Modified polyethylene glycol hydrogels for growth factor delivery and controlled tissue invasion

Carla Astrid Gustafsson
GSTCAR003

SUBMITTED TO THE UNIVERSITY OF CAPE TOWN

In fulfilment of the requirements for the degree MSc (Med) Biomaterials Faculty of Health Sciences

Supervisor: Associate Professor Neil H. Davies

Cardiovascular Research Unit, Department of Surgery

Date of submission: 23 April 2019

Declaration

I, *Carla Astrid Gustafsson*, hereby declare that the work on which this dissertation/thesis is based is my original work (except where acknowledgements indicate otherwise) and that neither the whole work nor any part of it has been, is being, or is to be submitted for another degree in this or any other university.

I empower the university to reproduce for the purpose of research either the whole or any portion of the contents in any manner whatsoever.

Signature: Signed by candidate

Date: 22/04/2019

Abstract

The prevalence of cardiovascular disease and myocardial infarction-induced heart failure has risen significantly over recent years, emphasising the need for new, effective therapeutic strategies. A promising alternative approach is the cardiac delivery of potentially cardioprotective and regenerative growth factors from biomaterial scaffolds.

One hydrogel system that has promise in this area is an injectable enzymatically degradable polyethylene glycol (PEG) hydrogel. Two modifications aimed at further optimising this system as a regenerative medicine scaffold were explored. Firstly, the covalent addition of heparin into the PEG backbone was assessed for its ability to stimulate angiogenesis by assessing the controlled release of basic fibroblast growth factor (bFGF), vascular endothelial growth factor (VEGF) and placental growth factor 2 (PlGF-2), and also assaying endothelial cell sprouting in an *in vitro* 3D spheroid angiogenesis assay. The second modification involved overlaying an increasingly hydrolytic degradability on top of the enzymatically degradable background of the hydrogel. The potential of this modification to regulate the rate of hydrogel replacement by invading tissue was assessed in the 3D spheroid assay and a subcutaneous implant study in a rat model.

The covalent coupling of heparin was found to substantially increase the rate of release of bFGF, VEGF and PlGF-2 over 20 days by 23%, 42% and 19%, respectively, relative to non-heparinised PEG hydrogels ($p<0.01$). A 3D spheroid-based angiogenesis assay was modified for use in quantifying endothelial cell sprouting in PEG hydrogels. bFGF and VEGF were shown to elicit a significant increase (2.3 – 2.4-fold increase) in average cumulative sprout lengths relative to that seen in the control spheroids ($p<0.01$). However, PlGF-2 did not stimulate a significant response (1.4-fold increase, p=NS). In follow up studies with heparinised hydrogels, it was found that the 3D angiogenesis was not rigorously established and ways forward are discussed.

Enzymatically degradable PEG hydrogels that retained their enzymatic degradability with increasing levels of potential for hydrolysis were formed by increasing the proportion of PEG-acrylate (PEG-Ac) and correspondingly decreasing the portion of PEG-vinyl sulfone (PEG-VS) monomers. PEG-Ac forms hydrolytically unstable bonds with the peptide crosslinker whilst

PEG-VS forms stable linkages. This approach was shown through swelling studies to be capable of generating a range of hydrolytic degradation rates. Sprouting of endothelial cells from PEG hydrogel embedded spheroids was shown to increase as the PEG-AC concentration increased. Importantly, the rate of tissue invasion *in vivo* was also shown to be positively correlated with the PEG-Ac concentration.

The increased utility of these hydrogels to act as delivery vehicles for therapeutic agents, through covalent coupling of heparin, is promising for their use as regenerative medicine scaffolds. Additionally, so is the ability to finely tune tissue invasion by manipulating their hydrolytic degradability.

Acknowledgments

I would like to thank my supervisor, Associate Professor Neil Davies, for all the guidance he has given me and patience he has shown throughout the course of my time in the Cardiovascular Research Unit. I would also like to thank Dr. Kyle Goetsch for his input, and the endless supply of doughnuts.

Every member of the Cardiovascular Research Unit has been an integral part of this journey. A special thank you must go to Emma Doubell for her friendship throughout the years and willingness to help wherever possible, and to Helen Ilsley for her input, assistance with all things laboratory related and processing of all histological sections. Ellen Ngarande, thank you for your help with flow cytometry. And to Mr Raymond Michaels, the work you do for all of us is so appreciated. To the lovely members of the Polymer Laboratory, past and present, thank you for an endless supply of PEG and laughter.

Lastly, I would like to thank Nick for being the most patient, encouraging partner, with the most fantastic Photoshop skills. And to my mum, Diane, and brother, Sven, I do not think I could have done this without all your support. To Helen and George, thank you for being such wonderful Cape Town parents.

I would finally like to thank the National Research Foundation, without the support of whom this work would not be possible.

Table of Contents

List of Figures

List of Tables

List of Abbreviations

Ang-1	Angiopoietin-1
Ang-2	Angiopoietin-2
bFGF	basic Fibroblast Growth Factor
BM-MSCs	Bone Marrow Mesenchymal Stromal Cells
CAM	Chick Chorioallontoic Membrane
CD31	Cluster of Differentiation 31, also known as Platelet Endothelial Cell Adhesion Molecule (PECAM-1)
CD34	Cluster of Differentiation 34, also known as the Human Hematopoietic Progenitor Cell Antigen
CVD	Cardiovascular Disease
DSL	Delta, Serrate, LAG-2
Dll1	Delta-like 1
Dll4	Delta-like 4
DNA	Deoxyribonucleic Acid
ECs	Endothelial Cells
ECM	Extracellular Matrix
EDC/NHS	1-ethyl-3-(-3-dimethylaminopropyl) carbodiimide/N-hydroxysulfosuccinimide
EDD	Embryo Development Day
EGF	Epidermal Growth Factor
FGF	Fibroblast Growth Factors
FGFRs	Fibroblast Growth Factor Receptors
Flk-1	Fetal liver kinase-1
Flt-1	Fms related tyrosine kinase-1 (mouse)
FLT-1	Fms related tyrosine kinase-1 (human)
GAGs	Glycosaminoglycans
HdFbs	Human dermal Fibroblasts
HF	Heart Failure
HIF-1α	Hypoxia Inducible Factor-1 alpha
HUVECs	Human Umbilical Vein Endothelial Cells
iHUVECS	immortalised HUVECs
Jag1	Jagged-1
Jag2	Jagged-2
KDR	Kinase insert Domain Receptor
LAD	Left Anterior Descending coronary artery

MMPs	Matrix Metalloproteinases
MI	Myocardial Infarction
MTT	3-(4,5-dimethylthiazol-2-yl)-2,5-diphenyltetrazolium bromide
NADPH	Nicotinamide Adenine Dinucleotide Phosphate
Nrp1	Neuropilin 1
PA-R	Plasminogen Activator Receptor
PDGF	Platelet Derived Growth Factor
PEG	Polyethylene Glycol
PEG-Ac	PEG acrylate
PEG-VS	PEG functionalised with vinyl sulfone groups
PGs	Proteoglycans
PlGF	Placental Growth Factor
PlGF-2	Placental Growth Factor-2
PIPAM	Poly-*N*-Isopropyl Acrylamide
PVA	Polyvinyl Alcohol
RGD	Arginine (R)-glycine(G)-aspartate(D)
ROS	Reactive Oxygen Species
S1P	Sphingosine-1-Phosphate
SMCs	Smooth Muscle Cells
Strep-HRP	Streptavidin-Horse Radish Peroxidase
TNF-α	Tumour Necrosis Factor-alpha
TGF-β	Transforming Growth Factor-beta
VEGF	Vascular Endothelial Growth Factor
VEGFR2	VEGF receptor 2
VS	Vinyl Sulfone
XTT	sodium 3’-[1-[(phenylamino)-carbony]-3,4-tetrazolium]-bis(4-methoxy-6-nitro) benzene-sulfonic acid hydrate

1. Introduction

1.1. Treating Myocardial Infarction-induced Heart Failure: The Need for Therapeutic Angiogenesis

Cardiovascular disease (CVD) is one of the main causes of death in developed countries, with myocardial infarction (MI) being one of the leading contributors [1]. This trend is not dissimilar in less developed areas, like South Africa, where it was reported in 2000 that CVD was the second largest cause of death after HIV/AIDS [2]. This is still the case, as CVD was responsible for 1 million deaths in 2013 in Sub-Saharan Africa alone [3]. With the rapid rate of urbanisation came changes in lifestyle and, thus, a major increase in CVD [4]. These lifestyle changes include dietary alterations and changes in physical activity. There has been a shift from diets containing cereals, vegetables and fruits, to those containing processed foods high in fat. In addition, due to the development that has taken place in these countries, individuals are also now engaging in less exercise [5].

Currently, health care practitioners are seeing an increasing proportion of patients survive their MIs, which can be accredited to improved management of acute arrhythmias and the implementation of reperfusion [1]. However, with this increased survival rate, comes a greater prevalence of MI-induced heart failure (HF), which current therapeutic strategies are not proving sufficiently efficacious to overcome [1].

1.1.1. Progression to infarction

Lifestyle, as well as genetic factors, play a major role in the development of CVD [6–8]. High plasma cholesterol levels cause lipids to accrue within coronary arteries and these levels alter the permeability of the endothelial cells lining the vessel walls, allowing lipids into the vessel wall itself. Immune cells are also able to penetrate the vessel wall by binding to proteins now expressed by the altered endothelial cells which then initiates the inflammatory process of atherosclerosis [9].

It is mainly through the rupture of this atherosclerotic plaque, and the thrombus formation that follows, that a coronary artery is occluded and an MI takes place [10,11]. This occlusion

of blood to the heart causes the region that the blocked vessel supplies to become ischemic [12]. This absence of oxygen and nutrients causes extensive cardiomyocyte death, producing an acellular, non-contractile area known as the "infarct" [13,14]. Due to the heart's very limited capacity for regeneration, this loss of cardiomyocytes at the infarct site is permanent [15].

The infarcted heart can then enter a vicious cycle of pathological remodelling driven, at least in part, by the increased workload on the surviving cardiomyocytes and the elevated stress in the ventricular wall due to thinning [16,17] as a consequence of cardiomyocyte loss. This elevated stress can be simplistically viewed as a consequence of Laplace's Law (first applied to the heart by Woods in 1892 [18]): "ventricular wall stress is directly proportional to the diameter of the ventricle and the ventricular pressure and is inversely proportional to the wall thickness of the ventricle" [16]. Eventually, this ventricular stress-driven process of adverse remodelling leads to HF [16] where the heart is unable to meet the metabolic needs of the body [19].

1.1.2. Current treatment strategies

Reperfusion of the blocked blood vessel by means of coronary angioplasty and/or the use of a stent are common strategies and can substantially limit infarct size and ventricular remodelling, positively influencing patient survival [20]. However, necrosis of the affected myocardium usually ensues quickly after the occlusion of the blood vessel. Thus, this necrosis often occurs before reperfusion takes place [21]. If the adverse remodelling is not prevented, eventually ventricular contractile function and cardiac output declines, which can progress to congestive HF [12]. Current treatments for MI and congestive HF include surgical procedures – like ventricular resection, balloon angioplasty, coronary artery bypass or the implantation of left ventricular assist devices – and pharmacological treatments, with diuretics and vasodilators being some of the strategies employed clinically, often in combination [12,22,23]. This approach lessens the symptoms but does not repair the damaged tissue [24]. Some patients are also not eligible or are entirely unresponsive to these current treatments [25]. Others continue to suffer symptoms of ischemic disease despite being given intense pharmacological treatments. Many of these individuals are not eligible for the invasive means of reperfusing the ischemic tissue by angioplasty or surgery [25].

Importantly, all of the above have proved inadequate in terms of long-term treatment [15]. For example, the use of diuretics may be a helpful pharmacological strategy in the short-term to relieve fluid accumulation, but will eventually trigger the Renin Angiotensin Aldosterone System due to the diuresis, vasoconstriction of renal blood vessels, and the accompanying decline in glomerular filtration rate [26,27]. This results in renal dysfunction and is indicative of a poor prognosis, with these patients needing dialysis and often being admitted to intensive care [28]. Although one of the main treatment goals is to achieve fluid balance in patients with chronic HF, hence the use of diuretics which prevent fluid reabsorption in the kidneys, a study (Acute Decompensated HEart Failure REgistry, or the ADHERE study) has found a higher mortality rate to be associated with the increased use of these diuretics [26,28].

The most effective "cure" for MI-induced HF is a heart transplant, however there is a great shortage of donors available at any given time [15]. If a patient does become a transplant recipient, they will need life-long immuno-suppression after surgery and further complications, like cardiac allograft vasculopathy, may ensue [29,30]. Thus, a need for more effective, alternative therapeutic strategies to treat the pathologies seen post-infarction is evident.

1.1.3. Therapeutic angiogenesis

One potential treatment approach that has emerged is therapeutic angiogenesis. Angiogenesis is defined as "the process of the formation of new blood vessels from pre-existing vessels" [31]. The goal of therapeutic angiogenesis is to bring about this angiogenic response in a patient as a form of therapy. This allows for the re-vascularisation of ischemic tissue with an increased blood vessel density potentially improving tissue function [32,33]. In part, the therapeutic outcome is believed to derive from ameliorating the microvasculature damage that occurs [34], increasing capillary supply to the surviving hypertrophic cardiomyocytes [35] and perfusing the cardiomyocytes surrounding the infarct zone [36]. Therapeutic angiogenesis is often achieved through the controlled release of growth factors, although stimulating the expression of certain angiogenic genes and delivering stem cells have also been utilised [37,38]. However, the genetic and stem cell approaches do not fall

within the scope of this review.

The Isner group are considered the pioneers of therapeutic angiogenesis. In Isner's seminal work, published in 1994, it was shown that by administering a single factor, vascular endothelial growth factor (VEGF), in a rabbit model of hindlimb ischemia, functional vasculature could be created [39]. Since the publication of this work, it has become apparent that delivery of growth factors without a delivery vehicle, referred to as bolus delivery, has adverse effects and does not allow for a sufficient therapeutic duration [40,41]. Studies into potential delivery vehicles ensued, and the field of therapeutic angiogenesis has since advanced, showing promise in treating not only MI, but other pathologies, including cardiovascular diseases [42] like coronary artery disease, peripheral artery disease and aortic atherosclerosis [32].

Patients with coronary artery disease and peripheral artery disease would also benefit greatly from a strategy like therapeutic angiogenesis. This is because some individuals with end-stage coronary artery disease suffer from chronic ischaemia and do not qualify for mechanical means of revascularisation [43]. Similarly, some patients with critical limb ischemia, the most severe type of peripheral arterial disease, do not qualify for revascularization by angioplasty or bypass. Patients with critical limb ischemia are faced with amputation or death if not urgently treated [44]. Thus, in the context of these ischemic diseases, the ischemic tissue provides an appropriate substrate for angiogenic therapy as the lack of oxygen causes the expression of receptors for pro-angiogenic factors as the tissue is primed to respond to the therapeutic angiogenesis therapies [45,46]. If one can stimulate angiogenesis, the ischemic area can become reperfused, circumventing the need for surgery and providing a patient ineligible for invasion-based reperfusion with a non-invasive alternative [32,44].

It follows that the process of angiogenesis and the molecules involved need to be understood in order to bring about therapeutic angiogenesis to treat ischemic cardiovascular disease.

1.1.4. The process of angiogenesis

Angiogenesis is involved in key physiological processes like embryonic development, inflammation and wound repair, but also in pathological situations like tumour growth [31,47]. It is a complex process involving multiple factors, thus presented below is a summary.

The main trigger for physiological or pathological angiogenesis in adults is ischemia, a lack of sufficient oxygen and nutrient supply to the tissues [48]. This stimulates the production of reactive oxygen species (ROS) by vascular cells, including endothelial cells (ECs), smooth muscle cells (SMCs), fibroblasts and perivascular adipocytes [49]. ROS are generated by these cells during electron transport within the mitochondria, where oxygen is reduced through electron additions to form a superoxide anion, hydrogen peroxide, a hydroxyl radical, and a water molecule [50]. ROS can also be generated by the actions of the enzyme NADPH (nicotinamide adenine dinucleotide phosphate) oxidase, which transfers electrons from NADPH to oxygen, creating a superoxide anion [51,52]. Angiogenesis is promoted by ROS directly, where hydrogen peroxide induces the expression hypoxia inducible factor 1-α (HIF-1α) which then stimulates the expression of VEGF in SMCs and ECs [48]. The HIF pathway is regarded to be the master regulator of angiogenesis [53]. Angiogenesis can also be indirectly stimulated by ROS through the creation of active oxidation products like peroxidised lipids, which is a VEGF-independent pathway [48,54].

The first step in the angiogenic process involves vasodilation stimulated by nitric oxide. In order for this dilation to occur, the junctions between the cells, as well as the contacts with perivascular cells, need to be loosened [47]. Angiopoietin-2 (Ang-2) plays a role here – by preventing Angiopoietin-1 (Ang-1) signalling, which promotes vessel stability, Ang-2 is able to destabilise the vessel and assist the detachment of pericytes and smooth muscle cells [55]. This also allows for ECs to migrate during the angiogenic process as this enables plasma proteins to extravasate and create a temporary extracellular matrix (ECM) for the ECs to move through [47]. The loosening of these cellular contacts is carried out by proteinases, including plasminogen activators and matrix metalloproteinases (MMPs), as well as other enzymes like chymases and heparinases [56]. Pro-angiogenic factors, like basic fibroblast growth factor (bFGF) and VEGF, stimulate the secretion of these proteases and plasminogen activators by ECs [57]. By degrading molecules in the ECM, further growth factors sequestered within are liberated and activated [56].

These liberated factors are involved in the activation of quiescent ECs, after which they then adopt one of two distinct endothelial phenotypes – that of the tip cell or the stalk cell. Tip cells are characterized by their location, their filopodia, and their migratory behaviour. These cells integrate directional cues, both attractive and repulsive, from their surrounding environment in order to set the path for sprout growth [58]. Tip cells are also involved in making new connections between sprouts in order to create a connected and functional vasculature [59]. The cells following on from the tip cell, the stalk cells, do not produce as many filopodia and respond differently to VEGF by proliferating. They are responsible for creating tight and adherens junctions to stabilise the sprout, a lumen and "luminal/abluminal polarity". This polarity is important as it leads to the deposition of a basal lamina and allows for recruitment and attachment of pericytes and vascular SMCs. These cells are instrumental in preventing vessel regression, allowing for the stabilisation and maturation of vessels [60,61]. In order for stalk cells to carry out these different functions, they respond to environmental queues differently and have different gene expression profiles compared to tip cells [58,62–64]. After extensive *in vitro* and *in vivo* assays, it has been found that VEGF and Notch signalling pathways are instrumental in the development of ECs into tip or stalk cells [64–66].

The Notch pathway is evolutionarily conserved and is needed for embryonic development, regulating tissue homeostasis, and maintaining stem cells in adults [67,68]. First identified in *Drosophila*, this pathway has since been shown to play a role in cell fate, tissue patterning, and morphogenesis by way of its role in cellular differentiation, proliferation, and a cell's ability to survive and apoptose [69,70]. There are four Notch receptors expressed by mammals, with Notch 1 and Notch 4 being expressed by ECs. Ligands known as Delta, Serrate, LAG-2 (DSL) ligands bind to Notch receptors. Of these DSL ligands, Delta-like 1 (Dll1), Dll4, Jagged-1 (Jag1), and Jag2 are expressed by ECs [71–74].

VEGF binds to its tyrosine kinase receptor, VEGF receptor 2 (VEGFR2), also referred to as KDR in humans and Flk-1 in mice [75]. Once this takes place, the cell-surface glycoprotein Neuropilin 1 (Nrp1), which is considered a non-tyrosine co-receptor, acts to improve VEGF binding and signalling [76,77]. After VEGF has bound to its receptor and the binding and signalling has been treated, the quiescent ECs are activated. This binding of VEGF then causes an increase in Dll4 expression in the tip cells – these would be the cells closest to the source

of the VEGF. Dll4 then stimulates Notch signalling in the stalk cells preventing the cells from becoming tip cells. Notch signalling also decreases VEGFR2 expression, making these cells less responsive to VEGF and thus reinforcing their stalk phenotype. Instead, these cells express VEGF receptor 1 (VEGFR1), also known as Flt-1 in mice and FLT-1 in humans, and begin to express Notch target genes. Contrary to this, tip cells experience low Notch signalling [78,79]. This allows them to continue to have their high levels of VEGFR2 and Nrp1 expression [78]. Furthermore, Jag1, produced by the stalk cells, prevents Dll4-Notch signalling in the tip cells when under the influence of a glycosyltransferase called Fringe [73,80]. This further differentiates the tip/stalk phenotypes and allows for spacing between tip cells by ensuring not every cell stimulated by VEGF becomes a tip cell [78].

During pathological angiogenesis, placental growth factor (PlGF) is upregulated and also plays a role by enhancing the response to VEGF. This occurs when PlGF shifts VEGF from its receptor, VEGFR1, making more available to bind to VEGFR2. The enhanced angiogenic response is the result of the activation of both VEGFR1 and VEGFR2 [81]. It is postulated that PlGF may stimulate angiogenesis through the transmission of intracellular signals mediated by VEGFR1 [82–84]. However, it is known that VEGFR1 has a weak tyrosine kinase activity and its intracellular signalling requires further study. PlGF may also influence angiogenesis through the formation of heterodimers with VEGF, if both are expressed within the same cell [84,85]. This dimer is able to bind to and activate VEGFR1, as well as induce dimerization of VEGFR1 and VEGFR2, if both of these receptors are present on the cell's surface [75]. Autiero et al. (2003) report that once PlGF activates VEGFR1, VEGFR2 can then be activated through transphosphorylation [86].

From the above, one can see that the highly coordinated process of angiogenesis involves many factors, both promoters and inhibitors. The formation of a mature vasculature necessitates this precise spatial and temporal regulation of factors [87] and research towards delivering growth factors increasingly aims to recapitulate this process sufficiently.

For researchers to ascertain whether their proposed treatment is capable of bringing about angiogenesis, appropriate angiogenic assays need to be devised. Many such assays exist, both *in vitro* and *in vivo* to enable this testing. However, one of the most pertinent technical challenges in studying angiogenesis is selecting an appropriate assay [88].

1.1.5. Studying angiogenesis *in vitro*

In vitro techniques make it possible to study the proliferation, migration and invasion of ECs – all processes that form a part of angiogenesis [89]. In this context, one can study a therapeutic's direct effect on endothelial cells and gain some indication of what one could expect *in vivo* [90].

Two-dimensional (2D) assays can be fast, highly reproducible assays to conduct [91]. An example is the proliferation assay, involving the seeding of defined number of cells (e.g. endothelial cells) into tissue culture treated wells. After seeding, cells are treated with the factors of interest and incubated for a minimum of 18 to 24 hours. Cells can then be counted, using a haemocytometer or automated cell counter, and cell numbers compared between treatments. In addition, a colorimetric assay can be employed [91]. These include MTT [3-(4,5-dimethylthiazol-2-yl)-2,5-diphenyltetrazolium bromide] or XTT [sodium 3'-[1-[(phenylamino)-carbony]-3,4-tetrazolium]-bis(4-methoxy-6-nitro)benzene-sulfonic acid hydrate] assays, which indirectly measure proliferation through measuring mitochondrial activity [91–93].

Cell migration assays can also be carried out, creating a 2D, *in vitro* model of cellular migration after basement membrane degradation, during the angiogenic process. Scratch assays are one such example [94]. These involve seeding cells in a monolayer and using an implement to create a scratch or "wound". Growth factors or other proteins of interest can then be administered and their effect on the rate of "wound" closure can be monitored. A more three-dimensional (3D) version of this assay makes use of the Boyden chamber, or modified versions thereof [95]. The one side of the chamber contains cells placed on top of a filter (which may be coated in an ECM protein) containing pores of a relevant size to facilitate the migration of the cell type used. The other side contains the chemoattractant i.e. growth factors of interest. The number of cells that migrate through the pores towards the chemoattractant can be quantified by staining cells on the underneath of the membrane and/or counting cell in the bottom [91,96]. The advantages of this assay include a high level of sensitivity to minor changes in chemoattractant gradients [97], and a high reproducibility and short duration, with the assay being conducted over a few hours [91].

In vitro cell culture has evolved from culturing cells in a monolayer, to culture conditions that are more representative of the *in vivo* environment, for example 3D assays involving cell spheres, consisting of one or multiple cell types, embedded in a matrix. 3D assays have allowed for the study of cell-cell interactions, as well as interactions between cells and their environment [98,99]. In addition, 3D cell cultures possess a greater stability and longer lifespan than 2D cultures. 3D cell spheres can be cultured for at least 4 weeks, as compared to 2D culture where cells need to be trypsinised regularly due to confluency [100].

An example of an *in vitro* angiogenesis assay is the 3D cell-coated microcarrier assay, pioneered by Nehls and Drenckhahn in 1995 [101]. In this assay, the outer surface of the microcarrier beads are coated with endothelial cells, after which the beads are suspended in a fibrin matrix (which can contain other cells in co-culture, for example fibroblasts) [102]. Sprouting/invasion into the matrix is then monitored over time and quantified. The downside of this assay is that it is very technical – achieving an even coating of cells can be very challenging and there will always be some beads that are not sufficiently coated, making reproducibility an issue [103,104].

Pioneered by Korff and Augustin, the spheroid sprouting assay is a challenging but powerful *in vitro* assay for angiogenesis [91,105]. Unlike other assays, the spheroid sprouting assay can theoretically, and if necessary, be conducted for several weeks depending on the cell type(s) [100,106,107]. Because there is no inflammatory response as there would be *in vivo*, this assay facilitates the study of the mechanisms, both at the cellular and molecular level, underpinning the angiogenic process [108]. As with the microcarrier bead assay, this assay provides a suitable way in which to study angiogenesis and test potentially pro-angiogenic compounds *in vitro* [108].

The assay usually involves endothelial cells, particularly human umbilical vein endothelial cells (HUVECs) but co-culture spheroids with multiple cell types have been used, embedded in a 3D matrix [109–111]. Most spheroid sprouting assays are conducted in collagen, but fibrin has also been used in the literature [108,109,112]. Spheroid formation relies on the need of adherent cells, like those involved in the angiogenic process, to adhere to a substrate [100]. Here, they are prevented from adhering to cell culture plastics (as they would in monolayer culture) by the addition of methylcellulose to the culture medium. The cells therefore have

no choice but to adhere to one another in order to survive [100,113]. This is most commonly achieved through a hanging drop method, or through the use of round-bottom culture plates that have not been tissue culture-treated [114,115]. In most spheroid assays, the sprout length or "extent of invasion" is measured, using micrographs captured, through use of computer software, and the number of sprouts is counted [108,109,116]. One can use these metrics to compare the effect of added growth factors, for example, or specific culture conditions [105].

The spheroid sprouting assay has many advantages, including the fact that it is more representative of the *in vivo* environment than 2D cell culture assays [105]. It also takes cell proliferation, migration, invasion and survival into account. The tunability of this assay is a further advantage, with one being able to control and alter experimental conditions to test any compound of interest, or the effect of a particular microenvironmental state, in a 3D scaffold of choice [108]. As stated by Korff and Augustin (1998), the spheroid cell culture model is a very powerful tool, allowing one to study the effect of EC survival/growth factors in a 3D environment representative of that found *in vivo*.

1.1.6. Studying angiogenesis *in vivo*

Once a therapeutic has been tested *in vitro* and has been determined to significantly influence the cellular processes of interest, like cellular invasion of a matrix, the next step is to assess its effects within a living organism. This is a necessary step in validating a potential therapeutic and moving towards clinical translation [117].

These *in vivo* assays include the embryonic chick chorioallontoic membrane (CAM) assay, the corneal angiogenesis assay and the subcutaneous implant model [118,119]. In the latter model, sponge-like polyurethane (P.U.) discs or Matrigel plugs have been implanted into the subcutaneous space in rodents [120,121].

In the past, researchers have used CAM assays to study angiogenesis, with the first CAM assay conducted by Rous and Murphy in 1911 [119]. Many consider it an *in vivo* assay, whereas some perceive it as an *ex vivo* model [122,123]. In this assay, the chick embryo takes 21 days to develop, with the CAM forming close to embryo development day (EDD) 4 and becoming

fully developed at EDD 14 [124,125]. When assessing angiogenesis, the assay usually commences on EDD 10 or 11 as this is when vascular expansion in the CAM is at its peak [126]. Usually the angiogenic response is evaluated macroscopically by looking at the formation of vessels at the site of implantation. This then establishes vascular density, the length of the vessels or vessel branching points/mm^2. Histological analyses can also be conducted, such as staining for CD31 (a marker specific to ECs) immunohistochemically [127].

As the embryo does not possess a mature immune system, this assay allows for the growth of xenografts without them being rejected [127,128]. The CAM assay has also been employed in testing biomaterials containing pro-angiogenic factors and/or cells [129]. Although a very cost effective, high throughput assay to study angiogenesis, there are a few disadvantages. When compared to *in vivo* assays, the assay has time constraints, with incubation period in the chick embryo being limited to between seven and ten days [127]. It is also important to recognise that the growth of blood vessels seen on the CAM is almost 2D in nature, and that the CAM environment is rather different to what one would find *in vivo* within an adult animal as it is highly specialised for the growth of the chick embryo [130]. The cells that respond in this assay are embryonic in nature and are thus already in an activated state. There are also drastic changes in vasculature from day to day as the chick embryo develops which need to be considered [130]. This assay also often requires animal ethics clearance when chick embryos are past a certain developmental stage [131].

An alternate assay is the corneal angiogenesis assay. Originally developed in a rabbit model in 1972 by Gimbrone et al. to study tumour angiogenesis, it has since been introduced into mice [118,132]. A pocket is made in the cornea, into which the therapeutic is placed. As the cornea is avascular and transparent, the premise is that any vasculature seen after applying the pro-angiogenic treatment of interest was stimulated as a result of that treatment and can easily be identified [91,117]. Quantification can be carried out by measuring the area of vessel penetration, chemotaxis of vessels toward the stimulus over time, or fluorochrome-labelled substances can be utilised for ease of quantification [117,133]. This assay has been used to study the angiogenic effects of growth factors like bFGF and VEGF [118,134].

Subcutaneous implant assays have also proved useful in assessing the angiogenic potential of a growth-factor releasing biomaterial. The degradation of the material can be studied as well

as its biocompatibility, in the context of immune and inflammatory responses, and cytotoxicity [135]. A specialised approach, specific to our group, involves impregnating P.U. discs with the biomaterial, which are placed in pockets under the skin in rats [120]. After a period of time, the discs are excised and can be histologically stained for endothelial cell markers (e.g. CD31 and CD34) and markers of vessel maturation (e.g α-smooth muscle actin) [120,136].

This model has some definite advantages. Referred to as the ectopic subcutaneous implant model, it is the least invasive of those used in *in vivo* tissue engineering research [135]. It also creates an environment of defined dimensions (that can easily be excised for analysis) that allows the process of angiogenesis to take place by allowing for cellular movement, as well as the necessary gaseous exchange and source of nutrients needed for vessel growth. Cells are able to move to the implant area and can penetrate the implanted disc, allowing for the formation of fibrous, vascular tissue [137,138]. Thus, this a suitable model to use when studying a therapeutic's pro-angiogenic capabilities.

1.1.7. Growth factor candidates for therapeutic angiogenesis

As previously mentioned, growth factors are involved in many important processes, with focus here on growth and remodelling of blood vessels [139,140]. There are many growth factors and cytokines that are being explored as therapeutic angiogenesis candidates, including the aforementioned bFGF and VEGF, as well as tumour necrosis factor-alpha (TNF-α), transforming growth factor-beta (TGF-β), placental growth factor 2 (PlGF-2), Ang-1 and Ang-2, and platelet derived growth factor (PDGF) [141,142]. The three growth factors of interest in this project are bFGF, VEGF and PlGF-2.

bFGF, also known as FGF-2, is an 18 kDa pro-angiogenic protein of 155 amino acids belonging to the FGF family, of which there are 18 members in mammals. This was the first successfully purified pro-angiogenic factor, isolated in 1984 by Folkman et al. from bovine cornea basement membrane [143]. Through binding to their transmembranous tyrosine kinase receptors (called fibroblast growth factor receptors or FGFRs), they are able to stimulate cell proliferation, migration, differentiation and enhance survival [31,144,145]. There are four

known tyrosine kinase FGFRs for these 18 FGFs to bind, namely FGFR1, FGFR2, FGFR3 and FGFR4 [146]. bFGF binds to either FGFR1 or FGFR2.

In order for activation to be successful, bFGF must bind to a proteoglycan, specifically heparin or heparan sulfate to stabilise the interaction of bFGF with its receptor FGFR1, and upon doing so, forms a complex consisting of two bFGFs and two FGFR1s [147][57]. The dimerisation of these receptors results in tyrosine kinase residue autophosphorylation. This activates downstream signalling cascades which stimulate the survival, proliferation, migration and differentiation of ECs [57].

bFGF has been utilised and studied both *in vitro* and *in vivo*. *In vitro*, it has been shown to affect endothelial cells not only by stimulating proliferation and migration, but also DNA synthesis and the production of plasminogen activator (PA) [148–150]. Murakami et al. (2008) conducted a study in which they inhibited FGF signalling in endothelial cells *in vitro* and in adult mouse and rat endothelial cells *in vivo*. This group found that disrupting FGF signalling resulted in dissociation of adherens and tight junctions, causing endothelial cells to come away from the vessel wall. Ultimately, vasculature was lost, elucidating the important role FGFs play in maintaining a lasting vasculature [151]. In addition to influencing endothelial cells, bFGF also affects SMCs and fibroblasts [152].

VEGF has become another factor of interest since its use in the pioneering work on hind limb ischemia by the Isner Group [39]. As mentioned above, VEGF (originally called vascular permeability factor or VPF) has receptors expressed by multiple cells types – e.g. endothelial cells, macrophages and keratinocytes – which all play a role in wound healing [141,153]. The soluble and membrane-bound form of VEGF usually binds to VEGFR1 or VEGFR2. Neuropilin-1 (Nrp-1) binds VEGF-A, the 165 amino acid variant produced by alternative splicing [141,142]. There are four VEGF isoforms, which range from 121 to 206 amino acids in length and are named accordingly [154].

Upon ligand binding, the VEGF receptors undergo dimerisation and autophosphorylation [155]. This leads to the activation of several pathways, namely the Ras/MAP-kinase, the PI3K/PTEN/Akt, the Jak/Stat and the PLC-γ/PKC pathways. VEGF's stimulation of cell proliferation occurs through the activation of Akt in the PI3K/PTEN/Akt pathway [155]. It has

been suggested that a crosstalk exists between VEGF and other signalling molecules, for example sphingosine-1-phosphate (S1P), during angiogenesis [156,157].

VEGF is able to promote the release of von Willebrand factor in the body, stimulate the expression of integrins, interstitial collagenase, PA and its receptor, plasminogen activator receptor (PA-R), and increase vascular permeability as well as fenestration [141]. One of the main issues with the therapeutic use of this growth factor is its short half-life *in vivo* [158,159].

PlGF is another member of the VEGF family. The 152 amino acid-long heparin-binding isoform, PlGF-2, is of particular interest due to its role in angiogenesis [142,160]. As a result of alternative splicing, there are four PlGF isoforms ranging in amino acid length – 131 (PlGF-1), 152 (PlGF-2), 203 (PlGF-3) and 224 amino acids (PlGF-4) [161–163]. These amino acid sequence lengths do not include the 18 amino acid-long signal peptide common to all the PlGFs [142]. PlGF-1 and PlGF-3 are the non-heparin binding isoforms, whereas PlGF-2 and PlGF-4 possess an additional 21 amino acid long heparin binding domain [161,163,164]. PlGF, discovered in 1991 by Maglione et al. in a human placental cDNA library (hence its name), is a member of the VEGF family and binds to the same receptors [165]. It has been known to bind to Flt-1, but not to KDR, which is thought to mediate most of the pro-angiogenic and pro-proliferative effects of VEGF. It is to be noted that the binding of PlGF-2 to its receptors is heparin dependent [166]. PlGF-2 has also been reported to bind to Nrp-1 [166].

This growth factor affects multiple cell types – endothelial cells, smooth muscle cells and inflammatory cells of the immune system – in order to bring about the growth of new blood vessels [167]. PlGF has been shown to be as effective as VEGF but does not cause the undesirable side effects like an increase in blood vessel permeability, oedema, hypotension or hemangioma formation [167,168].

Research has been conducted in which “naked” PlGF-2 has been delivered. Wu et al. (2015) administered PlGF-2 via an intravenous drip over 14 days in a porcine model of myocardial ischemia [160]. A significant increase in enhanced myocardial perfusion and contractility was seen at rest, and during a period of stress it was noted that no negative side effects were observed. It appears that this research group are the first to show the positive effect of PlGF-2 on myocardial perfusion and systolic function in a clinically applicable model [160].

It is to be noted that there is conflicting data in the literature when it comes to the concentrations of PlGF-2 needed to elicit a response, and the type of the response elicited. For example, Lang et al. stated that PlGF-2 affects endothelial cell proliferation, where others state this is not the case [148,166]. PlGF-2 has been shown to cause the migration of endothelial cells [166], however Bompais et al. (2004) found no increase in migration [169]. Thus, further research is needed to assess the effects of this growth factor.

1.2. Delivery of pro-angiogenic factors using functionalised, polymeric hydrogels

Although there is a prodigious amount of research into therapeutic angiogenesis approaches, delivery is still a major challenge [37,170]. Growth factors can be delivered as recombinant proteins by bolus administration. As this has adverse effects, researchers then began to use viral vectors to deliver factors. This method too had its disadvantages [171]. Thus, a strong case for controlled release using a biomaterial arose [172].

1.2.1. Bolus delivery of factors

Bolus administration of factors that are not encapsulated (i.e. “naked” factors) within a material presents multiple problems. [39]. Usually large doses are delivered, as was done by Wang et al. (2013), in a bid to overcome the short half-life of VEGF *in vivo* [159]. These high doses resulted in increased vascular permeability, causing fluid to leak out of the vasculature, leading to hypotension. This was confirmed in a study conducted by Hariawala et al. (1996) where VEGF (2 mg) was administered into the left coronary ostium in a porcine model of chronic myocardial ischemia [173].

Following on from a trial in pigs [174], a Phase-I trial (FGF Initiating RevaScularization Trial or FIRST) involving patients with coronary artery disease aimed to further investigate the safety and efficacy of recombinant bFGF [175]. In this trial, Simons et al. (2002) also saw hypotension occurring after single-bolus intracoronary injection, particularly in the patients given bFGF at the highest dose (30 µg/kg) [175,176]. Further indicating the potential for undesirable outcomes with a single delivery, the same group reported that there was also trend towards both hypotension and tachycardia in patients given high bFGF doses [176]. Higher growth

factor doses could result in an imbalance between factors that work in synergism, and it has been reported that this approach creates abnormal vasculature with a tendency to regress due to cellular and matrix detachment, followed by apoptosis [60,177–179]. In addition, the vessels formed during this high-dose administration are not very well perfused [180]. Cooper et al. (2001) have also shown that bolus delivery of bFGF can cause proteinuria [181].

As growth factors play a role in cancer growth, bolus delivery of "naked" factors could also unintentionally stimulate distant tumour-containing tissues because the factor is not localised to the target site [182,183], although this potentially devastating side effect has not been reported. As aforementioned, growth factors delivered "naked" have an extremely short half-life (VEGF: 35 – 50 minutes [184,185], and bFGF: 45 – 50 minutes [186,187] under normoxic conditions). Even under more disease-relevant conditions, half-life is still considered too short [188]. In a Phase-II clinical trial involving patients with coronary artery disease receiving VEGF by intracoronary infusion, it was reported that by 8 hours post-administration the level of VEGF present had already substantially decreased, resulting in only transient VEGF exposure [189]. This is usually owing to degradation by proteases in the body [190,191]. Thus, therapeutic duration is brief, and the dose that reaches the intended site is low [37,192].

1.2.2. Controlled release of growth factors

It is now known that localised delivery of these factors, and sustained delivery of low doses over time, rather than uncontrolled bolus delivery, are integral to the development of functional vasculature [193]. In the physiological context, the ECM is a repository of pro-angiogenic factors, which are only locally released into the surrounding tissue when needed [194]. Often, tissue regeneration takes weeks to months and requires an almost constant stimulation by growth factors [172]. On this basis, research focus began to shift towards the use of biomaterials, using natural or synthetic polymers as ECM-mimics for controlled growth factory delivery [195]. Gene therapy has also been explored as a way of stimulating local over-expression of the factors, and will be briefly discussed [196–198].

1.2.2.1. Gene therapy

Another means by which researchers have tackled the goal of sustained and targeted delivery is through gene therapy, involving the delivery of plasmid deoxyribonucleic acid (DNA) [196–198]. Though a potentially powerful approach, this extensively investigated area is beyond the scope of this thesis. It should be noted, however, that there are possible safety issues associated with gene therapy for such prevalent pathologies like ischemic hearts and limbs. The commonly used adenovirus vector, when used to treat an ornithine transcarbamylase deficiency [199], resulted in the death of one patient as a direct result of the immune response mounted against this vector [200]. Furthermore, retroviral-type vectors, used as DNA carriers to aid delivery, run the risk of causing insertional mutagenesis. A viral vector was used for transgene delivery in a study aiming to treat severe combined immunodeficiency, in which suffers possess a mutation in the gene encoding the γ chain (γc). Hematopoietic stem cells were isolated from each patient and transduced *in vitro* using a defective retroviral vector [201]. At first it seemed there were no adverse side effects, however a participant later developed acute lymphoblastic leukaemia caused by insertional mutagenesis [202].

1.2.2.2. Polymeric delivery of growth factors

A mentioned above, sustained delivery of growth factors is pertinent to the formation of stable vasculature, and the prevention of high-dose and off-target effects. As viral vectors do pose a level of risk, polymeric biomaterials have been considered for sustained delivery. These include microparticles, nanoparticles and polymer-coated liposomes, as well as injectable hydrogels which polymerise *in situ* [37,167,203,204].

Liposomes are composed of mammalian cell membrane phospholipids, making them biocompatible [205]. When phospholipids, with their polar heads and hydrophilic tails, are immersed in an aqueous solution they arrange into spherical structures consisting of one or more lipids bilayers, surrounding an aqueous core [203]. This allows liposomes to envelop both hydrophobic and hydrophilic compounds. By using liposomal delivery vehicles, bioactivity of protein cargo is prolonged by protecting from extremes in temperature, pH and ionic strength [203].

In terms of being applied to recombinant growth factor delivery, liposomes have been used to orally deliver epidermal growth factor (EGF) for the treatment of peptic ulcers [206,207]. They have also been employed to deliver EGF percutaneously for wound healing [208]. In the context of myocardial infarction, researchers have delivered VEGF-loaded liposomes [209]. However, these were "immunoliposomes" – liposomes altered by addition of anti-P-selectin antibodies, P-selectin being a cell-adhesion molecule. This was to aid in selectively targeting delivery to the infarct border zone in which a high inflammatory response is present, causing an upregulation of P-selectin resulting in leukocyte and stem cell recruitment to the infarcted area [210,211]. In this study, lasting improvements in cardiac functioning were observed up to 4 weeks post-MI and correlated with increases in vascular density and perfusion [209].

Although some studies have shown positive results, the use of liposomes comes with disadvantages. For example aggregate formation and vulnerability to dissociation by enzymes, causing them to leak their contents prematurely [212]. To mitigate this, liposomes can be coated in polymers like polyethylene glycol (PEG) as a means of steric stabilisation, assisting in creating "stealth" liposomes with improved cargo release kinetics [213–215]. Despite this improvement, liposomes possess relatively low growth factor loading efficiency, which remains a barrier to use as a delivery vehicle in this context [203]. Unlike cross-linked polymeric delivery vehicles, the duration of release from liposomal carriers usually tends to be shorter [216].

Binsalamah et al. (2011) made use of an alternative biomaterial in delivering PlGF-2. This growth factor was encapsulated in chitosan-alginate nanoparticles and administered by intramyocardial injection. A sustained release was seen over a 5-day period and resulted in a significant increase in left ventricular function, vascular density and anti-inflammatory cytokines, along with a decrease in scar area formation and levels of pro-inflammatory cytokines [167].

Albumin-alginate microcapsules have also been used as a delivery vehicle to administer hepatocyte growth factor (HGF) and bFGF intramyocardially in a chronic heart failure model in rats [37]. Through employing the microcapsule delivery mechanism, growth release was controlled and the dose needed was substantially decreased. Here, a total of 125 ng HGF and 500 ng bFGF were delivered, compared to the 10 - 100 μg/kg usually administered without a

delivery vehicle, which is much higher than the amounts present physiologically. In this study the release was successfully confined to the desired treatment area (the left ventricle), without leakage in to the systemic circulation [37].

1.2.2.2.1. Hydrogel-based delivery

Rather than using particles or polymer-coated liposomes, polymer hydrogels can be employed for growth factor delivery. A hydrogel can be defined as a cross-linked polymer network that retains water due to the presence of hydrophilic groups, similar to the natural tissues occurring in the human body [217]. Hydrogels are particularly attractive because they possess properties pertaining to both liquids and solids – meaning they are spatially confined and yet molecules are able to diffuse out [218].

There are many benefits to using hydrogels to deliver therapeutics. Their aqueous nature assists in maintaining the biological function of the encapsulated substances [219], with their cross-linked network allowing for the outward diffusion of the substances while simultaneously preventing larger, potentially interfering, molecules from entering the hydrogel [220]. Polymerisation of several hydrogels only requires mild reaction conditions, such that they can cross-link under biologically relevant conditions without affecting cellular viability [221]. Some hydrogels have the added advantage of being injectable, allowing for less invasive administration [204,222,223].

Hydrogels can either be made from natural sources – proteins and polysaccharides extracted from living organisms e.g. collagen, gelatin, alginate and fibrin – or from synthetic materials like polyvinyl alcohol (PVA) or PEG [172,224–226].

Natural Hydrogels

Natural hydrogels are known for their good biocompatibility and degradability [172]. These hydrogels are successful in mimicking the natural ECM as they are derived from naturally occurring ECM components, allowing for cellular attachment, as well as growth factor binding and release as would occur *in vivo* [227–229].

Animal and human clinical trials have taken place using natural hydrogels as delivery vehicles [76,230]. Marui et al. (2007) have employed gelatin hydrogels loaded with bFGF in the treatment of limb ischemia in a Phase I-IIa clinical trial. This treatment was shown to be safe and effective, with most patients showing increased healing of limb ulcers, without raising serum bFGF levels and without the need for gene or cell delivery [231].

Although used in clinical trials, the use of gelatin hydrogels is thought to be limited because of the material's lack of stability and poor mechanical properties when under physiological conditions [229]. Xing et al. (2014) have improved the stability and strength by removing divalent cations (Ca^{2+} and Fe^{2+}), while still maintaining the hydrogels cellular attachment capabilities [229].

Fibrin hydrogels were one of the first biomaterials employed in promoting wound healing and stopping bleeding [232]. When blood clotting proteins fibrinogen and thrombin are combined in the presence of Ca^{2+}, insoluble fibrin forms [233]. This unique means of polymerization allows gelation time to be controlled, and by altering reaction conditions one can alter the architecture of the hydrogel network [232].

In a canine model of MI, bFGF was incorporated into a fibrin glue to create a controlled release vehicle. Animals in Group I only underwent permanent ligation of the left anterior descending coronary artery (LAD), whereas in Groups II and III channels were created after infarct induction, transmurally and non-transmurally, respectively. These channels were then used to administer the growth factor-containing fibrin glue. Compared to the infarct-only control, an increased and persistent angiogenic response was seen, improving cardiac functioning and perfusion. However, the one shortcoming of this study was they did not include a control in which fibrin without bFGF was administered, or in which bFGF alone was administered without fibrin [234].

Although there are some benefits to the use of natural hydrogels, there exist a few disadvantages. These include the variation between the sources from which they are derived, and further variation between batches, leading to inconsistencies [235–237]. One cannot manipulate the chemistry or physical properties of these hydrogels to provide further spatial and temporal cues, which are pertinent for tissue regeneration [122,177,238], to the same

extent one can with their synthetic counterparts. By chemically modifying synthetic hydrogels, one can provide these cues, making synthetic biomaterials an ideal, and more clinically appropriate candidate for use in tissue regeneration [122,239,240]. One can also alter the composition of the hydrogel to fine-tune degradation rate, as well as its mechanical strength, making synthetic hydrogels like PEG a promising delivery vehicle [217,241].

Synthetic Hydrogels

As aforementioned, synthetic hydrogels can be made from a variety of polymers, including PVA and PEG, as well as polymers like polyacrylic acid and poly-*N*-isopropyl acrylamide (PIPAM), which can also be combined to create new hydrogels [242,243].

PVA hydrogels have proven to be stable and although historically used as nondegradable implants, they can be crosslinked with biodegradable linkages, making them better suited for a wider range of biomedical applications [218,244,245]. These hydrogels are commonly formed through a process of repeated freeze-thaw cycles, or “cryo-gelation”. This gives rise to a highly porous scaffold that allows for diffusion, however in their traditional form these hydrogels are ill suited for controlled release of therapeutics [245]. PEG hydrogels, however, have shown much promise.

1.2.3. Polyethylene glycol hydrogels for controlled release

PEG monomers can be functionalised with chemical end-groups e.g. vinyl sulfones and acrylates (Figure 1) allowing for the formation of complex hydrogels with different characteristics in terms of degradation and capacity for cellular invasion [246,247].

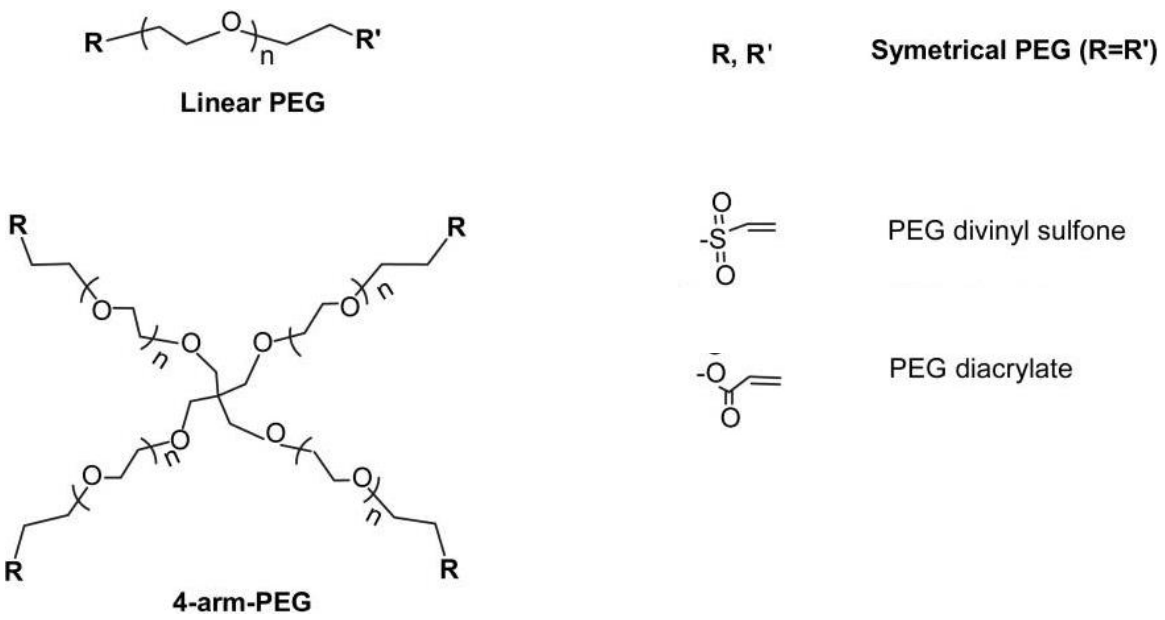

Figure 1: The structure of linear and 4-armed polyethylene glycol *and the possible functionalising end-groups, divinyl sulfones and diacrylates. Image adapted from Zhu (2010) [248].*

These PEG hydrogels are created by step-growth Michael-type addition reactions, also known as conjugate addition reactions, that are very selective [246,249–252]. Formation of these hydrogels involves the "thiol-ene" crosslinking of a dithiol linker, which can be a peptide with thiol-containing cysteine residues either end of enzymatically degradable peptide sequences (termed "bis-cysteine") with vinyl sulfone end-groups on the PEG (Figure 2) [249,250,253]. PEG functionalised with vinyl sulfone groups will, hereafter, be referred to as PEG-VS. The bond formed in this reaction is a stable thioether sulfone bond. Similarly, acrylated PEG monomers (PEG-Ac) crosslink with these thiol groups on MMP-recognition peptides [247,254,255] to form hydrolytically unstable thioether ester bonds form. PEG-Ac monomers will be further discussed in Section 1.3.

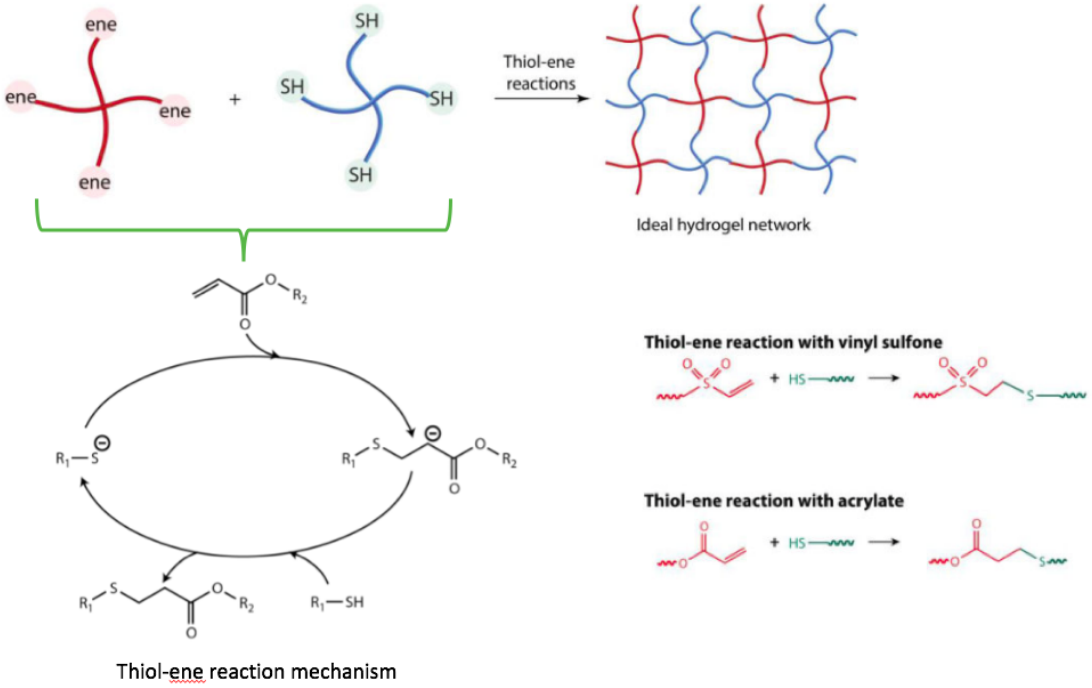

***Figure 2: Mechanism of thiol-ene hydrogel crosslinking**, as would occur between PEG-VS monomers and peptide crosslinkers like MMP-recognition peptides, as well as between PEG-Ac and the peptide crosslinkers. Image adapted from Kharkar et al. (2016) [253].*

Utilising these PEG gels has many advantages. They do not require any external stimulation to initiate this reaction, and no biologically incompatible leaving groups are generated through this reaction [256,257]. These hydrogels also do not elicit much of an immunological responses *in vivo* – they are relatively "biologically inert", and are able to enhance the pharmacology of protein cargo without altering their chemical structure and efficacy [30,258,259].

1.2.3.1. Enzymatic degradation

The Lutolf and Hubbell group developed an enzymatically degradable PEG hydrogel, which has since been utilised by other research groups including our own [239,255,260,261]. As aforementioned, enzymatically degradable PEG-VS gels are crosslinked using cysteine-functionalised peptide sequences, that are cleavable by enzymes naturally occurring *in vivo* [120]. This degradation is desirable as it allows for cell invasion and prevents the macrophage-centric immune response seen with non-degradable PEG hydrogels [262–264]. The crosslinking peptide sequences of interest here are those recognised by MMPs. MMPs encompass a large group of enzymes, of which there are 23 in the human body [265].

The sequence most commonly used is that of collagen type I's alpha chain substrate site. It has been found that substituting the "A" in the sequence (GPQGYIAGQ) for a "W", giving the amino acid sequence GPQGYIWGQ, increases activity [266]. *In vivo*, this sequence is cleavable by a range of different MMPs, and can thus be referred to as "PAN-MMP" [250].

Kadner et al. (2012) showed that enzymatically degradable PEG-VS gels cross-linked with MMP-1 specific recognition sequences delivered one week after cardiac infarction in a rat model significantly increased wall thickness and fractional shortening, as well as reduced end-diastolic diameter compared to the control that received saline instead of PEG [255]. Johnson et al. (2015) employed the same enzymatically degradable hydrogel in the heart but to deliver therapeutics, with the aim of reducing the inflammation. This was achieved by loading the PEG gel with coacervates filled with a morphogen (sonic hedgehog) and an anti-inflammatory cytokine (interleukin 10) [30]. A preservation of cardiac function was seen after MI, with the hydrogel improving coacervate retention post administration and integrating with the heart wall. Improved vascularisation was seen after 4 weeks, along with decreased fibrosis. The hydrogels themselves also act as a therapeutic, by reducing stress in the ventricle walls (in accordance with Laplace's Law) and restoring the shape of the ventricles [12,260].

Promoting cellular degradation of these scaffolds by MMPs relies first on cellular adhesion and invasion. In order to re-vascularise the area and bring about tissue regeneration, cells need to be able adhere to and invade the biomaterial as they would the ECM in the body [262].

Integrins, transmembrane receptors expressed on the surface of cells, mediate cell migration and adhesion by binding to ECM proteins (e.g. laminin, collagen and fibronectin) [267,268]. Many of these ECM proteins share a 3-amino acid monomeric peptide/integrin binding motif – arginine-glycine-aspartate, which is shortened to RGD using the amino acid single letter codes [268–270]. This short sequence can be easily synthesised and it has the advantage of being relatively stable and less subject to denaturation or degradation *in vivo* than the complete proteins [271]. It can also be incorporated in much higher concentrations than the entire sequence [271]. Due to their inert nature, PEG hydrogels do not inherently allow for cellular attachment. Therefore, to facilitate cellular adhesion, RGD can be incorporated

[218,271,272]. This is achieved with the PEG formulations described here by synthesis of the peptide sequence with incorporation of a single cysteine (Figure 3) [262].

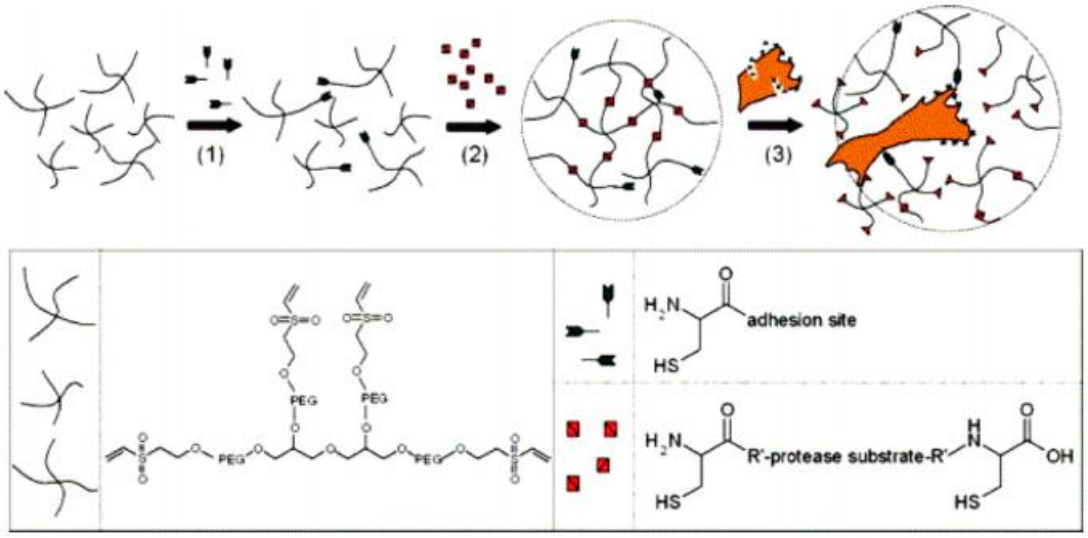

Figure 3: The stepwise formation of 4-armed PEG-VS hydrogels *by reacting with monocysteine-containing cell recognition peptides e.g. RGD (1) and bis-cysteine-containing enzymatically degradable peptides e.g. MMP (2) to enable cell attachment and eventual degradation of the hydrogel (3). Image adapted by Silva et al. (2009) from Lutolf et al. (2003) [262,273].*

1.2.3.2. Mechanical properties

The mechanical properties of hydrogels play a role in mechanotransduction, or the cellular conversion of mechanical information obtained from cellular surroundings into biochemical signals [274]. This influences how cells spread, migrate and differentiate [275]. Ehrbar et al. (2011) have shown that when the matrix has a low stiffness, cells tend to migrate in a manner not involving proteolytic degradation [276]. This is usually because hydrogels with a lower stiffness have a lower crosslink density as well as channels or defects within them. Thus, there are larger spaces for the cells to move through, making cellular migration possible without degradation of the surrounding matrix [262]. The higher stiffness matrix however restricted migration to that achieved by cellular proteolysis [276]. Thus, when creating a biomaterial one must consider matrix stiffness to allow for the desired cell invasion [259].

Small amplitude oscillatory shear rheometry is conducted to ascertain the mechanical properties of a hydrogel. G*, or the complex modulus, is a measure of how stiff an elastic

material is. In the case of a hydrogel, the material is both elastic and viscous. Thus, G* is divided into two moduli: the storage modulus (G') and the loss modulus (G''). When the G' value is greater than the G'' value, the hydrogel is more solid. When the G'' value is greater than the G' value, the hydrogels behaves more like a liquid [277].

1.2.3.3. Functionalisation with heparin

It has been argued that synthetic hydrogels lack an important ECM component involved in morphogen presentation – glycans (glycosaminoglycans – GAGs – and proteoglycans – PGs) [278]. Glycosaminoglycans are made up of repeating units, which are disaccharide derivatives, and can either be nonsulfated or sulfated. Heparan sulfate, as well as its related molecule heparin (Figure 4), can attach to serine-containing proteins to form proteoglycans [248,279]. Glycans, which are highly negatively charged, are able to aid the diffusion of nutrients and through swelling, relieve compressive stresses and prevent tissue from collapsing when pressure is applied [280].

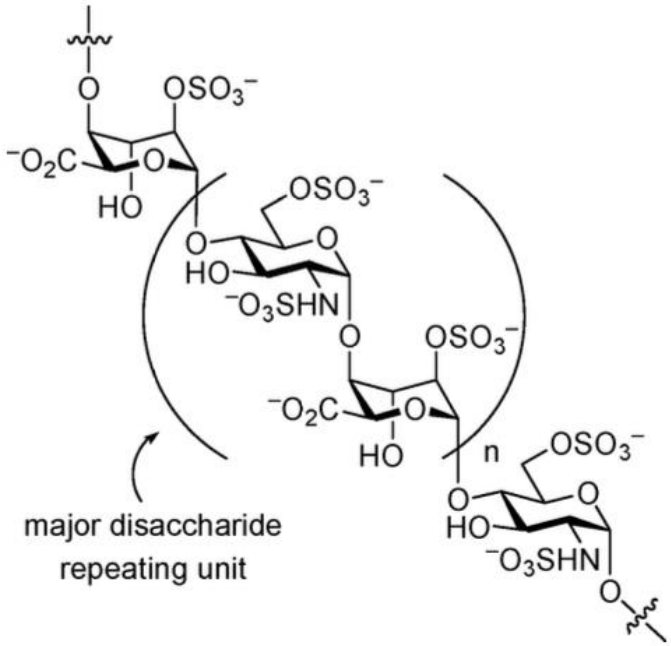

***Figure 4: The structure of heparin**, indicating the disaccharide unit that is repeated through the molecule. Image taken from Hung et al. (2012) [281].*

Heparin proteoglycan is found within mast cell granules, whereas heparan sulfate is found on the surface of cells and in the extracellular matrix. Heparin is more sulfated and can typically

outcompete heparan sulfate for binding to proteins [279]. There are in excess of 100 proteins that bind to GAGs through serine residues (with hyalorunan being an exception) to form proteoglycans [282,283]. These include proteins involved in cell adhesion molecules (e.g. fibronectin and laminin), lipid metabolism (e.g. lipoprotein lipase), coagulation (e.g. antithrombin) and many other processes [282].

Heparin has been widely used for its anti-coagulant effects since 1912 when these properties were first described by Doyon [284], with the first formulations suited for human trials only being produced in the 1930s [279,285]. However, heparin is more than just an anti-coagulant. It was in 1982 that Taylor and Folkman were the first to discover its pro-angiogenic nature through the use of the CAM assay [286]. Its pro-angiogenic nature stems from the ability of many growth factors to interact with heparin through heparin binding sites – essentially clusters of positive charge [279]. Heparin is able to prevent the degradation of these factors and prolong their half-life [192]. The presence of heparin has even been found to potentiate growth factor activity [287]. For example, as previously described, bFGF signalling involves a synergism with heparan sulfate/heparin. After secretion, bFGF is held within the ECM and on the cell surface by heparan sulfate/heparin and once released from the ECM, binds to cell surface heparan sulfate/heparin. This binding creates a ternary complex, stabilising the reaction between the ligand (bFGF) and the FGFR [145,288]. The presence of heparin or heparan sulfate also contributes towards VEGF binding to its receptor and confers stabilization upon the active conformation of VEGF. These proteoglycans are able to protect VEGF from degradation and have been shown to increase the angiogenic response this growth factor elicits from endothelial cells [289].

Heparin thus can be added to hydrogels and other biomaterials to increase their functionality [254]. This potentially allows for controlled release of growth factors, preventing their rapid clearance, and improving the pharmacology of the proteins without the need to alter their structure or alter their chemistry [290].

Heparin has been employed by our group to modify the surface of porous P.U. scaffolds – Bezuidenhoudt et al. used heparin to coat the surface of P.U. discs for subcutaneous implantation. They found this to increase vascularisation, without the normally associated rise in inflammatory response [136]. This was later taken a step further with the addition of

VEGF and PDGF to the heparinized surface of these scaffolds [291]. After 10 days, the dual release of these factors was found to increase vascularization within the scaffold, with this response lasting a minimum of 2 months post-implantation. Furthermore, heparin was found to enhance the angiogenic response elicited by the growth factors [291].

Very recently, this work has been extended by our group towards incorporation of the heparin directly into PEG hydrogels via acrylation of heparin [254]. This was done by reacting a heparin/heparan sulfate solution with acrolyl chloride (added by syringe pump) for an hour, followed by filtration and, finally, precipitation of the acrylated heparin/heparan sulfate. This was then vacuum dried and purified by dialysis against deionized water, and freeze-dried for long-term storage [254].

Although PEG hydrogels with acrylate or vinyl sulfone terminal moieties can potentially bind growth factors through interaction with their cysteine residues, this will result in a permanent covalent linkage. Thus, bound growth factors either interact directly with invading cells or contribute to a chemotactic gradient when released from a degrading hydrogel. The incorporation of heparin was postulated to allow for greater binding and enhanced chemotactic gradient formation due to the electrostatic nature of growth factor binding to heparin. An initial study showed that 8-armed monomeric PEG-Ac hydrogels could bind and release VEGF from these hydrolytically degradable hydrogels [254]. An increase in vascularization in subcutaneous implants in rats was observed after 4 weeks relative to non-heparinised PEG hydrogels containing VEGF. Limited release studies were performed on these hydrolytically degradable hydrogels.

This 8-arm heparinised hydrogel was investigated in the context of optimising delivery of bone marrow mesenchymal stromal cells (BM-MSCs) to the infarcted heart [261]. The fact that hydrogel gelation takes place *in situ*, as a result of the Michael-type addition reaction that occurs under normal physiological conditions, confers an advantage to using hydrogels in the heart – upon injection, the gelation prevents them from being ejected from the heart [257,290,292]. The aim of this study in which BM-MSCs were delivered was to better engraftment, and additionally improve the binding and release of the paracrine factors secreted by these cells. It was found that heparin-containing hydrogels were better able to bind VEGF and bFGF. When delivered along with BM-MSCs, improvements in cell engraftment

and retention were seen. Cardiac functioning was also improved, with less remodelling and fibrosis taking place [261].

Thus, these heparinized hydrogels have been investigated in the context of the 8-arm format, both for enzymatically and hydrolytically degradable versions. Further work is required on growth factor binding and release from the 4-arm formats, which are of interest as they allow for less stiff hydrogels to be generated [258], and the range of growth factors studied needs to be extended. It would also be of interest to determine the influence of heparin on the interaction of cells with growth factors when cells are invading the hydrogel. As described above, bFGF interaction with cells is enhanced through its binding to heparin [145,288]. This could most easily be examined in a suitable 3D *in vitro* angiogenesis assay.

1.3. Controlling cellular invasion of hydrogels by altering PEG composition

From the previous chapter it has been elucidated that, through chemical manipulation, the elastic modulus or stiffness (G') and general strength of these polymers can be altered to create a material that mimics the biological milieu [30,262,293]. By addition of sequences that allow for cell adhesion and enzymatic degradation of these scaffolds, thus promoting invasion, one further mimics the natural ECM. Thus, ultimately creating a material that can enable tissue regeneration *in vivo* [262]. Through the addition of proteins, like growth factors, one can further improve upon the regenerative capacity of these materials through the stimulation of angiogenesis [294]. This chapter focuses on a means of manipulating these hydrogels to control cellular invasion and, in turn, their replacement by tissue.

As has been elucidated in sections prior, part of what makes PEG such an attractive candidate for the delivery of alternative therapies is the control one can exert over its chemistry, and, in turn, over its mechanical properties e.g. stiffness [30]. Hydrogel stiffness is influenced by the distance between crosslinks and is very important when designing a biomaterial as it influences whether cells are able to penetrate the hydrogel [262]. Additionally, the mechanical properties of the scaffold have a major influence on cellular behaviour through mechanotransduction [295]. It is important in regenerative applications that degradation of the scaffold and tissue ingrowth take place simultaneously [239]. A major advance in this field was made when the peptide crosslinkers aforementioned were introduced, allowing the tissue replacement of the material to be directly linked with cellular proteolytic activity [262]. Determining the exact timing of this degradation is also crucial, but complex, and is influenced by a wide range of factors. For example, sufficient cellular matrix deposition must occur before the scaffold completely degrades. In the case of controlled release, the material needs to persist long enough to allow for the sufficient release of its cargo to allow for the generation of stable vasculature [296,297].

Ideally, a scaffold designed for regenerative purposes should allow for preferential invasion of desired cell-types that would aid in replacing the temporary scaffold with the desired site-specific tissue [250]. One would wish to be able to tailor the hydrogels such that only target cell types invade in order to ensure optimal cellular functioning [295]. Bracher et al. (2013) found that depending on which enzymatically degradable sequence/s one incorporates into

the hydrogel, one can intentionally encourage the invasion of specific cell types into the scaffold. By using a peptide recognised and cleaved by MMP-14, smooth muscle invasion was more pronounced than that of fibroblasts [250]. By altering the amounts of MMP-9 recognised peptide to a peptide sequence recognised by multiple MMPs (PAN-MMP), cellular invasion was controlled *in vitro* in a spheroid sprouting assay, as well as *in vivo* [120].

1.3.1. A novel, multi-modal approach to degradation

Based on the work by Kim et al. (2016), we now wanted to investigate whether we could employ 8-arm PEG hydrogels to control cellular invasion using a novel, multi-modal degradation system involving hydrogels that are both enzymatically and hydrolytically degradable [258]. A drawback of fully hydrolytically degradable gels is that this bulk degradation is not cell-driven, i.e. through their migration and movement into the scaffold. Thus many researchers turned away from hydrolytically degradable gels to investigate enzymatically degradable gels for tissue regeneration [120]. However, if one can combine hydrolytically degradable components with enzymatically degradable components, one should be able to solve this issue of degradation that is not cell-directed. There is then the potential to control cellular invasion and degradation by altering the molar ratios of hydrolytically degradable components to enzymatically degradable components. Zhu et al. (2015) state that "biomaterial degradation theoretically should be aligned with the pace of cell infiltration and neo-tissue formation to allow the structural and functional integration of host tissue with tissue developed in the region of the implanted biomaterial" [298]. For example, in the context of biodegradable arterial stents, there is a desire to create a stent that persists for a sufficient period to allow for vascular wall remodelling, but if the stent persists slightly passed this point complications begin to arise [299,300]. Thus, it would be ideal if one could tailor the degradation of the biomaterial to the milieu of interest.

Our group has previously shown that one can modulate fibroblast and smooth muscle cell invasion rate in our PEG gels [250]. We have also shown that we can control which cell types invade and can degrade our PEG hydrogels by utilising cell-type specific MMP sequences [120]. However, to the best of our knowledge, no other group has employed a multi-modal degradation approach to controlling PEG hydrogel degradation and cell invasion [301].

1.3.1.1. Multi-modal hydrogel chemistry

These hydrogels incorporate the integrin-binding sequence RGD and consist of 8-arm PEG monomers functionalised with both vinyl sulfone and acrylate end-groups. As described in the previous section, the cross-linking of these hydrogels involves the binding of PEG-Ac monomers with thiol groups within the bis-cysteine residues of MMP-recognition peptides forming thioether ester bonds [247,254,255]. Like with the 4-arm gels discussed in the previous chapter, the PEG-VS monomers are also joined to the thiol-containing peptides but by a thioether sulfone bond, which is very stable [260]. The ester bonds between the PEG-Ac and the peptide can be broken hydrolytically and would thus be broken first. As this occurs, more and more water enters the gels, further increasing the hydrolytic breakage of bonds [254,259]. As the PEG-Ac monomers come away, so a network of PEG-VS is left behind that can only be enzymatically cleaved at the MMP peptide sequences.

The premise is that upon injection *in vivo*, the initial structural support needed would be provided, but hydrolytic degradation throughout the bulk of the hydrogel would facilitate cell-directed enzymatic breakdown and thus potentially more rapid cellular invasion would occur as the hydrolytically degradable component increases.

Considering all the above, multi-modal degradation may be an attractive approach to tissue regenerative scaffolds. Hypothetically, it should allow one to combine the benefits that come with both hydrolytic and enzymatically degradable gels, thus creating a scaffold which one can exert considerable control over, creating gels even more suited to specific regenerative purposes. For example, in the context of wound healing, if dermal grafts degrade too quickly, undesired fibrosis takes place rather than a more regenerative form of tissue replacement [302]. Thus ,the potential tunability of the breakdown and replacement by tissue of this novel hydrogel could allow for its use in many other therapeutic situations, not just in the context of myocardial infarction and the cardiovascular system [258].

1.4. Study aims

The injectable PEG hydrogel system described above has significant promise as a scaffold for regenerative therapies.

The aims of this project were directed toward the optimisation of two critical aspects of the hydrogels as related to their regenerative potential:

1. The ability to bind and release growth factors bFGF, VEGF and PlGF-2 in a sustained, controlled manner and how this impacts the ability to stimulate angiogenesis. Here the hydrogel was to be modified by the covalent addition of heparin, and the effects assessed by establishing a suitable *in vitro* angiogenesis assay.

2. The degradation rate, and thus replacement by tissue *in vivo*. The effect of modification by exploiting both enzymatic and hydrolytic degradation was to be initially determined using the 3D *in vitro* assay developed in (1.), followed by analysis in a subcutaneous implant model in the rat.

2. Results and Discussion

2.1. Studies towards establishing an *in vitro* angiogenesis screening model

Optimising the angiogenic response within regenerative scaffolds is critical. Thus, the utility of a cell spheroid-based 3D *in vitro* angiogenesis assay was investigated as a means of analysing the efficacy of modifications that have and will be made to the PEG hydrogel system used in our laboratory. After experiments directed towards establishing an *in vitro* assay were completed, an attempt to assay a recent modification, namely the covalent addition of heparin into the PEG hydrogel, was carried out.

2.1.1. Rheological analysis of 4-arm 20 kDa PEG-VS hydrogels

The viscoelastic properties of 4-arm 20 kDa hydrogels were determined by small strain oscillatory shear rheometry. These hydrogels were formed by cross-linking PEG-VS monomers with MMP-1 recognition peptides. Prior to utilisation in an *in vitro* angiogenesis assay, the stiffness and hydrogel-like nature of the hydrogels needed to be established.

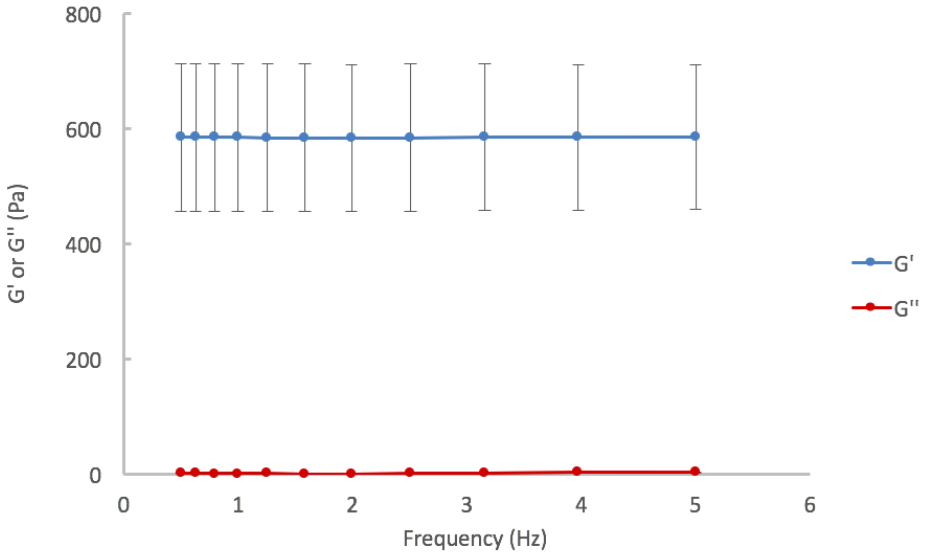

Figure 5: Rheological analysis of 3.5% 4-arm PEG-VS hydrogels. *Frequency sweep from 0.5 – 5 Hz showing both elastic (G') and viscous (G'') components. Results are here represented as mean ± SD, n = 9 hydrogels.*

The average storage modulus (G') for 3.5% 4-arm 20 kDa hydrogels was found to be 557 ± 107 Pa. This storage modulus obtained was somewhat higher than that which our group

previously obtained for the same hydrogel formulation of 254 ± 8 Pa [120]. It is hypothesised this may be indicative of batch variation for the PEG-VS monomer used. Although not possible to empirically test, as only one batch of each was available for this study, reports in the very limited literature available on rheological data for this type of hydrogel suggest this to be a plausible explanation and also indicate significant variance in storage moduli for similar hydrogel formulations [246]. A storage modulus of 290 ± 18 Pa was previously reported for a 10% 4-arm 20 kDa PEG-VS hydrogel containing RGD (unlike the hydrogels analysed here which did not contain RGD) and similarly cross-linked with a MMP-recognition peptide by the Hubbell group [303]. However, the Shikanov group reported a modulus of 3.8 kPa for a 5% 4-arm 20 kDa PEG-VS hydrogel crosslinked with a plasmin recognition sequence [258]. In the latter study, influence of this alternative cross-linking sequence may have played a role. It should be here noted that the MMP-1 recognition sequence used by the Hubbell only has a 2 amino acid difference when compared to that used in this study [262], suggesting this difference is unlikely to be a cause for the difference observed. Most importantly, the impact of removing crosslinking sites by blocking 12% of VS sites using l-Cysteine was found to substantially reduce G' from 3.8 kPa to 1.6 kPa in the Shikanov study [258]. This suggests that even minor reductions in modification levels of the PEG monomer termini with vinyl sulfones may be, in part, responsible for the discrepancies observed. Further detailed investigations to determine the precise cause are needed. For the purpose of this study, this was not necessary as only one batch of PEG-VS and one batch of MMP-recognition peptide were used throughout the duration.

Frequency sweeps for these hydrogels showed G' to be stable across the range from 0.5 – 5 Hz (Figure 5), confirming their hydrogel-like nature. Storage modulus is often nearly independent of frequency when the material tested is more hydrogel-like or solid in form, whilst a frequency-dependent storage modulus is characteristic of a more fluid-like material [304]. The gelled state of these viscoelastic materials was further confirmed by G' being orders of magnitude larger than the loss moduli, G'' [304,305].

Thus, the biomechanical properties of the hydrogel were established and the hydrogel was found to display hydrogel-like characteristics, allowing for progression to their utilisation in *in vitro* angiogenesis assays.

2.1.2. Characterisation of isolated human umbilical vein endothelial cells (HUVECs)

An *in vitro* angiogenesis assay requires the use of endothelial cells. Thus, prior to establishment of an appropriate assay which would allow for analysis of the angiogenic response in the synthetic PEG hydrogels, an isolation method for primary HUVECs needed to be set up in our laboratory.

HUVECs are considered one of the optimal cell types for use in angiogenic models, with Maruyama being the first to cannulate the umbilical vein and isolate primary endothelial cells [306,307]. Jaffe et al. (1973) then adapted this protocol to use collagenase instead of trypsin, and successfully propagated endothelial cells *in vitro*. This is now widely cited as the standard isolation protocol, with researchers adapting it slightly to suit their needs [308]. Advantages of utilising umbilical cord tissue include the fact that it is a readily available source, and that there are no ethical issues around the isolation of cells from tissue that would otherwise usually be discarded as waste. The tissue is easy to collect, without the need for any invasive procedures [309].

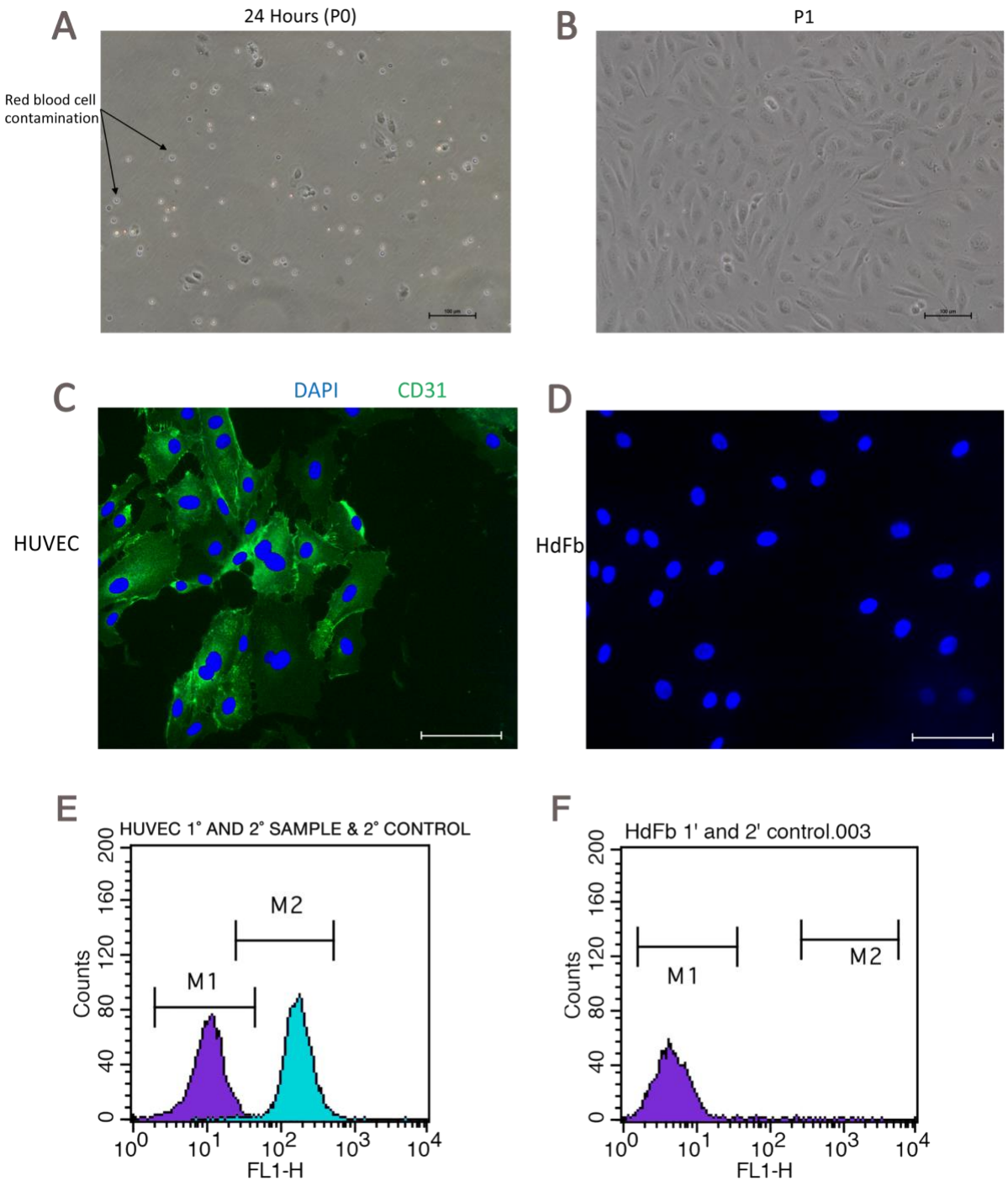

Figure 6: Assessment of endothelial nature of isolated cells. *Bright field micrographs showing morphology of isolated HUVECs after A) 24 hours, with slight red blood cell contamination. B) Cells at Passage 1 exhibiting the typical cobblestone morphology of endothelial cells. C & D) Immunocytochemical staining of HUVECs with anti-CD31 antibodies. Cells counterstained with DAPI. Human dermal fibroblasts (HdFbs) were used as a negative control. Scale bar = 100 µm. Flow cytometric analysis of isolated HUVECs: histograms showing E) secondary (2°) antibody control (2° antibody alone, purple peak) and the primary (1°) and 2° antibody sample (1° and 2°, turquoise peak), and F) HdFb negative control.*

A mixture of both larger cells and smaller, biconcave cells are visible on a micrograph from 24 hours after isolation (Figure 6A). The latter are red blood cells that are flushed out of the vein during isolation, but these blood cell contaminants are removed during media changes. After 3-4 days, the cells reach confluency and can be passaged. Upon approaching confluency, as seen for cells at P1 (Figure 6B), the cells start to have the typical cobblestone patterning indicative of ECs when cultured in a monolayer [310,311], suggestive of a successful EC isolation.

This observation required corroboration and extension by assaying the cells for the presence of a surface antigen expressed by ECs, namely Cluster of Differentiation 31 (CD31), by immunocytochemistry and flow cytometry. Immunocytochemical staining was conducted using a mouse primary antibody against human CD31. The secondary antibody used (goat anti-mouse) conjugated with a fluorochrome (Alexa Fluor 488). Thus, the cells showing green fluorescence in Figure 6C above could be identified as CD31-positive HUVECS. To confirm this, human dermal fibroblasts (HdFbs) were used as a negative control, as they do not express CD31. As expected, no green fluorescence was present (Figure 6D). This expression of CD31 was further confirmed by flow cytometric analysis. A clear shift in fluorescence intensity (FL1-H) can be seen between the isotype (secondary antibody) control and the sample stained with primary and secondary antibodies (Figure 6E), confirming the high percentage of cells that were CD31 positive. Here HdFbs were again used as a negative control and produced a peak like that of the isotype control, showing no CD31 was present (Figure 6F).

2.1.3. Establishing a spheroid sprouting assay as an *in vitro* angiogenesis assay within the context of synthetic PEG hydrogels

As these synthetic hydrogels, which mimic the ECM, have been and will be used extensively in regenerative medicine, a detailed understanding of the angiogenic response to them will facilitate their development as regenerative scaffolds. Furthermore, due to their defined nature, they can be extensively tuned to determine the influence that parameters such as stiffness, cell adhesion site density and degradability, have on angiogenesis in combination with pro-angiogenic growth factors.

Spheroid sprouting assays, as aforementioned, involve the formation of cell spheroids by addition of cells to a viscous methylcellulose-containing medium and incubation for 24 hours in round bottom, non-adherent culture wells. The spheroids formed are then suspended in a 3D environment (most commonly collagen or fibrin hydrogels) and allowed to sprout in response to pro-angiogenic stimuli [110]. Spheroid-based assays are a widely used method of assaying angiogenic responses *in vitro* in a manner that is more representative of *in vivo* responses than 2D methods [105,108]. Conducting an assay in 3D allows the endothelial cells to maintain a phenotype more like that seen *in vivo* [312–314].

Thus, this assay was chosen to establish an *in vitro* angiogenic assay in the context of our specific synthetic PEG hydrogel, which could then used to study the angiogenic response to three growth factors of interest – VEGF, bFGF and PlGF-2 [172] – the latter of which does not possess clearly established angiogenic potential [148,166,169]. Our group has previously explored the use of a 3D spheroid assay in the context of fibroblast and smooth muscle cell invasion into enzymatically degradable synthetic PEG hydrogels [120,250]. However, to our knowledge, an angiogenesis spheroid-based assay has not been established for the PEG hydrogel.

2.1.3.1. Trouble shooting

In establishing this assay with endothelial cells, a substantial amount of trouble shooting had to first be carried out before the effects of the growth factors could be analysed. VEGF and bFGF are widely known in the literature to elicit endothelial cell sprouting, thus these growth factors were used to assess the potential of this assay in the context of this PEG hydrogel. Because there are conflicting findings in the literature surrounding the sprouting response elicited by PlGF-2, this growth factor was also assayed to determine whether further insight into its *in vitro* angiogenic potential could be gained [148,166,169].

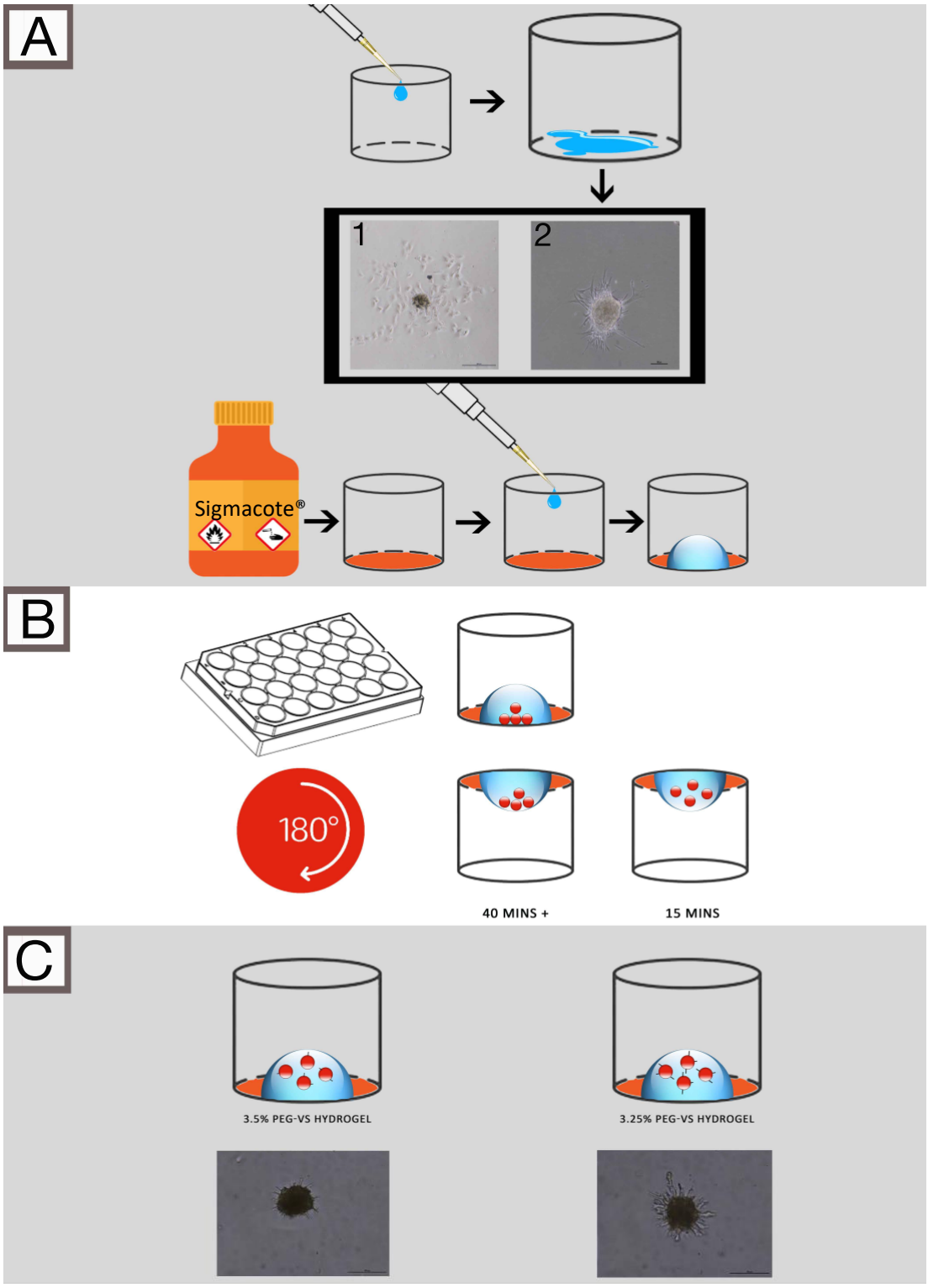

***Figure 7: HUVEC spheroid sprouting assay trouble shooting**. A) The charge of the tissue culture-treated surface caused hydrogels to spread excessively across the surface, substantially reducing the depth of the hydrogel droplet. This caused 1) spheroids to break apart (scale bar = 500 µm) or 2) cells to spread along the bottom of the well. Using Sigmacote® rendered the surface hydrophobic and allowed hydrogels to bead, forming domes of greater depth (scale bar = 100 µm). B) Spheroids sank to the bottom of the hydrogel during polymerisation at 37 °C, creating sprouting artefacts. Inverting the 24-well plate for longer than 15 minutes, the spheroids would fall to the surface of the hydrogel, preventing sprouting. C) Altering the concentration of PEG in the hydrogel from 3.5% (m/v) to 3.25% resulted in improved sprouting (scale bar = 100 µm).*

Due to the hydrophilicity of tissue culture treated plates, pre-polymerised PEG solutions tended to spread excessively prior to gelation [315] (Figure 7A). This resulted in the hydrogels flattening out in the well, causing the spheroids to sink to the bottom of the hydrogel, touching the bottom of the plate and thus breaking apart into single cells as the cells begin to spread (Figure 7A.1). In less extreme cases, this causes broad sprouts to form and spread along the bottom of the plate, rather than within the hydrogel itself (Figure 7A.2). A dome-shape hydrogel is preferred as it enables most spheroids to be surrounded by gel, creating a 3D environment with more vertical room for sprouting. To prevent spreading, the 24-well plate was siliconised by pre-coating with Sigmacote® (Figure 7A). This altered the surface charge, making the surface hydrophobic, reducing wettability and allowing a high contact angle to form with the resultant hydrogel droplet [316,317]

Although formation of dome shaped hydrogels did allow for more vertical space for spheroids to descend through while the gels set, the spheroids would still tend to sink to the bottom and, as above, cause cells to spread along the bottom of the plate instead of within the hydrogel. Inversion of the plate while the gels were setting (Figure 7.B) was investigated as a means of keeping spheroids remote from the plate surface. However, if the plate was inverted for too long, the spheroids all fell to the top of the hydrogel, with some breaching the apical surface. This again hindered sprouting and cracked the hydrogel (Figure 8). It was found that if the plate was inverted for no more than 15 minutes and then reverted, the spheroids did not fall to the apical surface of the hydrogel and were well distributed within the hydrogel (Figure 7B).

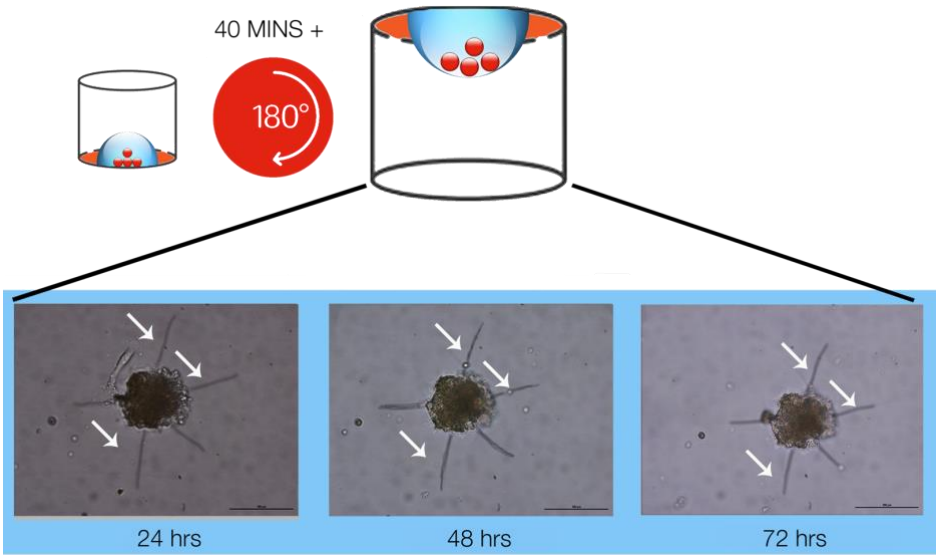

Figure 8: Consequence of inverting spheroid hydrogels for 40 minutes or more. *Micrographs taken at 24, 48 and 72 hours showing no spheroid sprouting. White arrows indicate cracks in the hydrogel caused by the spheroid breaching the hydrogel surface.*

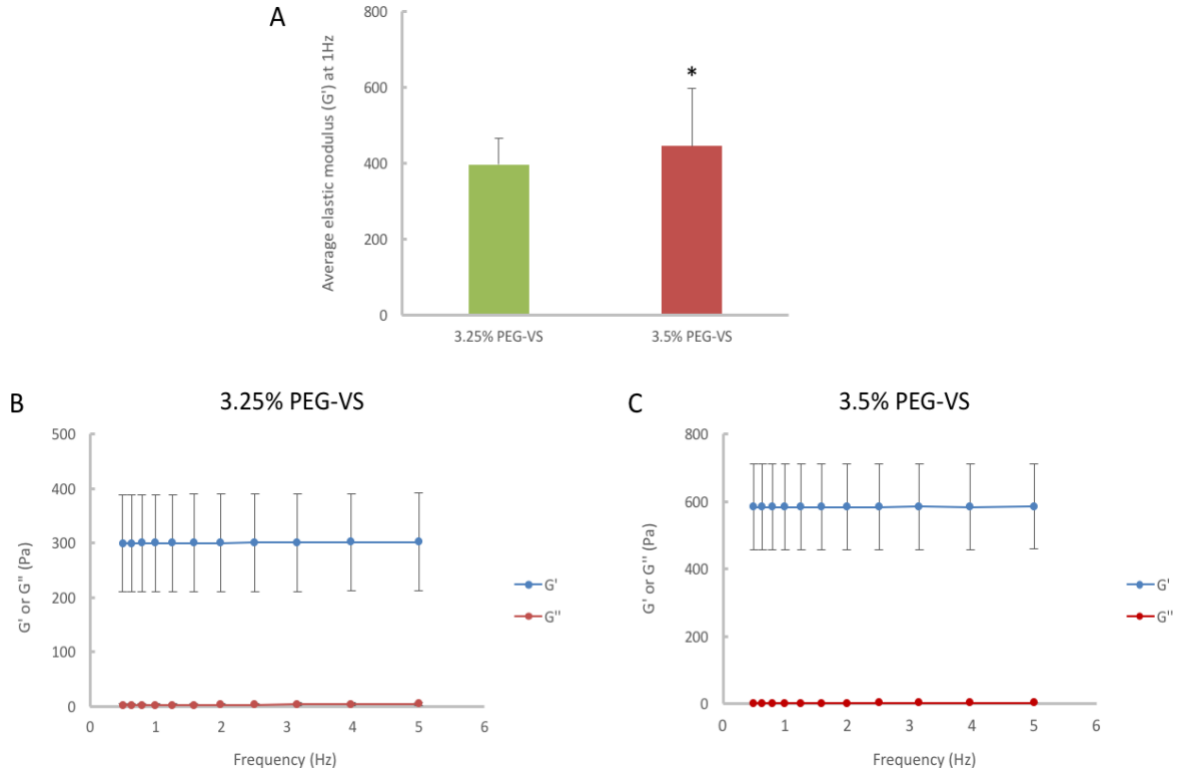

Figure 9: Rheological analysis of 3.25% and 3.5% PEG-VS hydrogels. *A) Comparison of storage moduli of 3.25% PEG-VS hydrogels and the 3.5% PEG-VS hydrogels. Frequency sweeps from 0.5 – 5 Hz showing both elastic (G') and viscous (G'') components for B) 3.25% PEG-VS hydrogels and C) 3.5% PEG-VS hydrogels. Results are here represented as mean ± SD. $p < 0.05$, n=5.*

Initially, sprouting was conducted in the enzymatically degradable 3.5% 4-arm PEG-VS hydrogels that underwent rheological analysis as shown in Figure 5. At this concentration, limited sprouting was observed. A reduction in the PEG concentration to 3.25% (m/v) was then investigated. This was found to be the optimal percentage for sprout length and now allowed the majority of spheroids to sprout (Figure 7C). It is to be noted that hydrogels containing less than 3.25% PEG-VS would not polymerise and, thus, could not be utilised in this assay.

Rheological analyses were conducted on these 3.25% and 3.5% PEG-VS hydrogels (Figure 9). There was a significant difference ($p = 0.02$) in stiffness between the non-heparinised 3.5% and 3.25% PEG-VS hydrogels (average G' of 445 ± 151 Pa versus 397 Pa ± 69, respectively, $n = 5$). This result is as one would expect – the addition of 0.25% less PEG-VS meant that fewer crosslinks were formed within the hydrogel per unit volume, thus hydrogel stiffness decreased, explaining the improvement in endothelial sprouting seen (Figure 7C). This was the last step in establishing this assay.

2.1.3.2. Ability of HUVEC spheroid assay to detect angiogenic responses in PEG-VS hydrogels

Initial experiments found that if spheroids were incubated for longer than 72 hours, the sprouts would begin to break apart, making analysis challenging (Figure 10).

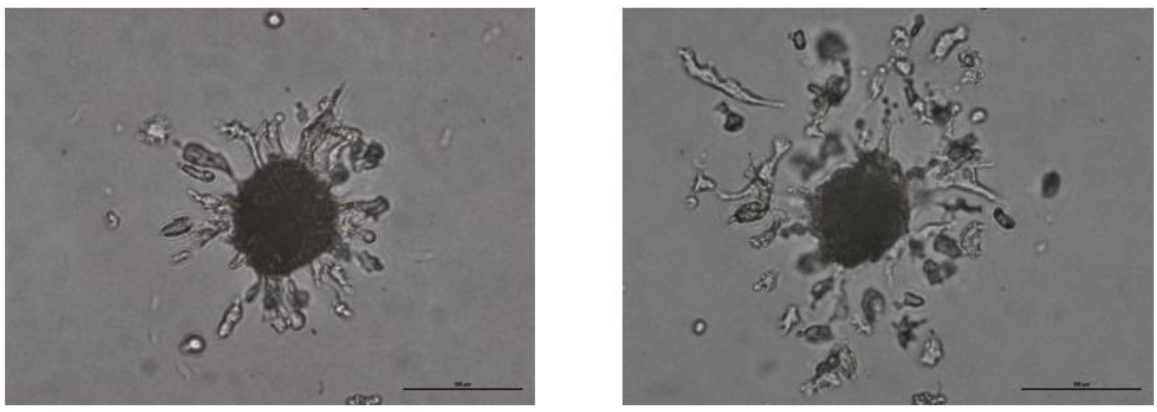

***Figure 10: Spheroid sprout disruption occurs at 96 hours**: Micrographs (20x mag) obtained at 24 and 96 hours of the same spheroid show sprouts begin to break apart, hindering analysis. Scale bar = 100 µm.*

Therefore, it was decided that 72 hours was the time point chosen for image analysis as the differences were most pronounced at this time point relative to the control. The angiogenic response to the three growth factors of interest – bFGF, VEGF and PlGF-2 – at 72 hours is presented in Figure 11. All spheroids were of a similar size (approximately 100 µm diameter) and similar round shape, with a very defined edge. By 72 hours, the bFGF- and VEGF-treated spheroids had the longest and most numerous sprouts (Figure 11). PlGF-2, at 40 ng/ml and 100 ng/ml, did elicit sprout growth. However, this response appeared very similar to that seen in the control (10% FBS, no growth factors) spheroids. Average cumulative sprout length per spheroid and average sprout number per spheroid were the two metrics used to assess the angiogenic response. All spheroids present within each hydrogel were included in the analysis, except those at the very edge/bottom of the hydrogel, or those that were close to other spheroids/had clumped together. This is because spheroids in these locations may have a different number and length of sprouts, as well as a different sprout orientation which may complicate analysis [116].

In the majority of literature reporting on angiogenic outcomes of EC spheroid sprouting in hydrogels, if reported, 5-10 spheroids are considered per treatment group [109,111,116,318–321]. A recent study by the original developers of the assay indicated that there is inherent variability in the assay [109]. Thus, the following approach was taken to determine that a reproducible angiogenic response was being observed. A total of 6-12 spheroids per group were assayed in 3 sequential experiments. A verified angiogenic response would be one that was found to be significant across all 3 biological repeats.

At 72 hours, bFGF and VEGF both elicited a significant response ($p \leq 0.01$) across all three biological repeats compared to the control, for average cumulative sprout length per spheroid (Figure 11). bFGF elicited average cumulative sprout lengths of 593 ± 277 µm, 403 ± 164 µm and 1167.9 ± 309 µm for Experiments 1-3. These cumulative sprout lengths were an average of 4-fold higher than the control, which exhibited average cumulative sprout lengths of 206 ± 113 µm, 133 ± 64 µm and 222 ± 112 µm for Experiments 1-3. VEGF also elicited relative increases in average cumulative sprout lengths with lengths of 549 ± 207 µm, 470 ± 249 µm and 1367 ± 350 µm for Experiments 1-3. Therefore, on the same weight basis, bFGF and VEGF

elicited virtually identical responses, with around 4-fold increases in average cumulative sprout length.

Regarding the number of sprouts per spheroid, bFGF-stimulated spheroids had average sprout numbers per spheroid of 19 ± 6, 13 ± 5 and 20 ± 3 for Experiments 1-3 respectively. This was an average of 2.3-fold more sprouts than the control (average sprout numbers of 10 ± 4, 6 ± 3 and 7 ± 2 were recorded for Experiments 1-3 respectively) and was significant for each biological repeat ($p<0.01$). Again, VEGF followed a similar trend with average sprout numbers per spheroid of 16 ± 4, 14 ± 6 and 22 ± 4 for Experiments 1-3 respectively. This was an average of 2.4-fold more sprouts than the control and was again significant ($p<0.01$). Therefore, with respect to average number of sprouts per spheroid as well, bFGF and VEGF elicited an almost identical response.

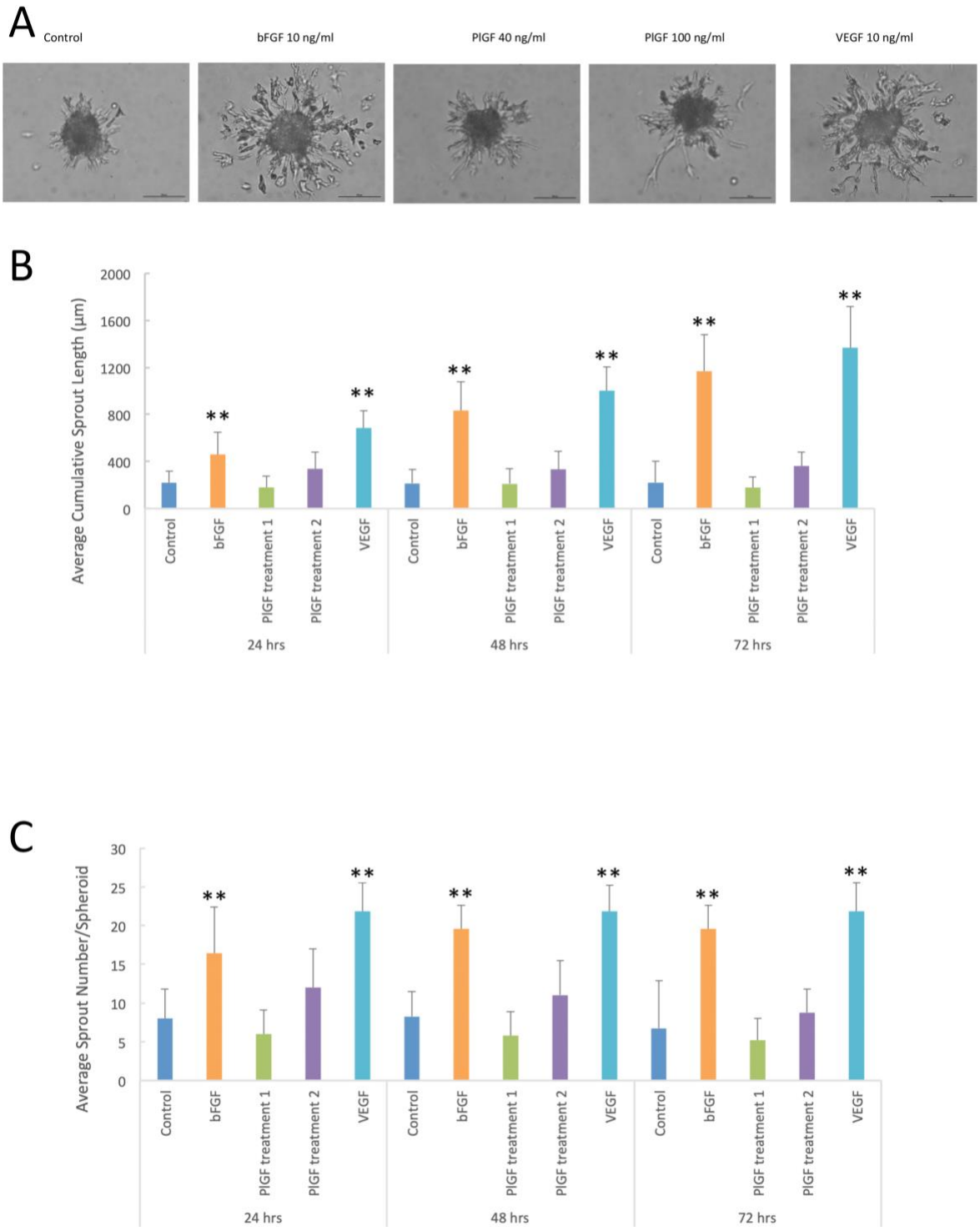

Figure 11: Spheroid sprouting assay with HUVECs. A) Micrographs showing HUVECs (single donour) sprouting over 72 hours. *Scale bar = 100 µm. Analysis of spheroid sprouting assays with HUVECs (P3-P5) from multiple donours. B) Average cumulative sprout length (µm) at 72 hours. C) Average sprout number per spheroid at 72 hours. For both B) and C) all growth factor concentrations were as follows: bFGF (10 ng/ml); PlGF treatment 1 (40 ng/ml); PlGF treatment 2 (100 ng/ml); VEGF (10 ng/ml). All treatments contained 10% FBS, including the growth factor-free control. ** = p ≤ 0.01 when compared to respective controls. Results are here represented as mean ± SD, n = 6-12.*

Where 3D spheroid-based angiogenesis assays have been used to directly assess the influence of VEGF and bFGF, the 3D matrix has been collagen at a concentration of 2 mg/ml. In this matrix, bFGF has been found to induce a 3-fold increase in cumulative sprout length after 24 hours at a concentration of 25 ng/ml (2.5 times higher than that employed here) [322] and up to 6-fold after 72 hours at 30 ng/ml [323]. More extensive but still limited data is available for VEGF. VEGF was found to increase cumulative sprout length by 2.5-fold after 24 hours [322] and around 3.5-fold after 72 hours at 25 and 50 ng/ml, respectively [323]. These concentrations are also higher than those used here but in a study that investigated the influence of VEGF concentration directly, concentrations from 8 – 642 ng/ml were found to induce similar response at 24 hours of around 2.5-fold relative to control [109]. Thus, for VEGF and bFGF similar relative increases in sprout length have been observed in collagen as were seen in PEG hydrogels here. The absolute responses were more with sprout lengths of around 800 - 1000 µm in 24 hours that increased to 1750 µm and 2750 µm for VEGF and bFGF respectively at 72 hours.

The slightly greater extent of sprouting often seen in collagen hydrogels is most likely the result of the lower stiffness of these types of hydrogels – 17 - 100 Pa for collagen [324–326], compared to the storage modulus of 397 ±69 Pa for the PEG-VS hydrogels used here. This is further reiterated by the fact that sprouting was substantially hindered in the 3.5% PEG-VS hydrogels, but by reducing the PEG concentration by 0.25%, and in turn the storage modulus, sprouting was improved. Mesh size may also play a role – with collagen having much higher mesh sizes of 15 µm on average, but can range from 1 - 20 µm [327] relative to the 20 nm of the PEG hydrogels [250]. The mesh sizes in the above natural hydrogels approximate that of cellular dimensions, which may allow for cells to move through these hydrogels by both mechanical and proteolytic means, whilst cellular invasion into the PEG hydrogels is entirely dependent on proteolysis [276].

Unlike bFGF and VEGF, neither of the two PlGF-2 treatments (40 ng/ml and 100 ng/ml) elicited average cumulative sprout lengths or average sprout numbers that were significant when compared to the control. The two different PlGF-2 concentrations used were based on the following literature: Hoffmann et al. (2013) found 40 ng/ml of PlGF-2 to significantly increase cumulative sprout length and sprout number in a spheroid-based angiogenesis assay in collagen. This same group conducted a HUVEC migration assay and found PlGF-2 (100 ng/ml)

stimulated almost as many cells to migrate as VEGF at the same concentration [328]. Thus, these two concentrations were tested.

Average cumulative sprout lengths of 290 ±98 µm, 174 ±163 µm and 179 ±87 µm were found for each experiment respectively with PlGF-2 at 40 ng/ml. PlGF-2 at 100 ng/ml elicited average cumulative sprout lengths of 326 ±77 µm, 198 ±76 µm and 362 ±120 µm, respectively. On average, the average cumulative sprout length of the 40 ng/ml treatment sprouts was only 1.2 times that of the control, and the average cumulative length of the 100 ng/ml treatment sprouts was only 1.6 times that of the control. The 40 ng/ml treatment generated average sprout numbers of 12 ±3, 8 ±3 and 5 ±3 per spheroid for Experiments 1-3 respectively. Similarly, the 100 ng/ml treatment generated average sprout numbers per spheroid of 15 ±2, 9 ±3 and 9 ±3. On average, the average sprout number per spheroid for the 40 ng/ml treatment sprouts was only 1.1 times the that of the control, and the average sprout number per spheroid for the 100 ng/ml treatment sprouts was only 1.4 times that of the control. None of these responses to the two PlGF-2 concentrations were significantly increased versus the control, but slight increases coupled with the increases observed as the PlGF-2 concentration increased, are suggestive of a slight angiogenic response. However, this may be below the range of sensitivity of the assay.

Hoffmann et al. (2013) conducted HUVEC sprouting assays but in collagen hydrogels (2 mg/ml) and only for a duration of 24 hours. This experiment showed that spheroids treated with their recombinant PlGF-2 (at 40 ng/ml) produced a significant increase in sprout length of about 2-fold, although it was less pronounced than that observed for VEGF where 3-fold increases were seen [328]. For sprout number a significant increase almost equivalent to VEGF was found. This far more robust response further suggests a possible impact of the PEG hydrogel's greater stiffness and smaller mesh size, although it is not immediately apparent why PlGF-2 should be individually impacted. Some have also seen no *in vitro* angiogenic response to PlGF-2 [166,169], further emphasising the wide range of response reported in the literature. More in depth studies need to be conducted to investigate this.

Thus, the *in vitro* angiogenesis assay utilising HUVEC spheroid sprouting has shown promise in detecting angiogenic responses in synthetic 4-arm PEG-VS hydrogels. This is important, as it should allow for future fine-tuning of these types of hydrogels for regenerative medicine

strategies. However, the assay does demonstrate a run-run variability which is undesirable. One manner in which to reduce this variability in future is through the use of immortalised HUVECs (iHUVECS) in generating spheroids. Heiss et al. (2015) showed that these cells displayed less variability in terms of spheroid sprouting, even over multiple population doublings, improving the robustness of the assay [109].

2.1.4. Controlled Release of Growth Factors from 4-arm PEG hydrogels

Our group has recently established a method of covalently attaching heparin into the PEG hydrogels [254]. We now wished to utilise the spheroid assay to investigate the influence of the attached heparin on the angiogenic potential of the above growth factors.

Heparin was acrylated on the secondary hydroxyls of the polysaccharide with on average 30-40% of the glucosamine containing disaccharides undergoing acrylation [254]. This acrylated heparin can then be coupled into the PEG hydrogel by a Michael addition reaction via the sulfhydryl containing peptides used for crosslinking. Prior to analysing the heparin containing 4-arm monomer PEG hydrogels in the angiogenesis assay, it was considered prudent to confirm their ability to entrap and release heparin binding growth factors. This has been shown by our group for VEGF and bFGF with the 8-arm monomer hydrogels [261] but not the 4-arm hydrogels. Additionally, PlGF-2 had not been previously assessed in the context of heparinised PEG hydrogels.

To determine VEGF, bFGF and PlGF-2 release from heparinised and non-heparinised hydrogels, growth factors were added to the hydrogel constituent mixtures prior to polymerisation. Each growth factor was loaded individually. bFGF and PlGF-2 were also loaded as a combination to test the effect of adding multiple factors. Once the hydrogels had set, they were washed to remove unbound growth factor and placed into iso-PBS. The elution rate of growth factors was quantified using ELISA over 20 days.

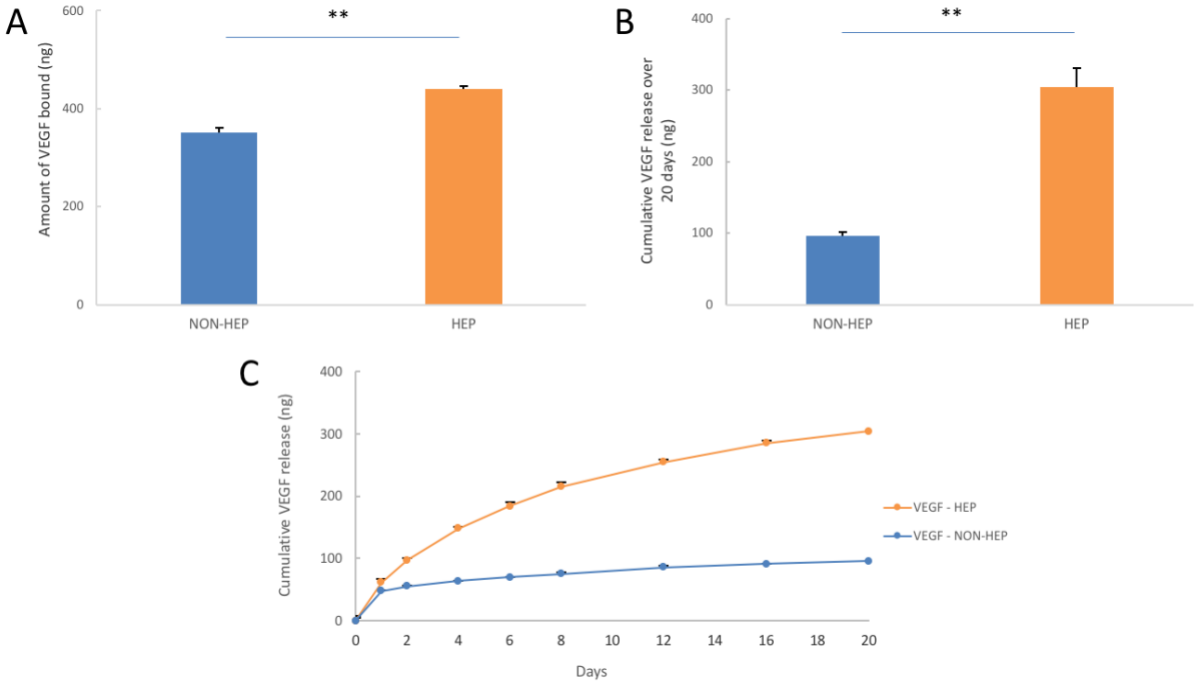

Figure 12: VEGF release from 4-arm PEG-VS hydrogels. *A) Comparison of total amount of VEGF (ng) bound to heparinised versus non-heparinised hydrogels. B) Comparison of total amount of VEGF released (ng) from heparinised and non-heparinised hydrogels. C) Cumulative release profile (ng) for VEGF over 20 days. Results are here represented as mean ± SD; n=4 gels per gel type. ** = p<0.01*

Error! Reference source not found.A above shows that, of the 500 ng VEGF added to each hydrogel, significantly more bound to the heparinised hydrogels (439 ±7 ng), as compared to the non-heparinised hydrogels (350 ±10 ng, $p<0.01$). The heparinised and non-heparinised hydrogels released 61 ±5 ng and 48 ± 8 ng, respectively, within the first day (**Error! Reference source not found.**C). This equates to 13.7% of the total VEGF bound (heparinised), and 13.9% of the total VEGF bound (non-heparinised), being released. Thereafter, the non-heparinised hydrogels only released an average of 2.5 ng each day until Day 20. This can be seen as the release curve flattens after Day 1. Conversely, the heparinised hydrogels released a relatively steady amount of VEGF each day, with a daily average of 12.7 ng of VEGF released until Day 20. The heparinised hydrogels released significantly more VEGF than the non-heparinised hydrogels ($p<0.01$) over the 20 days (**Error! Reference source not found.**B), with a total of 304 ± 27 ng being released (61% of total VEGF added) versus 96 ±6 ng (19% of total VEGF added), respectively. This is favourable as it shows heparin can be employed to improve both the binding and the controlled release of VEGF from these particular hydrogels.

The binding of VEGF to PEG hydrogels has been previously investigated by our laboratory in collaboration with the Hubbell group [122]. Initially, it had been surmised that only mutant VEGF constructs containing unpaired cysteines would be able to couple into the PEG backbone. Surprisingly however, it was found that native $VEGF_{165}$ could couple almost as efficiently [122].

It has been postulated that the unaltered VEGF could potentially bind to PEG-VS via its thiol-containing cysteine residues although these exist as disulphide cysteines [254,329]. The resultant thioether-sulfone bond would be very stable, and would thus not facilitate growth factor release until the VEGF is released by enzymatic cleavage [257,330]. A concern therefore exists that some structural alterations may result from the permanent coupling of a PEG molecule to a critical residue such as cysteine. This concern was part of the rationale behind introducing heparin within the PEG-VS hydrogels. But more importantly, it was hypothesized that this type of binding would allow for a greater chemotactic effect to be generated with VEGF being bound into the hydrogel in a manner analogous to that in which it is incorporated into the extracellular matrix [331,332].

The interaction between heparin and growth factors like VEGF is electrostatic – there exist electrostatic forces between the –N and –O sulphated groups within the heparin and the amino acid residues lysine and arginine within the growth factors. This electrostatic interaction enables a more pronounced growth factor release as the interaction is not indefinitely stable, as the formation or dissociation of these interactions is influenced by a thermodynamic equilibrium [333]. The fact that the heparin used in these hydrogels is acrylated further facilitates growth factor release via hydrolysis of the hydrolytically vulnerable ester bond. Such that when the heparin detaches from the PEG through hydrolysis, so does the growth factor, allowing for its release in a heparin/growth factor complex [254,259]. The use of heparin to bind the growth factors is further advantageous in that it mimics the physiological milieu – in the body, growth factors are sequestered in the ECM by glycosaminoglycans, thus controlling their local concentration, diffusion, degradation, involvement in cell signalling and enhancing their bioactivity [334]. This controlled release plays an important role in orchestrating tissue repair and regeneration [335]. Because hydrogels already emulate the aqueous nature and mechanical properties of tissues in the body, the addition of heparin further enhances their mimicry, boosting their therapeutic

potential [336]. The above data also confirm our findings for the 8-arm PEG hydrogels [254] and indicates that, indeed, a more pronounced chemotactic effect could be achieved when used as a therapeutic angiogenesis vehicle.

After ascertaining that VEGF could be successfully bound to and released from the hydrogels in a controlled manner over 20 days, the binding of the other factors of interest, bFGF and PlGF-2, was investigated. Furthermore, the effect of combining two growth factors on the capacity for binding and release was assayed. This was achieved by creating hydrogels using 500 ng each of bFGF and PlGF-2 (combination hydrogels). It has been shown in the literature that dual delivery of angiogenic factors can elicit more beneficial responses [291,337].

Similarly to the binding seen with VEGF, significantly more bFGF bound to the heparinised hydrogels than the non-heparinised, for both the bFGF alone (436 ±17 ng versus 356 ±16 ng, $p<0.01$) and the bFGF/PlGF-2 combination treatments (429 ±3 ng versus 349 ±19 ng, $p<0.01$) (
Figure **13**A). There was no statistically significant difference in bFGF binding when added alone or in combination with PlGF-2 (p=NS). This leads to the conclusion that adding more than one growth factor may not significantly impact the total binding of individual factors. When considering bFGF release in
Figure **13**B, the non-heparinised hydrogels released 22 ±4 ng (bFGF alone) and 19 ±5 ng (bFGF in combination) on Day 1. Similarly, the heparinised hydrogels released 19 ±3 ng (bFGF alone) and 16 ±5 ng (bFGF in combination). However, as with the VEGF release seen in **Error! Reference source not found.**, much more bFGF was released from the heparinised gels (an average of 7 ng/day) compared to the non-heparinised (an average of 0.8 ng/day) over the following 19 days (
Figure **13**B and D). In total, heparinised hydrogels released 150 ±10 ng (bFGF alone) and 148 ±14 ng (bFGF combination), whereas non-heparinised hydrogels released 37 ±5 ng and 35 ±7 ng, respectively. On average, heparinised hydrogels released 30% of the total bFGF added, and non-heparinised gels released 7%. This again demonstrates the effect heparin has on enhancing binding and establishing controlled release, thus increasing chemotactic potential.

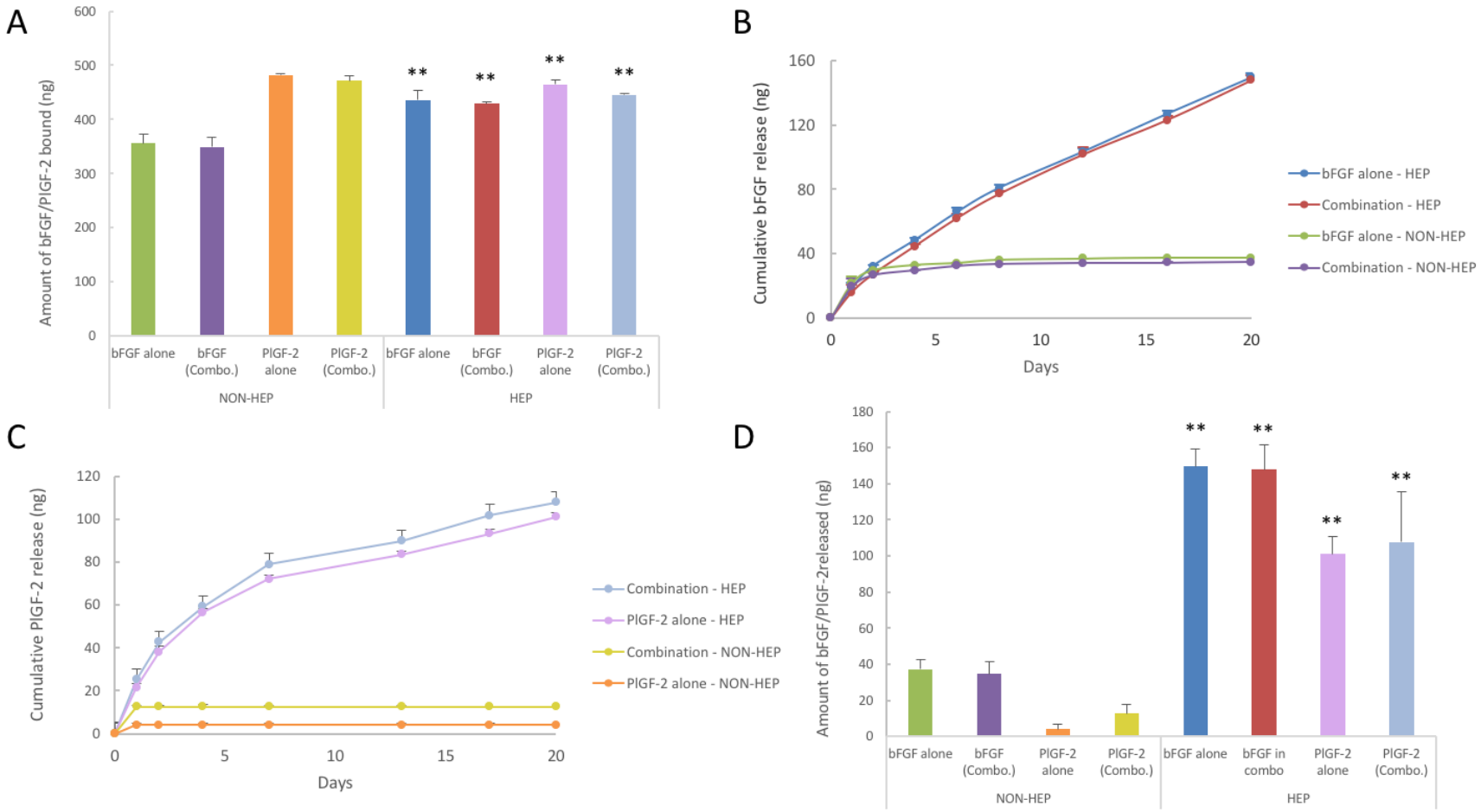

Figure 13: bFGF & PlGF-2 release from 4-arm PEG-VS hydrogels*. A) Total amount of growth factor bound to heparinised (Hep) versus non-heparinised (Non-hep) hydrogels when bFGF was added alone, and in combination (Combo.) with PlGF-2. Cumulative release profile for B) bFGF and C) PlGF-2 over 20 days. D) Comparison of total growth factor release from heparinised and non-heparinised hydrogels for bFGF alone and in combination with PlGF-2. Results are here represented as mean ± SD; n=4 gels per treatment. ** = p < 0.01 when compared to respective non-heparinised hydrogels.*

Surprisingly, unlike with VEGF and bFGF, the non-heparinised hydrogels bound a small but significant amount more PlGF-2 than the heparinised (
Figure **13**A). Non-heparinised hydrogels bound 482 ±3 ng (PlGF-2 alone) and 472 ±9.6 ng (PlGF-2 combination), whereas the heparinised hydrogels bound 465 ± 7 ng (PlGF-2 alone) and 445 ±3 ng (PlGF-2 combination). This might suggest that PlGF-2 may have more accessible cysteine residues. However, similar trends were seen with the cumulative PlGF-2 release from heparinised hydrogels (
Figure **13**C and D) when compared to VEGF and bFGF. Heparinised hydrogels released 101 ±10 ng (PlGF-2 alone) and 108 ±28 ng (PlGF-2 combination), which is an average of 21% release of the total PlGF-2 added. Non-heparinised hydrogels released much less: 4 ±3 ng (PlGF-2 alone) and 13 ±5 ng (PlGF-2 combination) on Day 1, which is only an average of 2% of the total PlGF-2 added. After Day 1, the non-heparinised hydrogels released no more PlGF-2 (
Figure **13**C). The heparinised hydrogels released an average of 4 ng/day over the remaining 19 days.

Despite the difference in binding between the heparinised and non-heparinised hydrogels, the heparinised hydrogels still released much more PlGF-2. The lack of release from the non-heparinised hydrogels is again postulated to be due to the probable covalent nature of the bonds formed between the PlGF-2 and the PEG-VS. Although heparin did not increase binding here as it did for the other growth factors, chemotactic potential is still enhanced due to increased release rate. This must also indicate that a portion of the PlGF-2 bound to heparin must have been sequestered away from binding via its cysteine residue to the vinyl sulfone moieties. The cumulative released amounts for bFGF and VEGF, where more is released from the heparinised hydrogels than the difference between the two hydrogels in total growth factor initially bound, also indicates this sequestration occurs with these growth factors.

Compared to the other releases from the heparinised hydrogels, the amount of PlGF-2 released was the least – 21% release versus 30% (bFGF) and 61% (VEGF). This could be because PlGF-2 binds to heparin/heparan sulfate with an extremely high affinity, with a K_D of approximately 1.5 nM [338]. As aforementioned, VEGF and bFGF have K_D values of 60.9 and 39 nM, respectively [339,340]. The binding of PlGF-2 to heparin has been shown to be so strong that Martino et al. (2014) fused PlGF-2's heparin binding domain onto VEGF, bone

morphogenetic protein-2 (BMP-2) and platelet-derived growth factor-BB (PDGF-BB). Thus, creating engineered growth factors with a "super affinity" for ECM proteins like heparan sulfate, increasing binding by 2- to 100-fold [339]. This may explain why the least amount of PlGF-2 was released when compared to the other factors. Therefore, it can be seen that, as growth factor affinity for heparin increases (VEGF affinity < bFGF affinity < PlGF-2 affinity), binding is enhanced (VEGF binding < bFGF binding < PlGF-2 binding) and growth factor release declines, with PlGF-2 having the lowest release, bFGF an intermediate release and VEGF the highest release.

The Werner Group have utilised a hydrogel similar to ours, in which heparin activated with 1-ethyl-3-(-3-dimethylaminopropyl) carbodiimide/N-hydroxysulfosuccinimide (EDC/NHS) was bound to the amine terminal end-groups of their 4-arm star PEG, effectively acting as a crosslinker [341,342]. However, their growth factors were not incorporated into the hydrogels before gelation, as done here, but were bound into the hydrogel after hydrogel polymerisation. Unlike the release seen in the figures above, these hydrogels allowed for a substantial burst release – over 90% of VEGF and 75% of bFGF were released on Day 1, after which the release rate became minimal – 0.33 ng/day (VEGF) and 1.3 ng/day (bFGF) [341]. In the experiments presented above, only 20% of the VEGF and 12% of the bFGF were released on Day 1. Thus, although these hydrogels were shown to bind VEGF and bFGF as our system did, the release appeared less optimal. It is possible that proteins, like growth factors, contain amine groups and so undesired binding between the EDC/NHS heparin and these groups within the proteins could occur [343]. This would be a more likely occurrence than growth factors binding to our PEG via cysteine residues, as cysteine is one of the least abundant amino acids within a protein [344].

It can be concluded that VEGF, bFGF and PlGF-2 could all be bound to the hydrogels, with heparin enhancing binding in the case of VEGF and bFGF. Heparinised hydrogels for all growth factors could release significantly more growth factor than the non-heparinised over a sustained period. Thus, these hydrogels would be suitable delivery vehicles *in vivo*, allowing the desired controlled and sustained release of factors that remain bioactive.

2.1.5. Spheroid sprouting assay in heparinised 4-arm PEG-VS hydrogels

As the release data in **Error! Reference source not found.** and Figure **13** show, heparinised hydrogels were very effective at capturing the growth factors, allowing for a sustained, controlled release of these factors over 20 days.

Schreiber et al. (1985) and Steffens et al. (2004) state that heparin can potentiate growth factor activity and can increase the angiogenic response of endothelial cells [287,289]. The electrostatic interactions with growth factors play a role in protein stabilisation/activation and also increase cellular receptor affinity [345,346]. Klagsbrun and Baird (1991) showed that heparin stabilises bFGF's interaction with its receptor, allowing a dimer consisting of two receptors and two bFGF molecules to form [347]. This leads to autophosphorylation, which then triggers the migration, proliferation and differentiation of endothelial cells, ultimately leading to angiogenesis [57]. When heparin is not present, bFGF exhibits a greatly reduced receptor affinity and thus reduced angiogenic potential [348].

Based on this, the hypothesis was that incorporating heparin into the hydrogels would mimic the physiological scenario, and allow for improved growth factor capture and release, potentiating their activity, and thus further promoting sprouting [287,289].

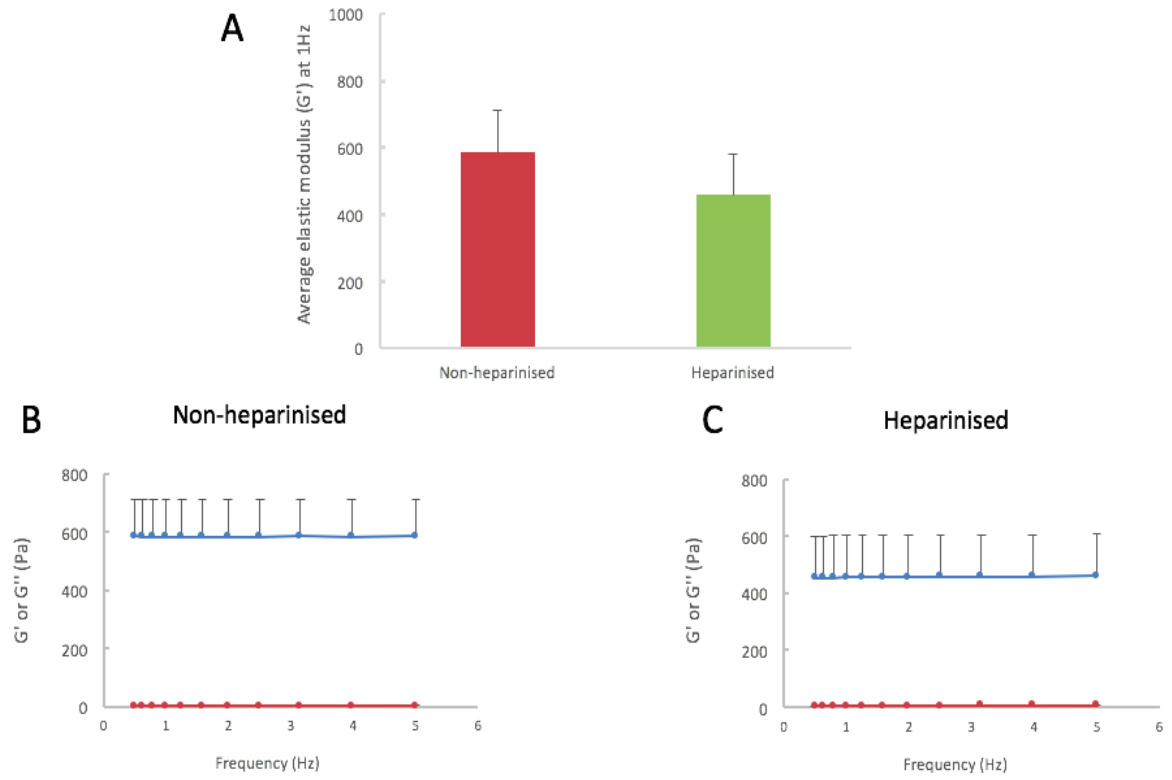

Figure 14: Rheological analysis of non-heparinised and heparinised 3.25% 4-arm PEG-VS hydrogels*. A) Average storage moduli (G') of the non-heparinised compared to the*

heparinised 3.25% PEG-VS hydrogels, p=NS. Frequency sweeps from 0.5 – 5 Hz showing both elastic (G') and viscous (G'') components for the B) non-heparinised hydrogels and the C) heparinised hydrogels. Results are here represented as mean ± SD, n=4.

Rheological analyses were conducted on both heparinised and non-heparinised 3.25% PEG-VS hydrogels and the results then compared to those obtained for 3.5% PEG-VS hydrogels. This was to determine whether altering the amount of PEG would significantly affect the viscoelastic properties of the hydrogel. It was found that there was a non-significant drop in stiffness after heparin addition, from 397 ± 69 Pa (3.5% PEG-VS) to 300 ± 89 Pa (3.25% PEG-VS) (Figure 14A). Frequency sweeps for these hydrogels showed G' to be stable across the range from 0.5 – 5 Hz (Figure 14B and C), confirming their hydrogel-like nature. Their gelled state was confirmed by G' being orders of magnitude larger than the loss moduli, G'' [304,305]. These findings indicate that the addition of heparin does not significantly alter the viscoelastic properties/stiffness of the hydrogel. This is suggestive that the presence of heparin will not influence cell invasion behaviour biomechanically [221,275,349]. This finding was perhaps not entirely unexpected, as the relative amount of heparin added was low – 210 µg heparin per 14 mg PEG, which equates to approximately 1 molecule of heparin per 70 molecules of PEG, if one makes the assumption that the heparin molecules were of the same molecular weight. Although this dose of heparin is considered high in terms of haemostatic effect if injected as a bolus, the heparin-PEG is injected such that it gels *in situ* and only allows for controlled release over an extended period. Previous *in vivo* studies have shown no adverse bleeding effects using the same heparinised hydrogel [261,350].

After concluding that heparinisation does not significantly alter the storage modulus of the hydrogel, these heparinised 3.25% PEG-VS hydrogels were employed to ascertain the effect of heparin on HUVEC sprouting.

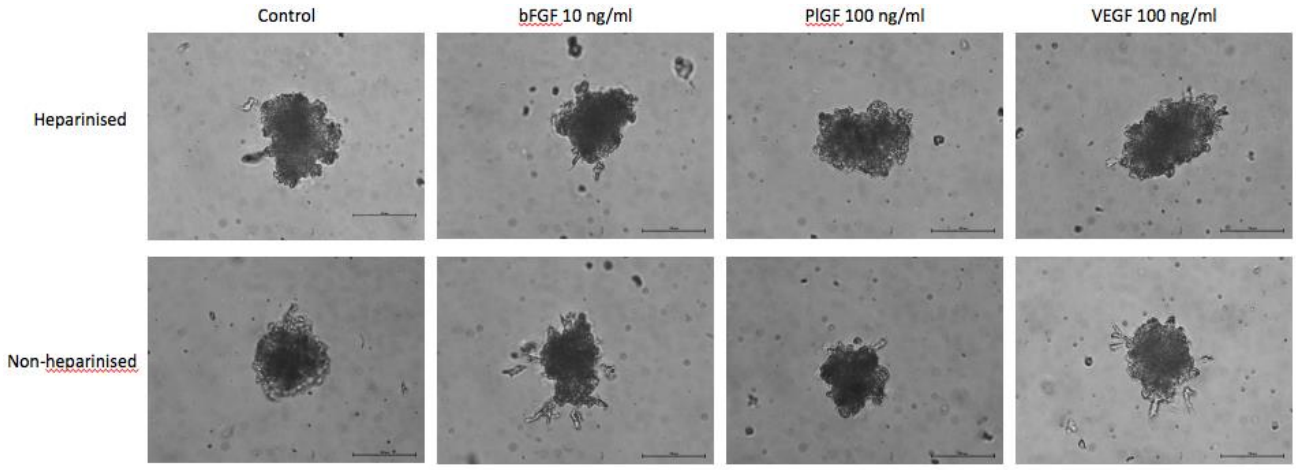

Figure 15: Spheroid sprouting assay with HUVECs within heparinised hydrogels. *Micrographs showing malformed HUVEC (P3) spheroids after 72 hours in both heparinised and non-heparinised control hydrogels. Scale bar = 100 µm.*

Unlike the spheroids seen in Figure 11, these spheroids did not form properly – they were not round and lacked the condensed appearance and defined edge seen with the previous spheroids (Figure 15). This was seen for both spheroids embedded in heparinised hydrogels and those embedded in the non-heparinised control hydrogels. Furthermore, no sprouting was now observed under any conditions, including those previously found to promote invasion. Initially, this was thought to be due to the purchasing of a new batch of round-bottom 96 well plates, although sourced from the same manufacturer. A round-bottom plate from the first batch was then used, but the same malformed spheroids were seen. A range of HUVECs at different passages and from different donors were used, however this did not improve spheroid shape. A new batch of methylcellulose was then ordered as it was thought that perhaps the previous batch had deteriorated and did not create a solution of the desired viscosity to allow for round, condensed spheroids to form. This again did not improve spheroid formation. This apparent irreproducibility of the assay was not resolvable within the time constraints of the project.

Although it was not possible to analyse the influence of heparin on the angiogenic potential of growth factors in PEG hydrogels, the above experiments did reveal a fragility in the *in vitro* spheroid assay. As the initial studies show that angiogenic effects can be readily discerned in this assay, further approaches towards generating a more stable assay will be undertaken in the laboratory. These include changing the medium when culturing spheroids within the methylcellulose solution from the standard medium containing only 10% FBS to the enriched endothelial growth medium [MCDB containing 10% FBS, hydrocortisone (10 mg/L), L-glutamine (292 mg/L), EGF (10 µg/L) and bFGF (5 µg/L)] as is used in the monolayer culture of HUVECs. This would provide a more nurturing environment and could allow for better spheroid formation. This approach was previously avoided due to concerns regarding interference of the growth factors present in the enriched medium with downstream analyses. When generating HUVEC spheroids, Korff et al. (2001) make use of a commercial medium by Promocell GmbH containing 2% FBS, EGF (0.1 ng/ml), bFGF (1 ng/ml), heparin (90 µg/ml), hydrocortisone (1 µg/ml) and 0.4% bovine hypothalamic extract, sold as "Endothelial

Cell Growth Supplement" [110]. Some of these additives could be used to further fortify the enriched endothelial growth medium in future.

As mentioned above, conducting future assays utilising iHUVECS could reduce the variability and irreproducibility as these cells are immortalised, and reduce the effect of passage number and donor variability [109]. It is hoped that these further modifications will allow for the establishment of a more rigorous *in vitro* angiogenesis assay that can be used as a tool for optimising the PEG hydrogel system as a regenerative scaffold.

2.2. 8-arm PEG hydrogels to control tissue invasion

One of the main aims in the field of regenerative medicine is to create a scaffold that can successfully guide the regeneration of the damaged tissue [351]. Although it is generally thought that fast replacement of a scaffold by functional tissue is optimal, it has become apparent that many factors influence this rate and that not all physiological situations will have the same requirements [352]. By tailoring the degradation rate of the scaffold, one can potentially tailor the rate of cellular invasion to better suit the specific milieu [274,353–355]. For example, in a study by Drueke et al. (2004) into full thickness wounds, it was found that in dermal grafts, implants that degraded quickly stimulated undesirable fibrosis, which causes scar formation [302]. However, when considering vascular grafts, a scaffold with a fast rate of degradation prevented calcification as cells were able to infiltrate rapidly [356]. A study conducted by our laboratory showed that, in the context of the infarcted heart, functional improvement was not seen when rapid hydrogel replacement occurred due to hydrogel topography, but a hydrogel shape that allowed for slower degradation was able to return function [255]. Thus, it is necessary that the hydrogel replacement rate by tissue can be controlled. The studies detailed in this chapter investigate a novel means of achieving such regulation in the enzymatically degradable hydrogels by the introduction of increasing levels of hydrolytic degradability.

The below studies shifted focus from hydrogels formed from the 4-arm PEG monomers (MW:20 kDa) to those from 8-arm monomers (MW:20 kDa). These types of hydrogels have been utilised by our group previously as injectable therapies for the infarcted heart [30,255,261]. One clear advantage of the increased number of arms in the monomer is that they are able to polymerise faster than the 4-arm. In a study by Kim et al. (2016), a time sweep test was performed and it was found that the rate at which hydrogel formation took place was dependent on the number of arms available for crosslinking [258].

The aim of the below study was to determine whether tissue ingrowth into these hydrogels can be controlled *in vivo*. The central premise of the approach employed to regulate tissue invasion was as follows. A hydrogel formed by crosslinking PEG-VS monomers with bi-cysteine containing MMP recognition peptides can only be degraded by cellular-based enzymatic hydrolysis of the peptide crosslinker. This does allow for total replacement of the hydrogel by

tissue but, as described above [122,262], it would be desirable to be able to speed up this process in some instances. Another type of 8-arm PEG monomer with acrylates as arm termini (PEG-Ac) can form hydrolytically degradable linkages with the peptide sulfhydryls, again via a Michael addition reaction, as aforementioned. Therefore, a hydrogel created with a combination of PEG-VS and PEG-Ac monomers, and crosslinked with an MMP-1 recognition peptide sequence, would possess some crosslinks which are solely cleavable by cellular MMPs, and others which are prone to degradation by both hydrolysis and proteolysis. Thus, it was hypothesized that by introducing increasing proportions of the hydrogel that can be hydrolytically degraded, in addition to the enzymatically degradable component, an increased rate of tissue invasion might be achieved.

As the heparinised form of the PEG hydrogels has increasingly become a focus in our group, with its potential for greater regenerative capacity [254,261], heparinised hydrogel formulations were utilised. Cellular invasion into the different hydrogels was initially studied *in vitro* using a spheroid sprouting assay, and tissue invasion investigated *in vivo* using a subcutaneous implant assay in rats.

2.2.1. Rheological analysis of heparinised PEG-VS/Ac hydrogel stiffness

To determine whether altering the PEG composition within a hydrogel – i.e. altering the PEG-VS:PEG-Ac ratios – altered initial hydrogel stiffness, rheological analyses of each hydrogel type were conducted. The hydrogels containing only PEG-VS monomers are here referred to as 0% PEG-Ac hydrogels, as they contain no acrylate. The 25% PEG-Ac hydrogels contain 75% PEG-VS monomers, with the remaining 25% of the monomers being PEG-Ac. 50% PEG-Ac hydrogels have an equal amount of PEG-Ac and PEG-VS monomers, whereas the 75% PEG-Ac monomers contain only 25% PEG-VS. The 100% PEG-Ac hydrogels are formed through crosslinking PEG-Ac alone with the dithiol peptide.

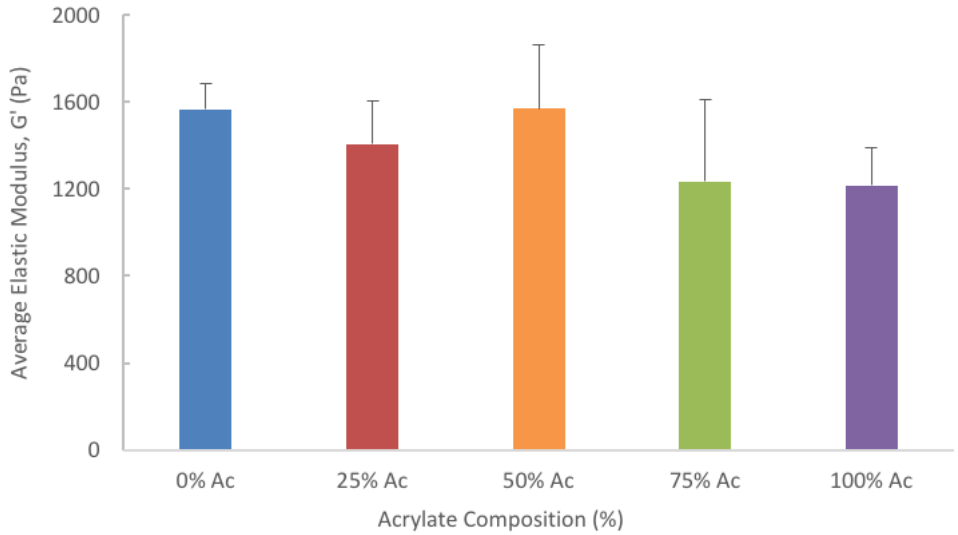

Figure 16: Rheological analysis of 4% 8-arm heparinised PEG hydrogels with increasing proportions of PEG-Ac. *Average elastic modulus, G' (Pa), of each type of hydrogel is shown. Results are here represented as mean ± SD, p=NS, n=4 hydrogels.*

The elastic modulus, or hydrogel stiffness (G'), at a frequency of 1 Hz ranged from 1217 ± 171 Pa to 1570 ± 290 Pa (Figure 16). Although the G' values were taken at a frequency of 1 Hz (Figure 16), the G' values do not fluctuate at other frequencies (Figure 17). G' remains relatively constant during the frequency sweep from 0.5 to 5 Hz. As mentioned in the previous chapter, for gelled viscoelastic materials such as these hydrogels, one would expect G' to be orders of magnitude larger than G'', which can be seen below (Figure 17) for all of the formulations of 8-arm PEG hydrogels [304,305]. Again, it is here demonstrated that storage modulus is virtually independent of frequency when the material is hydrogel-like or solid [304]. There was no significant difference in hydrogel stiffness between groups, suggesting that replacement of the PEG-VS monomer with PEG-Ac, had no substantial effect on hydrogel stiffness and that, biomechanically, the various hydrogels are reasonably similar in nature.

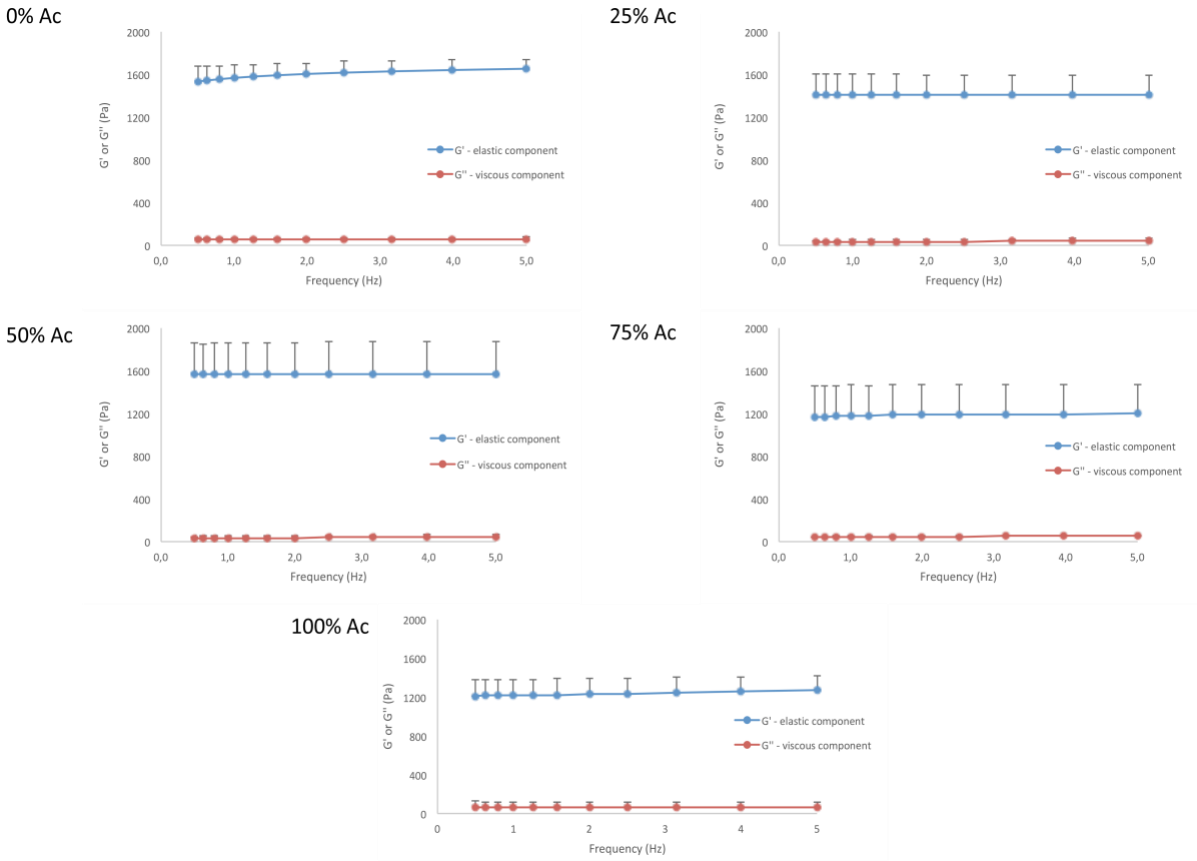

Figure 17: Frequency sweeps from 0.5 – 5 Hz*. Graphs show both elastic (G') and viscous (G'') components for the heparinised hydrogels ranging from 0% acrylate (*PEG-Ac*) to 100% acrylate, n=3 hydrogels.*

Vinyl sulfones react more selectively and rapidly with thiols through Michael addition than acrylates [357]. It was postulated that this difference should not influence the final stiffness of the hydrogels as the thiol groups present in the crosslinking peptide sequence are stoichiometrically balanced with the sum of the vinyl sulfone and acrylate groups. This is a requirement for effective polymerization to occur [246]. Thus, although thiols will react more rapidly with the vinyl sulfone end groups, it would be expected that the remaining thiols will be available to react with the acrylate groups. The finding that the hydrogels achieve similar final stiffnesses indicates that the above postulate is reasonable.

2.2.2. 8-arm PEG-VS/Ac hydrogels swelling assay

The hypothesis was that the introduction of increasing amounts of hydrolytically degradable ester linkages into the hydrogel should influence the invasion rate of cells into the hydrogels after implantation. A greater proportion of PEG-Ac would result in more rapid global hydrolysis throughout the hydrogel and this hydrolytic breakdown of the matrix would *de facto* reduce the number of enzymatically degradable linkages needed to be cleaved by invading cells. The hydrolytic degradation of links within the hydrogel will increase the effective hydrogel mesh size through swelling of the hydrogel [358]. Thus, the swelling of the various hydrogels in iso-osmotic PBS at 37 °C was determined by weighing hydrogels after preparation (W_0) and then periodically over a period of 30 days (W_t) , after which the swelling ratio (W_t/W_0) of the mass of swollen hydrogel, to that of the initial mass at time of polymerisation, was determined [359] (Figure 18).

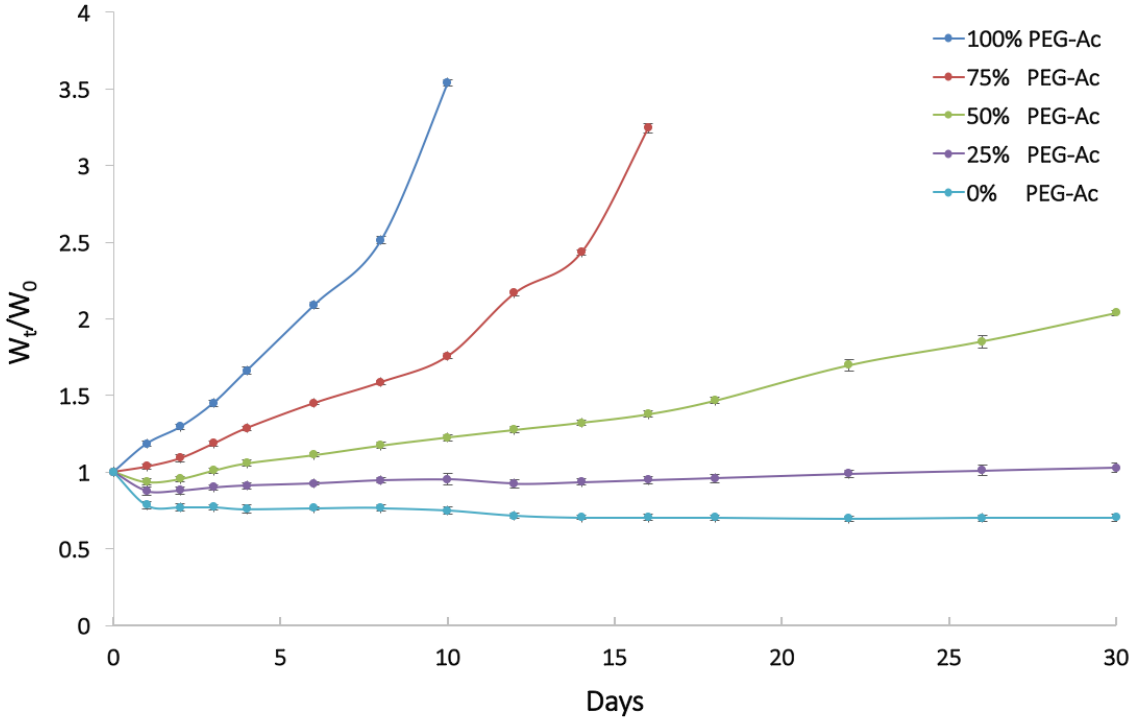

Figure 18: 4% 8-arm PEG swelling assay of 0% acrylate (0% PEG-Ac) - 100% acrylate (100% PEG-Ac) hydrogels. *The experiment was conducted over 30 days, with hydrogels weighed after preparation (W_0) and at regular intervals after exposure to iso-osmotic PBS (W_t) to calculate the hydrogel swelling ratio (W_t/W_0). Results are here represented as mean ± SD, n=4 hydrogels.*

Slightly surprisingly, the 0%, 25% and 50% PEG-Ac gels showed a decrease in mass over the first day. It is not clear what has caused this apparent deswelling but this initial decrease in

mass was found to be reproducible. It is possible that leaching of the heparin that did not couple into the hydrogel resulted in a drop in osmotic pressure with concomitant loss of water. This loss may then have been subsequently masked by elevated hydrolysis due to increasing PEG-Ac concentration.

Of the five different hydrogels, the 100% PEG-Ac hydrogels were the first to degrade. With the exception of the 0% PEG-Ac, which was composed only of PEG-VS, all the hydrogels showed increased swelling relative to Day 1. This was expected as this hydrogel is only enzymatically degradable and has no capacity for hydrolytic degradation. By Day 30, a 17.5% increase in weight was seen for the 25% PEG-Ac hydrogels and a 117% increase for the 50% PEG-Ac hydrogels. No 100% PEG-Ac hydrogel was visible for weighing at Day 12, indicating the hydrogel had degraded to the point of disintegration between Day 10 and 12. Similarly, the 75% PEG-Ac hydrogels were seen to degrade between Day 16 and 18. The remaining hydrogels, from 0 – 50% PEG-Ac, persisted until the last measurement on Day 30.

Thus, as predicted, the rate of hydrolysis was proportional to the percentage of hydrolytically degradable monomer present. This observation fits with the assumption that degradation of crosslinked polymeric hydrogels follows pseudo first-order kinetics, where hydrolysis rate is proportional to the number of degradable bonds and that the water concentration is constant throughout [360]. It could be seen that the hydrogels with the highest percentage (100%) of the hydrolytically degradable PEG monomer (PEG-Ac) degraded first, followed by the 75% PEG-Ac gels. The other hydrogels followed the same trend in swelling but persisted over the 30-day period due to the increasing presence of PEG-VS, the component that forms cross-links that are only enzymatically degradable. As no MMPs were available to cleave these bonds, degradation could not take place. Clearly a stable network, that could persist after complete or substantial hydrolysis had taken place, was not present in the 100 and 75% PEG-Ac hydrogels. Further extension of the hydrolysis period would need to be carried out to determine whether the polymer networks formed by the remaining PEG-VS monomers in the lower PEG-Ac percentage hydrogels are stable. Importantly, this swelling study demonstrates that there will be an increased rate of degradation due to hydrolysis alone, and that this should potentially allow for increased cleavage of the remaining enzymatically cleavable crosslinks by invading cells.

2.2.3. Assessing cellular invasion into 8-arm PEG-VS/Ac hydrogels utilising a spheroid sprouting assay

As it had been established that the hydrogels underwent more rapid hydrolysis with increasing PEG-Ac content, it was decided to evaluate the influence of this on cellular invasion *in vitro* prior to the ultimate goal of assaying the impact on tissue invasion *in vivo*. A spheroid sprouting assay like that established in Chapter 1 was thus utilised to study endothelial cell invasion within the different types of hydrogels.

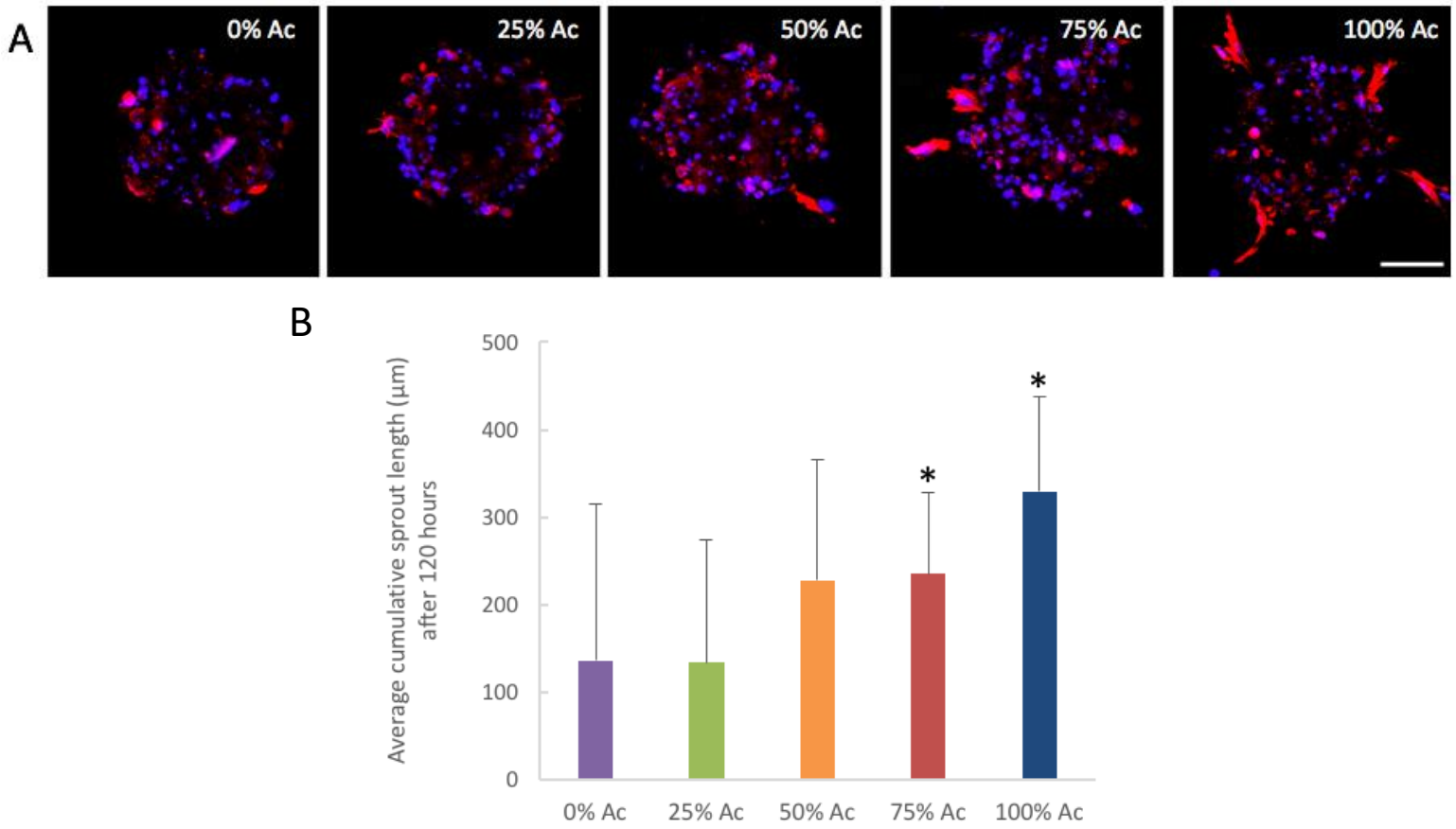

Figure 19: Spheroid sprouting assay with HUVECs. *A) Fluorescent confocal images showing sprouting at 120 hours for 0%-100% acrylate (Ac) gels. Nuclei are stained in blue and actin filaments in red. Scale bar = 50 µm. B) Average cumulative sprout length (nm) at 120 hours for 0-100% Ac hydrogels.* * = p<0.05 when compared to 0% Ac. Results are here represented as mean ± SD, n=7-14 spheroids per hydrogel type.*

Based on the swelling assay, one would expect the 100% PEG-Ac hydrogels to show the most sprouting over time. This is because these hydrogels would have swelled most rapidly due to bonds being broken hydrolytically, and potentially allowed both direct cellular movement, through any paths created by the hydrolysis, and a reduced need for peptide crosslinker

proteolysis. Paths referred to above were defined previously as physically interconnected passages formed by macroscopic cavities and little cracks in the hydrogel into which sprouts can extend [276]. It is to be noted that, unlike the spheroid assay presented in the previous chapter, this assay was allowed to take place over 120 hours to allow sufficient time for sprout formation. This is because these 8-arm PEG hydrogels are made up of a more densely cross-linked network than the 4-arm PEG hydrogels, potentially resulting in slower sprouting than that seen in the 4-arm hydrogels. A higher invasion was already seen in the previously presented 4-arm hydrogels by 72 hours (Figure 11), compared to that seen here after 120 hours. This does indicate that as expected, the 8-arm hydrogels, with their smaller mesh size and greater density of crosslinks, do impact on invasion. A longer invasion time was investigated, however the sprouts began to break apart, rendering analysis difficult. Why this occurs is unclear.

As expected, the 100% PEG-Ac and 75% PEG-Ac hydrogels had the highest average cumulative sprout lengths (329 ± 108 µm and 235 ± 93 µm) after 120 hours (Figure 19). When compared to the 0% PEG-Ac hydrogels, average cumulative sprout lengths were significant ($p<0.05$) for both the 100% and 75% PEG-Ac hydrogels. The 50% PEG-Ac hydrogels, with an average cumulative sprout length of 228 ± 138 µm, were however not significant when compared to the 0% PEG-Ac hydrogels. Sprouts within the two hydrogel types with the least acrylate (0% and 25% PEG-Ac) were not very long, with average cumulative sprout lengths of 136 ± 179 µm and 134 ± 140 µm, respectively. Thus, there was a trend towards increased invasion of cells as the hydrolytically degradable component increased. It should be reiterated that in all hydrogel formulations, the concentration of enzymatically degradable peptide crosslinkers is identical. The findings from the spheroid invasion assay suggested that the central premise that increasing hydrolytic breakdown would enhance cellular invasion was valid.

2.2.4. Subcutaneous implant model to investigate tissue invasion into 8-arm PEG-VS/Ac hydrogels *in vivo*

After showing with the *in vitro* spheroid assay that cellular invasion into the various hydrogels was augmented by increasing the proportion of PEG-Ac, the rate of replacement by tissue ingrowth was assayed *in vivo* in a rat subcutaneous model.

In the subcutaneous implant model, our hydrolytic and enzymatically degradable hydrogel hybrids were polymerised within highly porous P.U. discs. These discs allowed for simple retrieval of the implanted hydrogel and defined sectioning, staining and analysis [120]. This approach thus allows for an accurate quantification of hydrogel replacement by tissue as the volume initially occupied by hydrogel is defined [120].

Upon explanting the discs 2 weeks after implantation, the 0% PEG-Ac hydrogel was still intact and filled the disc – shown as a uniform pink or purple staining (Figure 20, see chevrons). As seen in the H & E stained sections, it appears histological processing may have caused some dehydration and wrinkling of the hydrogel within the disc. Very little cellular invasion is evident in the discs containing the 0% and 25% PEG-Ac hydrogels at this point. The presence of some empty spaces in the 25% PEG-Ac hydrogel, is potentially due to some level of hydrolytic break down having taken place. Theses spaces were not seen in the 0% PEG-Ac discs. Reinforcing this hypothesis, a greater area of these type of spaces were seen in the 50% PEG-Ac discs. Substantially more cellular invasion was able to take place within the 75% PEG-Ac discs, and further empty spaces were visible. At this 2-week time point, the 100% PEG-Ac hydrogels were already fully invaded, as seen in the H & E stained section.

When the equivalent hydrogels were explanted after 4 weeks, further invasion was seen in all the discs where there was still capacity for ingrowth (Figure 20 and Figure 21). After this period, the 0% PEG-Ac discs again had the most hydrogel remaining. Very little to no hydrogel remained within in 50% and 75% PEG-Ac discs. At this time point, a few empty spaces were visible within the remaining hydrogel in the 0% PEG-Ac discs. It is possible this is indicative of remote cellular proteolytic activity from cells present in the surrounding subcutaneous area.

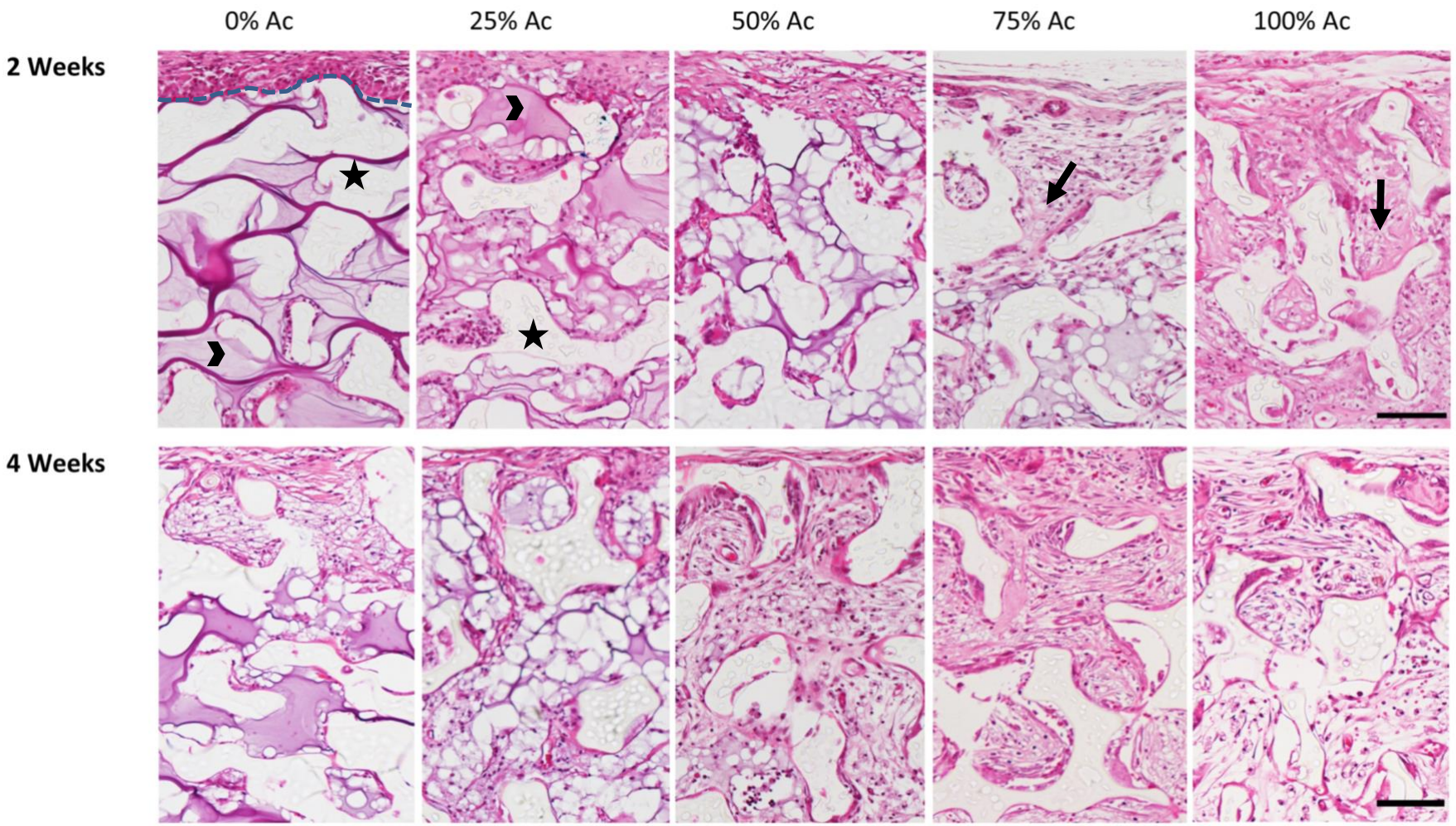

Figure 20: Cellular invasion of P.U. discs impregnated with the different 8-arm PEG hydrogels explanted at 2 weeks and 4 weeks. *Explanted discs were histologically sectioned and stained (hematoxylin and eosin). The blue dashed line indicates the edge of the P.U. disc. Chevrons indicate remaining PEG hydrogel and arrows depict tissue ingrowth. Stars denote the struts of the P.U. discs. Scale bar = 100 µm, n=4.*

Analysis of the amount of tissue present in the micrographs confirmed complete invasion of the 100% PEG-Ac discs at 2 weeks, and indicated that almost complete tissue invasion had taken place for the 75% PEG-Ac discs (89 ±6%, Figure 21). The curves of cellular invasion generated for 2 weeks and 4 weeks were both sigmoidal in shape (R^2>0.99 for both time points: logistic A with offset curve fit). The upward shift of the 4-week curve relative to the 2-week curve, shows that invasion increased in all hydrogel discs, with the exception of the 100% PEG-Ac containing discs as these were completely ingrown at the earliest time point. The largest relative increase in tissue invasion was seen in the 50% PEG-Ac containing discs, with the amount of tissue present increasing from 25 ±7% to 92 ±4%, which is almost complete replacement of hydrogel by tissue.

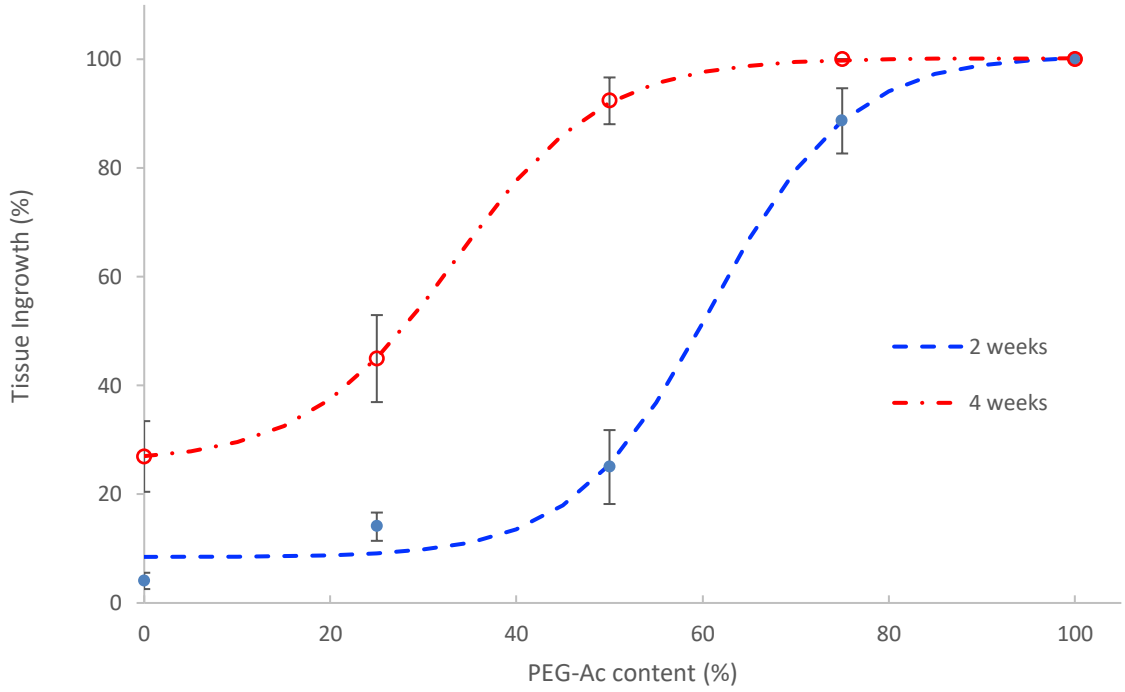

Figure 21: Tissue ingrowth (%) for each type of 8-arm PEG hydrogel*. Results are shown after 2 weeks and 4 weeks and represented as mean ± SEM, n=4.*

Further than simply assessing cellular invasion, one can evaluate extracellular matrix deposition by ascertaining the amount of collagen produced by hydrogel-invading cells [361]. Because invasion of the P.U. discs is constrained by the ingrowth volume available, collagen deposition could potentially be used to gain further insight into invasion rate. Furthermore, it was of interest to determine whether collagen deposition was also temporally regulated by

hydrogel acrylate content. The physiological response to the implanted biomaterials seems to initiate in a manner similar to that of wound healing, which has three phases: inflammation, tissue formation, and tissue remodelling. These tend to overlap rather than occurring one after the other [362,363]. During inflammation, immune cells like neutrophils and macrophages arrive at the site to clean the wound, removing bacteria and phagocytosing material [362]. After a few days, granulation tissue forms consisting of new ECM and blood vessels. Fibroblasts migrate in to the wound, differentiate into myofibroblasts, and begin to deposit collagen, after which angiogenesis can commence [362]. Thus, collagen deposition necessarily follows cellular invasion.

Once this has occurred, cells would infiltrate and begin forming new tissue. At 2 weeks after implantation, picrosirius-stained collagen (seen in red in Figure 22) can only be seen outside the P.U. discs for the 0% and 25% PEG-Ac hydrogels, with only small amounts being present within the disc itself in the 50% PEG-Ac hydrogel. In comparison, more collagen can be seen for the 75% PEG-Ac hydrogels, however considerably more was visible in the 100% PEG-Ac discs and the staining seemed more intense. Collagen could be seen within all the discs explanted after 4 weeks. The collagen content of the 50% PEG-Ac hydrogels at this time point appeared comparable to that seen within the 2-week 100% PEG-Ac hydrogels. The 75% PEG-Ac hydrogels seemed to have a similar amount of collagen present to that observed within the ingrowth area of the 100% PEG-Ac hydrogels, however in some areas the intensity of staining was diminished.

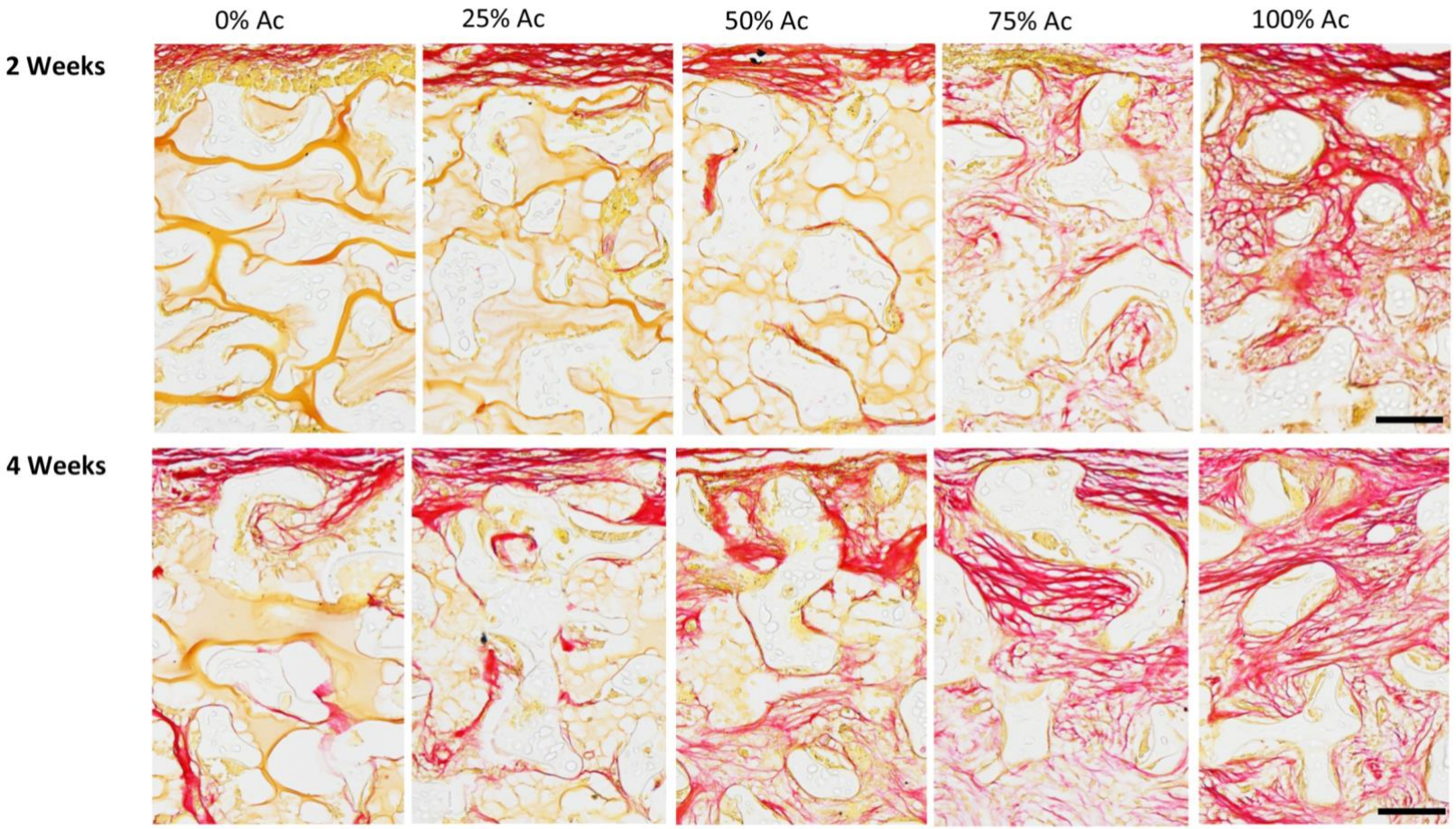

Figure 22: Collagen deposition within P.U. discs impregnated with the different 8-arm PEG hydrogels explanted at 2 weeks and 4 weeks. *Explanted discs were histologically sectioned and stained (picrosirius red). Scale bar = 100 µm, n=4.*

It can be seen that, as the acrylate composition of the hydrogels increases, so does collagen deposition (Figure 22 and Figure 23). This is because the faster the hydrogel degrades, the faster cellular infiltration can take place. The faster cellular infiltration takes place, the sooner the cells will start to produce and secrete ECM proteins such as collagen. Upon analysing the images in Figure 22, it became clear that the relationship between collagen deposition and the PEG-Ac: PEG-VS ratio was sigmoidal in nature (Figure 23, $R^2 >$ 0.99 for 2 and 4 weeks). In relation to the 2-week curve, the 4-week curve altered position by shifting up and to the left, with there being a significant increase in collagen deposition in all hydrogel groups.

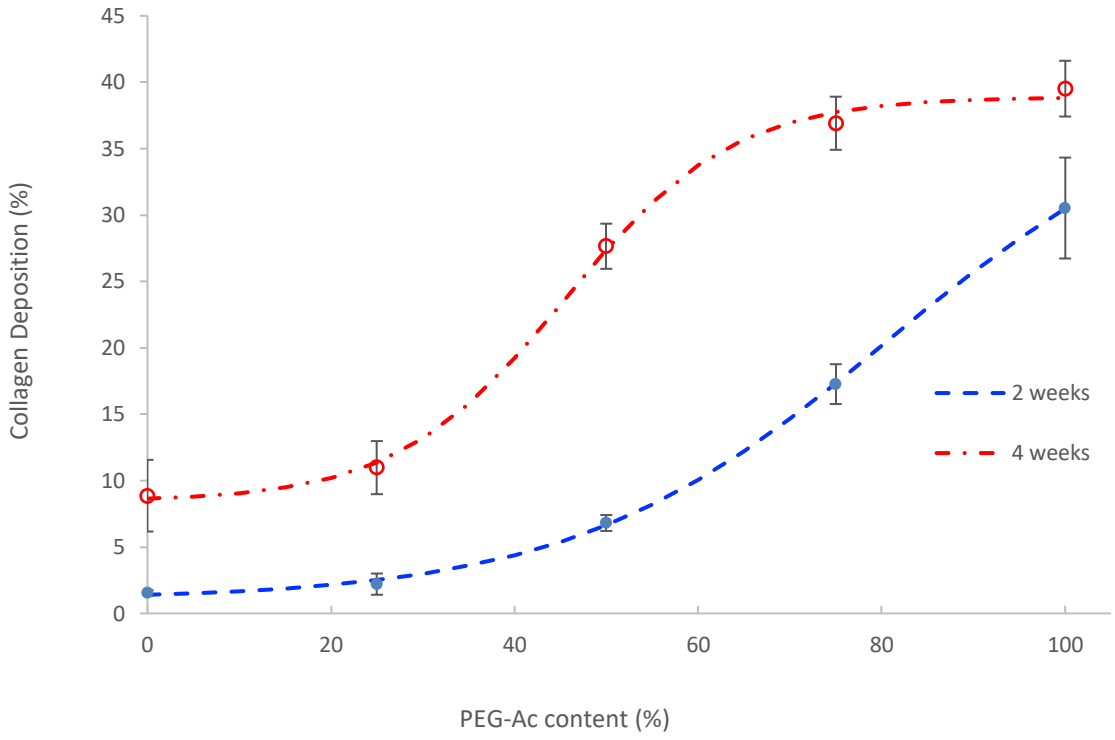

Figure 23: Collagen deposition (%) for each type of 8-arm PEG hydrogel. *Results are shown after 2 weeks and 4 weeks and represented as mean ± SEM, n=4.*

One can see there is a slight delay in collagen deposition (Figure 23) relative to cellular ingrowth in Figure 21. This is probably due to the sequence in which the wound-healing like response occurs. With inflammation occurring first, followed by cellular infiltration

and matrix deposition [362]. Although the 100% PEG-Ac discs were fully invaded by 2 weeks, at this point there was only a 30.5 ±4% collagen deposition. After 4 weeks, these explants had a collagen content of 39 ±2%. Similarly, the 75% PEG-Ac hydrogel explants were 37 ±2% collagen at 4 weeks. However, image analysis revealed that at 2 weeks, 100% PEG-Ac hydrogel explants showed a 77% increase in collagen deposition compared to the 47% increase (17 ±1% to 37 ±2%) seen in the 75% PEG-Ac hydrogel explants, with this difference being significant ($p<0.05$). Collagen synthesis and deposition appeared to cease once 40% of the ingrowth space was taken up by collagen, with both these hydrogels reaching this point. It makes sense that the hydrogels with the slowest degradation rate (0% PEG-Ac) and thus the least cell invasion will, in turn, show the least amount of collagen deposition – 1.6 ±0.2 % after 2 weeks and 8.8 ±3 % after 4 weeks. Therefore, this study further validates that the regulation of tissue hydrogel replacement, as well as tissue maturation, can be achieved by titration of hydrolytic cleavage points within the hydrogel.

3. Conclusion

The sustained, targeted delivery of pro-regenerative factors has shown great potential to bring about regeneration in various pathological contexts, including CVD and MI-related pathologies. Biomaterials like PEG have been employed for such delivery, but also have the potential to be used as scaffolds with the ability to guide the process of tissue replacement. With each physiological situation possessing its own requirements and optimal rate of replacement, a biomaterial like the PEG hydrogel used here with tunable biodegradability affords much desired control over the regenerative process.

The viscoelastic properties and hydrogel-like nature of the 4-arm 20 kDa were established prior to utilisation of these hydrogels in an *in vitro* angiogenesis assay. The storage modulus was found to be 557 ± 107 Pa by small strain oscillatory shear rheometry, which did differ from the literature and was likely due to PEG-VS monomer batch variation.

The next step towards optimising the angiogenic response within the PEG scaffolds was to investigate the angiogenic response elicited by the growth factors VEGF, bFGF and PlGF-2. Spheroid sprouting assays were established using HUVECs, confirmed as CD31-positive by immunocytochemistry and flow cytometry, to achieve this. VEGF and bFGF were found to elicit significant sprouting responses after 72 hours, with average cumulative sprout lengths being 4-fold higher than those of the control. Average sprout numbers per spheroid were found to be significantly (2.3 – 2.4 times) higher than the control. However, PlGF-2 did not elicit significant increases in sprout lengths when compared to the control, or increased sprout numbers.

By conducting growth factor release assays with quantification by ELISA, it was found that heparinised PEG-VS hydrogels were able to successfully increase growth factor binding and release for all three of the factors of interest over 20 days. It was observed that as growth factor affinity for heparin increases (with VEGF having the lowest affinity, followed

by bFGF and PlGF-2), binding is enhanced and growth factor release declines – PlGF-2 had the lowest release, followed by bFGF and VEGF. Combining two growth factors, bFGF and PlGF-2, was found to have no effect on the binding and release of the individual factors.

Further than binding growth factors, heparin itself is also pro-angiogenic and can present growth factors in a manner that enhances angiogenesis. Therefore, the effect of sprouting within heparinised hydrogels was of interest. These spheroids did not properly form, revealing a fragility within the assay. Troubleshooting could not be concluded due to time constraints, however it is thought that by fortifying the medium in which the spheroids form, this problem may be overcome in future. Utilising immortalised HUVECS may also reduce variability, making the assay more robust.

The focus then shifted from the 4-arm PEG monomers to an 8-arm monomer previously utilised in the infarcted heart by our group, which is able to polymerise faster and possesses increased functionality. Here, the aim was to determine whether tissue ingrowth into these hydrogels can be controlled *in vivo*. Unlike the hydrogels used previously, these hydrogels contained varying amounts (0 – 100% m/v) of PEG-Ac and PEG-VS monomers, affording the hydrogel varying degrees of hydrolytic and enzymatic degradation superimposed on the existent enzymatically degradable background.

Although the hydrogels contained differing concentration of the two monomers, the initial storage moduli were found to be similar across all the hydrogels, with G' ranging from 1217 ±171 Pa to 1570 ±290 Pa (p=NS). A hydrogel swelling assay over 30 days revealed that the hydrogels containing the most hydrolytically degradable monomers (100% PEG-Ac), degraded first between Day 10 and 12, followed by the 75% PEG-Ac between Day 16 and 18. The remaining hydrogels, from 0 - 50% PEG-Ac, persisted until the last measurement on Day 30, showing that the hydrolytic degradation rate was controlled.

This swelling assay informed the trends seen when a spheroid sprouting assay was conducted within these different 8-arm hydrogels. The hydrogels which degraded the fastest (100% PEG-Ac and 75% PEG-Ac), showed the most significant sprouting when compared to those that were not able degrade at all (0% PEG-Ac). Importantly, the *in vivo* subcutaneous implant assay which followed showed the rate of tissue replacement was proportional to the concentration of PEG-Ac. By altering the proportion of hydrogel additionally vulnerable to hydrolysis in the enzymatically degradable hydrogels, the rate of tissue invasion was controlled. When assessing collagen deposition, this was also found to positively correlate with PEG-Ac concentration. Analysis of collagen allowed for the delay in invasion of 75% PEG-Ac relative to 100% PEG-Ac hydrogels to be discerned.

In conclusion, a suitable *in vitro* angiogenesis assay was established to assess cellular invasion within the 4-arm hydrogel system, although it is clear that further modifications are required to render this assay more robust in our hands. When heparinised, these hydrogels were shown to have improved capture and release of growth factors, further adding to the current knowledge of such biomaterials as delivery vehicles. By altering the concentration of the two different monomers within the 8-arm hydrogel, control over the rate of tissue invasion was achieved. Thus, further optimisation of the PEG hydrogel system in several critical areas has been achieved and should allow for increased use of this hydrogel in regenerative medicine applications.

4. Methods

Recipes for making reagents e.g. cell culture media and PBS can be found in Appendix 1, Tables A1 to A8. All specialised reagents, general reagents, consumables and equipment used for experiments are detailed in Appendices 2 – 5, Tables A9 to A14, including catalogue numbers and supplier information.

4.1. Cell culture

The cells used for *in vitro* experiments were Human Umbilical Vein Endothelial Cells (HUVECs) isolated from waste tissue after obstetric procedures, and were between Passage 2 (P2) and P5. Human dermal fibroblasts (HdFbs) were used as a negative control for some experiments between P3 and P6. These were obtained from laboratory stocks. All cell culture was conducted within a laminar flow hood after sterilization of surfaces by UV light exposure for 15 minutes. Surfaces were then further decontaminated using 70% ethanol. All items entering the hood were also decontaminated using 70% ethanol.

4.1.1. Cell culture media

Experiments involving HUVECs were conducted in MCDB 131 medium (Table A1, Appendix 1), with 10% filtered foetal bovine serum (FBS) and 2% penicillin-streptomycin – hereafter referred to as “standard culture medium”. For cell culture prior to seeding for experiments, this medium was further supplemented with hydrocortisone (100 mg/L) as well as L-Glutamine (292 mg/L), EGF (10 µg/L) and bFGF (5 µg/L) – hereafter referred to as “enriched culture medium”. HdFbs were cultured in Dulbecco’s Modified Eagle’s Medium (DMEM) with 10% filtered FBS and 2% penicillin-streptomycin – hereafter referred to as “standard DMEM medium” (Table A2, Appendix 1).

4.1.2. HUVEC isolation

Ethical approval was obtained from the University of Cape Town's Human Ethics Committee (HREC REF: 407/2017), in accordance with the Declaration of Helsinki. After obtaining the mother's written consent, umbilical cords were collected after caesarean section at Vincent Pallotti Hospital, Cape Town.

HUVECs were isolated using an adapted protocol [364] as follows: All umbilical cords were collected in Collection Medium (Table 1) on the day of birth. The cords were either utilised upon arrival at the laboratory or stored at 4 °C for 24 – 48 hours, as Jimenéz et al. (2013) obtained comparable results when isolating either 24 or 48 hours after birth [307]. All cells were isolated under sterile conditions, using sterile drapes, gloves and instruments in a laminar flow hood.

Table 1: Media and solutions used during HUVEC isolation

Medium/Solution	Constituents
Collection Medium	Medium 199
	Gentamicin (0.2%)
Rinse Solution	Medium 199
	Gentamicin (1%)
	Heparin (0.2%)
Collagenase Solution	Collagenase (0.7 g/L or 0.07%)*
	PBS
Inactivation Solution	Medium 199
	FBS (20%)

* See Table A7, Appendix 1 for recipe and method

The end of the cord was trimmed to remove any blood clots and the umbilical vein identified (Figure 24). The vein was then cannulated, securing the cannula by tying a suture around it. To remove as much blood as possible, 20 ml of Rinse Solution (Table 1)

was then flushed through the vein using a 20 ml syringe into a kidney dish. The Collagenase Solution (Table 1) was then flushed through until no more Rinse Solution (pink in colour) could be seen flowing out of the vein. The bottom end of the cord was clamped and the vein distended with more Collagenase Solution. Once fully distended, the top part of the cord was clamped just below the cannula. The cord was massaged gently for approximately 2 – 3 minutes to create turbulence inside the vein so as to dislodge endothelial cells. The clamped cord was then placed inside a 1 L jar containing sterile PBS (Table A3, Appendix 1, pre-warmed to 37 °C) and then placed into a 37 °C incubator for 12 minutes.

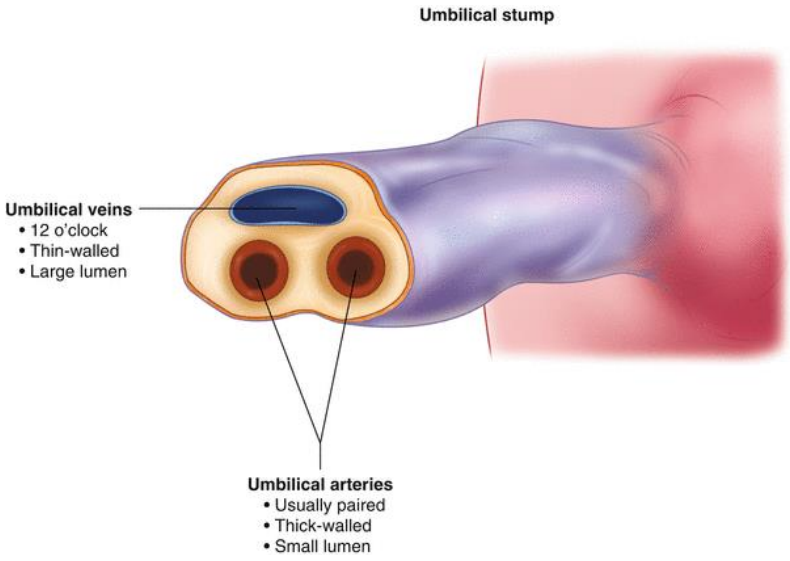

Figure 24: Diagram of the umbilical blood vessels and their defining features *[365].*

The jar was then removed from the incubator and the cord placed over an open 50 ml tube. The clamps were removed and the solution allowed to flow into the tube. The Inactivation Solution (Table 1) was then flushed through the vein until no more Collagenase Solution (yellow in colour) could be seen exiting the vein. The tube was centrifuged at 244 x g for 5 minutes (Megafuge 1.0R, Heraeus Sepatech, Germany). After removal of the supernatant, the cell pellet was re-suspended in enriched culture medium and pipetted into a collagen-coated well in a 6-well plate. Collagen coating was conducted by addition of 400 µl collagen type I (from bovine skin, diluted to 100 mg/L in sterile PBS)

to each well for 2 hours at 37 °C. The solution was then discarded and wells rinsed with an equal volume of sterile PBS three times. When prepared in advance, the plates were sealed and refrigerated at 4 °C with 2 ml sterile PBS in each well to prevent the collagen coating from drying out.

The above process, from the initial cord rinse step, was repeated to obtain a second yield of HUVECs which were placed in to another collagen-coated well in the 6-well plate. The plate was then placed into an incubator at 37 °C with 5% CO_2. After 24 hours, wells were rinsed with sterile PBS to remove red blood cell debris and fresh enriched culture medium was added.

4.1.3. Cell passaging

Once cells were approximately 80% - 85% confluent, culture vessels were rinsed twice with sterile PBS, with the volumes as follows: 1 ml for 6-well plate, 2.5 ml for a 25 cm^2 (T25) flask or 5 ml for a 75 cm^2 (T75) flask). This was followed by the addition of 0.25% trypsin-EDTA (volumes as above) for 2 minutes at 37 °C. Once the cells had lifted, the trypsin-EDTA was inactivated with the addition of an equal volume of enriched culture medium (with 20% FBS) if the cells were to be passaged further, or standard culture medium if the cells were to be seeded for an experiment. This was to minimize any influence of growth factors from enriched culture medium on downstream experiments. The entire volume was then aspirated and pipetted into a 50 ml tube and centrifuged at 400 x g for 5 minutes. The supernatant was then poured off and the pellet re-suspended in 1 ml enriched culture medium.

A cell count was then carried out as follows: 20 µl of the cell suspension was added to a microcentrifuge tube containing an equal volume of Trypan Blue (0.4% m/v). A haemocytometer and coverslip were cleaned with 70% ethanol, after which the coverslip was placed over the haemocytometer grid and 10 µl of the cell/Trypan Blue solution was

loaded under the coverslip. A cell count was then conducted. The four corners of the grid were counted, an average was obtained, and the number of cells/ml of media calculated as per the equation below:

$$number\ of\ cells/ml = average\ number\ of\ cells\ across\ the\ 4\ grids\ \times\ 2\ \times\ 10\ 000$$

The desired number of cells were then seeded for experimental use and the remainder of the cell suspension was either added to a flask containing fresh enriched culture medium in order to continue passaging the cells, or frozen as detailed below.

4.1.4. Freezing of cells

When primary HUVECs were first trypsinised and counted as mentioned above, at least one vial of cells was frozen to create a stock. Cells stocks up to P4 were created. This was conducted in the following manner:

Firstly, a 15% (v/v) DMSO stock was prepared in enriched cell culture medium and frozen in 1.5 ml aliquots. Before trypsinisation, an aliquot was thawed in the fridge and kept cold. Cells were trypsinised and centrifuged according to the protocol mentioned above. A cell count was carried out and the cell solution diluted, if needed, to create a solution with approximately 500 000 cells per 600 µl. This volume was then added to a cryovial, followed by the slow addition of an equal volume of 15% DMSO, and mixing by pipetting up and down, to achieve a final DMSO concentration of 7.5%.

Due to the sensitive nature of these endothelial cells, a cell freezing device (Mr. Frosty, Nalgene, MA), filled with isopropyl alcohol at room temperature, was used to freeze the cells. This controls cell freezing to a rate of 1 °C per minute. Once the DMSO was mixed in, the cryovial was placed straight into the Mr. Frosty and frozen at -65 °C overnight.

The following day, the cells were removed from the -65 °C freezer, and cryovials placed into a liquid nitrogen storage tank (- 196 °C) for long-term storage.

The same procedure as above was followed when creating frozen stocks of surplus HdFbs.

4.1.5. Thawing frozen HUVECs and HdFbs

The desired cryovial was removed from the liquid nitrogen tank and quickly thawed in a 37 °C water bath. The contents were then placed into a T25 or T75 flask, depending on the number of cells in the vial, containing enriched culture medium (HUVECs) or standard DMEM medium (HdFbs) with 20% FBS, rather than the standard 10% FBS used during passaging. The flask was then placed into the incubator, with a change of medium to that containing 10% FBS taking place 24 hours later.

4.2. Assaying CD31 expression of HUVEC isolates

The endothelial cell phenotype of all cell isolates was determined by immunostaining for the endothelial-specific marker CD31 and assessed by immunocytochemistry or by flow cytometry.

4.2.1. Immunocytochemical staining of cells

4.2.1.1. Collagen coating coverslips

Round coverslips (12 mm diameter) were placed into the wells of a 24-well plate and coated with 100 µl collagen type I from bovine skin (100 mg/L) as described for the collagen coating of the 6-well plates above. After rinsing, the coverslips were covered

with 500 µl sterile PBS and the plate was stored at 4 °C until the day of cell seeding. Before cells were seeded, the plate was brought to room temperature.

4.2.1.2. Seeding and staining cells

The optimal dilution for both primary and secondary antibodies was initially established. HUVECs were cultured to P4 and trypsinised as aforementioned. HdFbs were used as a negative control.

A cell count was conducted and 75 000 cells seeded onto the collagen-coated coverslips in a 24-well plate with a total of 400 µl of the respective media. After incubation at 37 °C for 24 hours, the cells were fixed using 1 ml cold methanol for 15 minutes. The seeded coverslips were then blocked with 1% BSA-PBS for 45 minutes to prevent non-specific antibody binding and then washed four times with 1 ml PBS for 5 minutes. 400 µl of the primary antibody (monoclonal mouse anti-human CD31) was added at the following concentrations: 1:500, 1:1000 and 1:2000 and incubated at 4 °C overnight. The wash steps were then repeated to remove unbound antibody. The fluorescently tagged (Alexa Fluor 488) secondary antibody (goat anti-mouse) was added at concentrations of 1:2000, 1:4000 and 1:8000 and incubated for 30 minutes at room temperature in the dark. The wash steps were again performed. Coverslips were carefully lifted using curved forceps and placed cell-side down onto a microscope slide with a drop of Fluoroshield containing DAPI nuclear stain.

Cells were then immediately viewed using a Nikon 90i microscope and micrographs captured at 400x magnification. The optimal primary antibody dilution was found to be 1:500, and the optimal secondary antibody dilution to be 1:2000. These dilutions were then used to assay all HUVEC isolates.

4.2.2. Flow cytometry analysis

HUVECs and HdFbs were trypsinised as previous described, however, instead of inactivating the trypsin with a cell culture medium containing FBS, a solution of PBS, 10% FCS and 1% sodium azide (Solution I) was used. The cells were then split into two separate microcentrifuge tubes – one to receive only secondary antibody (secondary antibody control) and one to receive both primary and secondary antibodies. The microcentrifuge tubes were centrifuged at 800 x g for 3 minutes. After resuspending with 300 µl of ice-cold Solution I, the cells were labelled with an equal volume of primary antibody (monoclonal mouse anti-human CD31 at 1:500 dilution, diluted in 1% BSA-PBS). The tubes were wrapped in foil and incubated at room temperature for 30 minutes. Cells were then centrifuged as above, and the pellet resuspended in 450 µl ice cold PBS. This was repeated 3 times. The secondary antibody [goat anti-mouse: AlexaFluor 488 F(ab') 2 fragment of goat anti-mouse IgG (H+L)] was then diluted (1:1000) in a 1% BSA-PBS (Solution II). After the last centrifugation, the pellet was resuspended in 450 µl Solution II. After incubation at room temperature for 30 minutes, cells were centrifuged 3 times as above. After the last wash, the pellet was resuspended in Solution III – PBS containing 3% BSA and 1% sodium azide.

CD31 expression was detected in the HUVEC and HdFb samples using a Beckon Dickson FACSCalibur flow cytometer system and shown as a shift from the mean fluorescence measured. A count of 10 000 cells was conducted, and cells gated based on forward and side scatter (FSC and SSC, respectively) to exclude non-viable cells and any debris within the samples.

4.3. PEG hydrogels

4.3.1. Preparation of the PEG monomers

4-armed and 8-armed PEG-OH monomers, both with a molecular weight of 20 kDa, were utilised to form PEGs with vinyl sulfone (PEG-VS) and acrylate (PEG-Ac) termini. This was conducted by the Polymer Laboratory of the Cardiovascular Research Unit at UCT, using a previously described protocol [254]. The 8-arm PEG-Ac was purchased from JenKem (TX).

In brief, the protocol for all PEG-VS was as follows: PEG-VS was created by deprotonation of the PEG-OH using sodium hydride, followed by addition of divinyl sulfone ($C_4H_6O_2S$), in excess. To quench any residual sodium hydride, acetic acid was added. This was then followed by precipitation in ether, repeated a total of three times. The PEGs were then frozen in 50 ml centrifuge tubes. The tubes were covered with Parafilm, into which holes were made to allow vacuum removal of air/vapours, and placed into the freeze dryer flask attachments. The samples were then freeze-dried overnight, after which they were stored at -20 °C. The desired amounts of PEG were weighed out as needed from this stock.

4.3.1.1. Lyophilising PEG

The 4-arm and 8-arm PEGs were reconstituted in sterile Nanopure water to a concentration of 2% (m/v). This was then aspirated into a 20 ml syringe and filtered into a 50 ml centrifuge tube using a syringe filter unit (pore size 0.2 µm) so as to sterilise the PEG for cell culture. Aliquots were made so that each tube contained 5 mg or 10 mg of PEG. The lids of the tubes were then tightly closed and the tubes immersed in liquid N_2 to flash freeze the PEG. The lids were then opened slightly and the tubes placed into the freeze-dryer flasks and inserted into the freeze dryer. The samples were left to freeze-dry overnight, after which they were stored at -20 °C.

4.3.2. Preparation of the acrylated heparin

Heparin molecules containing OH-termini were deprotonated and acrylated with acryloyl chloride in the same manner mentioned above, to form acrylated heparin (Hep-Ac) [254]. ^{1}H NMR was conducted by the Polymer Laboratory, and it was found that 40% of the heparin disaccharide units were acrylated through this process.

4.3.3. Formation of the 4-arm PEG-VS hydrogels

These PEG hydrogels consisted of 4-arm PEG-VS monomers and an MMP-1-degradable peptide linker sequence (here referred to as MMP-1 peptide) in a molar ratio of 2:1, respectively. For experiments where cells were embedded in the PEG hydrogel, cellular adhesion was required. To achieve this, RGD was added in a molar ratio of 12.5 PEG:1 RGD. Some hydrogels were heparinised by the addition of the Hep-Ac aforementioned. In these hydrogels, Hep-Ac was added as 1.5% (m/m) of the PEG.

“Master mixes” of all the constituents were created to limit variability between hydrogels. Each individual hydrogel was then pipetted from this homogenous mixture. When making up the hydrogel for experiments, the PEG and RGD were first reconstituted from freeze-dried powder with 0.3 M triethanolamine (TEOA, pH 7.4, see Table A8, Appendix 1). The reconstituted PEG and RGD were then combined in their respective amounts – see Table 2 below for an example of the volumes used to create a 100 µl 4-arm PEG hydrogel. Volumes were adapted as needed. The solution was incubated for 30 minutes in a 37 °C water bath, after which the required amount of TEOA was added. The MMP-1 peptide was also reconstituted from freeze-dried powder with TEOA, after which it was the last constituent added to prevent the hydrogel from setting too soon. If desired, heparin (Hep-Ac) could also be added. After addition of all the constituents, the hydrogels had a final PEG concentration of 3.5 or 3.25% (m/v).

Table 2: Making a 3.5% 100 µl 4-arm PEG-VS hydrogel

Hydrogel constituents	Initial stock concentration	Volume (µl)
PEG-VS	10 mg/100 µl (10%)	32.5
RGD	0.1 mg/ 60 µl	7.2
Heparin*	1.5 mg/100 µl	3.24
TEOA	0.3 M	40.96
MMP-1 peptide	1 mg/ 23.8 µl	16.1
Total volume	100 µl	

*For non-heparinised hydrogels, the heparin volume was replaced by TEOA

4.3.4. Formation of the 8-arm PEG-VS/Ac hydrogels

For these 8-arm PEG hydrogels, the MMP-1 peptide and PEG monomers were combined in a molar ratio of 4:1, respectively. When cellular adhesion was needed, RGD was added in the same 12.5:1 molar ratio as for the 4-arm PEG hydrogels aforementioned. If desired, Hep-Ac could be added at the same concentration as above. To create hybrid PEG-Ac/PEG-VS hydrogels, 25%, 50%, 75% or 100% of the PEG-Ac volume was replaced with PEG-VS. These hydrogels were made up to a final PEG concentration of 4% (m/v).

Table 3 below shows an example of the volumes used to create a 100 µl 8-arm 25% PEG-Ac hydrogel. Volumes could again be adapted as needed. 8-arm PEG hydrogels containing 25% PEG-Ac and 75% PEG-VS – referred to as 25% PEG-Ac hydrogels – were created using the stock concentrations and volumes in Table 3. Using the same stocks, PEG-Ac and PEG-VS ratios were altered to create the other hydrogels (Table A5, Appendix 1). When hydrogels were prepared for the in vivo subcutaneous implant study, iso-PBS (Table A4, Appendix 1) was used to reconstitute constituents and make the hydrogels up to a final volume.

Table 3: Making a 100 µl 8-arm 25% PEG-Ac hydrogel

Hydrogel constituents	Initial stock concentration	Volume (µl)
8-arm PEG-VS	10 mg/100 µl (10%)	30
8-arm PEG-Ac	10 mg/100 µl (10%)	10
RGD	0.1 mg/ 60 µl	9.84
Heparin*	1.5 mg/100 µl	4
TEOA/Iso-PBS	0.3 M	13.16
MMP-1 peptide	1 mg/ 23.8 µl	33
Total volume	100 µl	

4.3.5. Rheological analyses of PEG hydrogels

For rheological analyses of PEG hydrogels, flat discs are optimal [246]. Hydrogels were set between two glass plates with spacers. First, the glass plates were siliconised by coating them with Sigmacote®. The plates were air dried, rinsed with distilled water and buffed dry with tissue paper. 4 glass coverslips were placed on either side of the plates, giving the hydrogels a thickness of approximately 4 mm.

The 4-arm and 8-arm PEG hydrogels were made in the same manner as described above, with each hydrogel 100 µl in size. After adding all constituents together, the hydrogels were pipetted onto a glass plate, after which the second plate was lowered and used to sandwich the hydrogels. To keep the glass plates together, foldback office clips were used on either side.

The hydrogels were left to set at room temperature for one hour and then immersed in distilled water overnight. The plates were carefully separated using a blade, and hydrogels lifted off the glass plates using a siliconised glass coverslip.

Once lifted, the hydrogels were placed into 35 x 10 mm siliconised petri dishes containing distilled water and equilibrated for 1 hour.

Small strain oscillatory shear rheometry was conducted in a similar manner to that described by Goetsch et al. (2015) using a Kinexus Pro rheometer (Malvern Instruments, U.K.), with the upper geometry being a flat plate with a 20 mm diameter. The lower geometry was set to 37 °C with the rheometer hood closed. Once it had reached temperature, the hood was opened and a hydrogel placed onto the lower geometry. The upper geometry was lowered onto the hydrogel until a normal force (N) of approximately 0.5 N was reached, with the gap being 0.5 – 0.65 mm for all hydrogels analysed. A frequency sweep was conducted from 0.5 to 5 Hz with 1% strain to obtain the storage (G') and the loss (G'') moduli. The G' and G'' values of the hydrogels analysed were represented and compared at 1 Hz.

4.3.6. Swelling analysis of heparinised 4% 8-arm PEG-Ac/PEG-VS hybrid hydrogels

The constituents for heparinised 4% 8-arm PEG-Ac/PEG-VS, were combined as described above. 20 µl hydrogels were formed on flattened Parafilm and allowed to set for one hour at 37 °C (n=4 per hydrogel type). The hydrogels were weighed to establish their initial weights. They were then swelled in microfuge tubes containing 300 µl iso-osmotic PBS with 0.02% sodium azide and 2% penicillin/streptomycin at 37 °C in a shaking incubator set to 50 revolutions per minute (RPM) for 30 days. The hydrogels were weighed at regular intervals over this 30-day period.

4.4. Establishment of of HUVEC spheroid sprouting assays

The spheroid sprouting assay pioneered by Korff and Augustin [105], conducted in collagen hydrogels, was here adapted to study invasion into our PEG hydrogels.

4.4.1. Siliconising 24-well plates for use in spheroid assays

To create hydrogel droplets, the 24-well plates needed to be siliconised. This was done by addition of Sigmacote® to each well in the laminar flow hood. The Sigmacote® was left for a few seconds and then removed. The plates were then inverted onto paper towel and left to dry inside the laminar flow hood overnight. The wells were then washed with sterile Nanopure water, and again inverted and left to dry overnight. The plates were then placed into sterilisation bags and sterilised using ethylene oxide.

4.4.2. Preparation of methylcellulose

MCDB 131 medium was prepared with a pH of 7.4 and filter sterilised. Methylcellulose (3.6 g) was weighed into a 500 ml Schott bottle containing a magnetic stirrer bar and sterilised by autoclaving. 150 ml of the sterile medium was poured into a sterile measuring cylinder. The cylinder was sealed with foil and placed into a 60 °C water bath for 15 minutes. This warmed medium was then added to the methylcellulose and stirred for 20 minutes at room temperature. Another 150 ml of medium was then added and the solution stirred at 4 °C overnight. The solution was then split into 50 ml sterile centrifuge tubes in the laminar flow hood. The tubes were then centrifuged for 2 hours at 5000 x g in a fixed head centrifuge at 23 °C, followed by a 40-minute centrifugation at 23 °C in a swinging bucket centrifuge at 3130 x g. The supernatant was then collected, pooled in sterile Schott bottles and stored at 4 °C. This solution is here referred to as methylcellulose solution.

4.4.3. Formation of spheroids and placement into PEG-VS hydrogels

HUVECs were cultured in enriched culture medium to between P2 and 4 and allowed to reach 75% confluency. The cells were then trypsinised, resuspended in standard culture medium and counted as detailed above. HUVECs were diluted to 5000 cells/ml with 6 ml methylcellulose solution and 24 ml standard culture medium. 150 µl of this cell suspension was added to each well of a round-bottom, 96-well plate (not tissue culture-treated) to create spheroids of 750 cells. It is this viscous, methylcellulose-containing medium, as well as round, untreated wells that drives spheroid formation. The plate was incubated at 37 °C for 24 hours.

PEG hydrogels were formed as per Table 2 or Table 3. Whilst the PEG-RGD mixture was incubated for 30 min at 37 °C, the spheroids created were assessed using a light microscope to ensure selection of the ones with the smoothest edges and those free of debris. The selected spheroids were harvested using a 1 ml pipette tip (cut so as to reduce sheer forces) and pooled into a 15 ml centrifuge tube. The tube was then centrifuged at 244 x g for 3 minutes to pellet the spheroids. The supernatant was slowly removed and the pellet washed by addition of 200 µl TEOA, after which the previous centrifugation step was repeated. The spheroid pellet was then carefully aspirated along with 100 µl of the supernatant and added to a 0.6 ml centrifuge tube and centrifuged in a microfuge at 100 x g for 3 minutes. Supernatant was removed from the tube (approximately the amount of TEOA one would need to make up to the final volume) and the pellet resuspended in the PEG-RGD mixture, followed by the MMP-1 peptide solution and heparin if desired.

20 µl hydrogels containing between 3 – 5 spheroids each were pipetted into the siliconised wells of a 24-well plate. Once the hydrogels had set for one hour, 1 ml of culture media, supplemented with VEGF (10 ng/ml), bFGF (10 ng/ml) or PlGF-2 (40 ng/ml and 100 ng/ml), was added. In the case of the negative control, only culture media was added.

Spheroids were incubated for 72 hours at 37 °C and 5% CO_2, with micrographs captured using a phase contrast microscope (Nikon Eclipse Ti-S). Spheroids were incubated for 120 hours in the case of the 8-arm hydrogels, and fluorescent staining carried out.

4.4.4. Fixation, fluorescent staining and visualisation of 8-arm PEG-Ac/PEG-VS hybrid hydrogels

After capturing micrographs at 120 hours, the media was removed and the hydrogels washed twice with PBS. The spheroids were then fixed using 10% formalin in PBS for 30 minutes. The wash step was then repeated and the hydrogels permeabilised with 0.1% Triton-X in PBS for 4 minutes. The hydrogels were then washed 3 times and spheroids stained using ActinRed 555 Ready Probes reagent by adding one drop of the reagent to 5 ml PBS. This solution was vortexed and 1 ml removed and added to 4 ml PBS. The hydrogels were then immersed in this diluted solution for 20 minutes at room temperature, after which they were washed 5 times with PBS. The spheroids were counterstained with Hoechst 33258 nuclear stain (1:4000 dilution) for 10 minutes at room temperature, followed by a PBS wash repeated 3 times. The hydrogels were then immersed in PBS and the plate was covered with tin foil until they were viewed using a ZEISS LSM510 Confocal microscope.

For viewing, hydrogels were lifted out of the plate and placed onto glass coverslips to allow for viewing at a higher magnification than that possible when viewing the hydrogels in the 24-well plate. Z-stacked micrographs were obtained and ZEISS Efficient Navigation (ZEN, blue edition, 2012) image acquisition and processing software used to compress the Z-stacked micrographs.

4.4.5. Analysis of results

The length of each sprout was determined using ImagesPlus software v2.0 (Motic, Hong Kong) – see
Figure **25** below which shows the software interface.

Figure 25: *Measuring the length of each spheroid sprout using Motic ImagesPlus software.*

Once all the sprouts on the spheroid had been measured, cumulative sprout length was calculated by adding all the sprout lengths together. After all spheroids' sprouts in that treatment group were measured, the cumulative sprout lengths were averaged to generate the average cumulative sprout length. Spheroids that were close together or touching, were excluded from the analysis, as well as spheroids too close to the hydrogel edge. All other spheroids were included in the analysis, regardless or sprout length or number. Sprout number per spheroid was also established.

4.5. Sustained release of growth factors from PEG hydrogels

As 3.5% 4-arm PEG-VS gels were initially utilised in the spheroid sprouting assays, growth factor release from these hydrogels was assessed.

4.5.1. 3.5% 4-arm PEG-VS hydrogels frow growth factor release

To create cumulative release profiles, showing the release of each growth factor over a period of 20 days, 5 µl 3.5% PEG-VS (m/v) hydrogels were created.

Petri dishes (35 x 10 mm) were lined with sterile Parafilm strips. The PEG hydrogels were created as in Table 1, with the hydrogel master mix volume adjusted accordingly. Each hydrogel contained 500 ng of growth factor, with the combination hydrogels containing 500 ng of bFGF and 500 ng of PlGF-2. The growth factors were added to the master mix prior to the MMP-1 peptide, with their volume deducted from the TEOA volume seen in Table 1 so as not to alter the total mix volume.

Four 5 µl gels per treatment were pipetted out onto the Parafilm and set at 37 °C for 50 minutes. Once set, the hydrogels were lifted off and placed into individual microfuge tubes containing 250 µl iso-osmotic PBS (with 1% BSA and 2% penicillin-streptomycin). The tubes were placed into a shaker (50 RPM, 37 °C) for one hour (“Wash 1”) to remove unbound growth factor. This was repeated with the hydrogels placed into fresh iso-osmotic PBS (“Wash 2”).

The hydrogels were then again placed into fresh iso-osmotic PBS and only moved on the following days thereafter: Day 1, 2, 4, 6, 8, 12, 16 and 20. The eluent in each instance was frozen at -20 ° C after collection.

After the conclusion of the release assay on Day 20, the eluent samples (iso-PBS + eluted growth factors) were diluted accordingly and analyses were conducted by use of enzyme-linked immunosorbent assays (ELISAs).

4.5.2. ELISAs to quantify growth factor release

DuoSet® ELISA Development System kits were obtained for human PlGF, VEGF and bFGF from R&D Systems (MN). Only PBS was used (pH 7.2 – 7.4) to dilute the capture antibody and reagent diluent (concentrated BSA, purchased from R&D Systems) solutions. All dilutions were carried out according to the manufacturer's instructions and all incubations took place at room temperature.

In brief, the capture antibodies were diluted to their respective working concentrations with PBS. 100 µl of this was then added to each well of an immunosorbent 96-well plate and incubated overnight. Note that during each incubation period the plate was covered with Parafilm to prevent evaporation and contamination. The wells were washed with 400µl wash buffer (0.05% Tween®20 in PBS) three times and then blocked with 300µl reagent diluent (diluted accordingly) and incubated at 1 hour. The wash step was then repeated. 100 µl of each eluent sample, diluted (1:100) with reagent diluent, was added to the wells and incubated for 1 hour 30 minutes.

The growth factor standards were prepared by serial dilution using fresh growth factor (that purchased from Peprotech, and used for the release assays, not that supplied in the kit). The standard curve was carried out in duplicate. After a 2-hour incubation period, the wash step was repeated and 100µl of biotinylated detection antibody added to each well. After a 1 hour 30-minute incubation, the wells were washed once again and 100µl of streptavidin-horse radish peroxidase (strep-HRP) was added to each well.

After the wells were incubated with strep-HRP at room temperature for 30 minutes, the wells were again washed and 100 µl of the substrate solution (a 1:1 mixture of Solutions A and B – hydrogen peroxide and tetra-methyl-benzidine respectively – supplied in the colour reagent pack, R&D Biosystems) was added to each well. The plate was then incubated for 15 - 20 minutes and monitored for colourimetric changes. To stop the reaction, 50 µl of the stop solution (2 N H_2SO_4) was added to each well and the optical density read at 450 nm, with background correction at 570 nm, using an iMark microplate reader (BioRad, CA).

The amount of growth factor released (ng/ml) on each selected day was calculated using the standard curve and used to create cumulative release curves. The amount of growth factor bound was calculated by subtracting the amount of growth factor contained in each wash from the total amount of growth factor loaded into each hydrogel.

4.6. *In vivo* study: subcutaneous implant assay

This study was approved by the Animal Research and Ethics Committee of the University of Cape Town (HSF AEC 014/016) and was in keeping with the Principles of Laboratory Care and followed the guidelines within the National Research Council's Guide for the Care and Use of Laboratory Animals (National Institutes of Health, publication # 86-23).

The 2 mm x 5.4 mm (thickness x diameter) polyurethane (P.U.) discs used were manufactured by the Polymer Laboratory as previously described by Bezuidenhout et al. (2002) [366]. The discs possessed an 82% porosity and pore sizes of 157 ± 1 µm. Sterilisation of the discs took place by immersion in a tube of 70% ethanol which was sonicated for 20 minutes. After placing the discs into the wells of a sterile 96-well plate, 100 µl of the hydrogel solution (Table 3 and Table A5, Appendix 1) was pipetted onto the first disc. The disc was then repeatedly squeezed with a 1 ml syringe plunger to allow for air removal and hydrogel infiltration.

4.6.1. Subcutaneous implantation and subsequent removal of polyurethane discs

The subcutaneous implants were carried out in male Wistar rats (n=4) as previously described by Goetsch et al. (2015) [120]. Note that aseptic technique was used for surgical procedures.

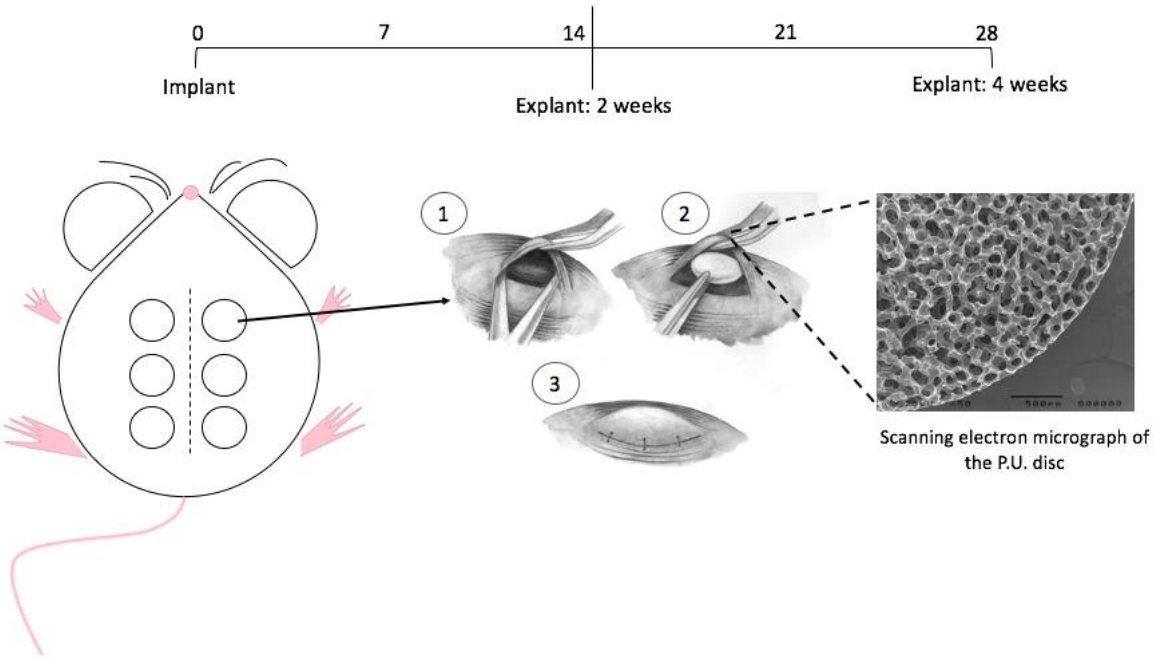

Figure 26: Schematic depicting subcutaneous implant model in rats. *P.U. discs were impregnated with the different hydrogels before polymerisation. Subcutaneous pockets were made along the dorsal midline (1) into which the discs were placed (2), with 6 randomised discs per rat. The pockets were then sutured closed (3). Explants took place at 2 and 4 weeks. Surgical images adapted from Pelhares et al. (2009). Scanning electron micrograph shows the porous nature of P.U. discs.*

After induction of anaesthesia using isoflourane, the animals were shaved and the surgical area prepared with povidine iodine. Longitudinal incisions, approximately 1 cm in length, were made on either side of the dorsal line (Figure 26). A pocket for each disc was then made, subcutaneously, by blunt dissection. The discs were then implanted into the pockets, with each rat obtaining one disc from each of the 5 groups. The incisions were then sutured closed using single 4.0 prolene sutures. It is to be noted that the individual

carrying out the surgery was blinded to the treatment groups and the implant position randomised for each animal.

After 2 weeks had elapsed, half of the impregnated P.U. discs were excised, with the other half to be excised after 4 weeks. To do this, the animals were euthanised by halothane inhalation. The discs were then surgically excised post mortem.

4.6.2. Histological processing and staining of implants

The excised discs were cut in half with a scalpel so that the cross-sections could be stained and visualised. Each half was placed into a separate sample jar containing 10% buffered formalin for fixation. 24 hours later, the discs were placed into 70% ethanol before being processed.

4.6.2.1. Wax processing and embedding

The P.U. discs were removed from the ethanol and placed into histology cassettes. The cassettes were then placed into wire mesh baskets and immersed in graded alcohol (70% to 90%), for 60 minutes in each. The samples were then immersed in 100% alcohol three times for 60 minutes each. This was followed by 3 changes of iso-octane, and then 3 changes of paraffin wax for 60 minutes each at 60 °C, with the final change being 120 minutes.

The cassettes were then opened, the samples placed into embedding moulds and hot wax poured in. Once the blocks were turned out, the samples were sectioned using a microtome.

4.6.2.2. Staining

Once mounted on microscope slides, sections were stained with haematoxylin and eosin (H&E) to quantify tissue invasion. First, the sections were dewaxed using trimethylpentane for 10 minutes. This was repeated twice more. The sections were then immersed in 100% alcohol three times, followed by two immersions in 96% alcohol and two in 70% alcohol. This was followed by immersion in distilled water. The slides were then placed in haematoxylin and then under running tap water, both for 5 minutes. The slides were then moved to eosin for 30 seconds, dipped into distilled water and then immersed in the alcohols mentioned above. Coverslips with a drop of Canada Balsam were then inverted and placed on top of the sections and allowed to dry.

In order to visualise the presence of collagen fibres, a picrosirius red stain was used. The sections were dewaxed as aforementioned, followed by staining with Weigert's haematoxylin for 8 minutes and a wash under tap water for 10 minutes. Picrosirius red staining was then conducted for 1 hour, and the sections wash twice in acidified water. Water was removed from the slides by shaking and the sections were dehydrated using three changes of 100% ethanol. Coverslips were then mounted onto the samples and allowed to dry.

4.6.2.3. Microscopic viewing and analysis

The H&E- and picrosirius red-stained sections were viewed at 100 x magnification using a Nikon 90i microscope and micrographs captured. These were then stitched together using the Nikon Eclipse software to form one image of the entire disc cross-section. Analysis was then conducted using Visiopharm Integrated Systems (VIS) analysis software by an individual that was blinded to the treatment groups. The amount of tissue ingrowth was quantified manually from the H&E-stained sections. Collagen fibre presence was then

quantified by training the VIS software to detect picrosirius red staining using the decision forest classifier machine learning model.

4.7. Statistical analyses

All statistical analyses were conducted using IBM SPSS Statistics v25.0.0 (IBM Corporation, NY), unless otherwise stated below, with statistical significance being defined as $p<0.05$ (*) and $P<0.01$ (**). Errors bars are either represented as standard deviation (SD) or standard error of the mean (SEM).

Once normal distributions were confirmed by Shapiro-Wilk testing, mean values between groups were compared using One-way Analysis of Variance (ANOVA) followed by the Tukey HSD post-hoc test for the spheroid assays.

Analyses of all other data were conducted using Student's T-tests [two-sample equal variance (homoscedastic)] in Excel (Microsoft Office for Mac version 15.32).

5. Appendices

Appendix 1: Recipes and reagents

All of the constituents for the solutions below were first dissolved in a beaker containing 800 ml Nanopure water. The pH was then corrected to pH 7.4 using NaOH/HCl and the solution brought up to the final volume of 1 L in a volumetric flask, unless otherwise specified. If needed, the solutions were then sterilised by autoclaving. For cell culture media, sterilisation was carried out using a vacuum pump attached to a 0.22 µm low protein-binding Schott bottle filter and stored at 4 °C.

Table A1: MCDB 131 culture medium recipe and constituents (for 1L)

Constituents	Amount added
MCDB 131 (powdered)	1 bottle (11.6 g)
Sodium bicarbonate	1.18 g
Nanopure H_2O	1 L

Table A2: DMEM culture medium recipe and constituents (for 1 L)

Constituents	Amount added
DMEM (powdered)	1 bottle (13.4 g)
Sodium bicarbonate	3.7 g
Nanopure H_2O	1 L

Table A3: Phosphate-buffered saline (PBS) recipe and constituents (for 1 L)

Constituents	Amount added
NaCl (137 mM)	8 g
KCl (2.7 mM)	0.2 g
KH_2PO_4 (1.4 mM)	0.2 g
$Na_2HPO_4.12H_2O$ (8 mM)	2.9 g
Nanopure H_2O	1 L

Table A4: Iso-osmotic PBS recipe and constituents (for 1L)

	Constituents	Amount added
Solution A	$NaH_2PO_4.H_2O$	20.7 g
Solution B	$NaH_2PO_4.12H_2O$	53.7 g
Solution C	NaCl	9 g
Iso-osmotic PBS	65 ml Solution A + 435 Solution B + 500ml Solution C	

*Note that pH was correct to pH 7.4 using Solution A and B, not NaOH or HCl

Table A5: 8-arm PEG-VS hydrogels for subcutaneous implants – to make a 100 µl hydrogel

Gel constituents	Volume (µl)
8-arm PEG	For 0% PEG-Ac hydrogels:
PEG-VS	40* 40 µl total
PEG-Ac	0*
	For 25% PEG-Ac hydrogels:
PEG-VS	30* 40 µl total
PEG-Ac	10*
	For 75% PEG-Ac hydrogels:
PEG-VS	10* 40 µl total
PEG-Ac	30*
	For 100% PEG-Ac hydrogels:
PEG-VS	0* 40 µl total
PEG-Ac	40*
MMP-1	33**
Heparin	4 (of a 1.5% solution in iso-PBS)
RGD	9.84
Iso-PBS	13.16
TOTAL	**100**

* of a 10% stock solution in iso-PBS

** of a solution made by addition of 9 mg MMP-1 recognition peptide to 214.2 µl iso-PBS

Many experiments to follow involved the use of growth factors, all of which were obtained from Peprotech, Rocky Hill, NJ. Before growth factors could be utilised in these experiments, they were reconstituted using diluents specified by the manufacturer (Table A6) to a stock concentration of 1 μg/μl and stored at -20 °C.

Table A6: Solutions for reconstitution of growth factors

Growth factor	Diluent
bFGF	5 mM Tris, pH 7.6
EGF	Sterile, de-ionised H_2O
PlGF-2	
VEGF	

When diluting growth factors to concentrations needed experiments, sterile 0.1% BSA-PBS was used. The carrier protein (BSA) was included to prevent binding of the growth factors to the storage tubes.

Table A7: Collagenase recipe and constituents

Constituents	Amount added
Collagen type II powder	168 g
Nanopure H_2O	240 ml

Once the collagen powder was weighed, it was added to the PBS and was stirred in a beaker (covered with tinfoil to prevent exposure to light) until dissolved. The solution was then filtered and aliquoted into 50 ml tubes. The tubes were covered in tinfoil and frozen at -20 °C. When ready to use, the tubes were slowly thawed at room temperature.

Table A8: Triethanolamine (TEOA) recipe (0.3 M)

Constituents	Amount added
TEOA	2.24 g*
Nanopure H_2O	50 ml

*Note the TEOA was weighed rather than volumetrically measured due to its viscosity.

After the 2.24 g of TEOA was weighed, 30 ml of Nanopure H_2O was added. The solution was vortexed and then corrected to pH 7.4 (with NaOH or HCl) and made up to a final volume of 50 ml using a volumetric flask. The solution was then sterilised using a syringe filter.

Appendix 2: Details of all specialised reagents used

Table A9: Growth Factors

Product	Producer / Supplier	Product Catalogue Number
Human fibroblast growth factor-basic (bFGF) 154 a.a.	Peprotech, Rocky Hill, NJ	100-18B-100UG
Human epidermal growth factor (EGF)		AF-100-15 250µg
Recombinant human placental growth factor-2 (PlGF-2)		100-56-100UG
Recombinant Human vascular endothelial growth factor 165 (VEGF)		100-20-10UG

Table A10: ELISA kits, ancillary products and consumables

	Product	Manufacturer	Product Catalogue Number
ELISA kits	DuoSet® ELISA Development system – Human bFGF	R&D Systems, Minneapolis, MN	DY233 and DY233-05
	DuoSet® ELISA Development system – Human PlGF		DY-264
	DuoSet® ELISA Development system – Human VEGF		DY293B-05
Ancillary products	Reagent diluent concentrate 1		DY997 – 21ml
Consumables	Maxisorp 96-well plates, non-sterile	Nunc, Roskilde, Denmark	44-2404-21

Table A11: PEG hydrogel constituents

Product	Manufacturer	Product Catalogue Number
PEG-OH 20 kDa, 4-arm	Nektar Therapeutics, Huntsville, AL	0J000P04
PEG-OH 20 kDa, 8-arm		0J000P08
PEG-Ac 20 kDA, 8-arm	Jenkem, Plano, TX	no catalogue number
RGD (GCGYGRGDSPG, MW = 1025.06g/mol)	GenicBio Synthetic Peptide, Shanghai, China	100 mg, no catalogue number on tube
MMP-1 (GCREGPQGIWGQERCG, MW = 1732.91g/mol)	GenScript USA Inc., Piscataway, NJ	U5878BB230-1 (100 mg per vile)

Appendix 3: Details of all general reagents used

Table A12: Details of general reagents used

Product	Producer / Supplier	Product Catalogue Number
Actin Red™ ReadyProbes® Reagent	Life Technologies	R37112
Alexa Fluor® 488 goat anti-mouse IgG secondary antibody	Molecular Probes®, (Life Technologies, USA)	A11029
Bovine serum albumin (IgG-free, Protease-free)	Jackson ImmunoResearch, Westgrove, PA	001-000-162 – 50g
Collagen type I (bovine skin)	Sigma-Aldrich®, St Louis, MO	C4243-20ML
Collagenase type II (HUVEC isolation)	Worthington Biochemical Corporation, Lakewood, NJ	LS004174
Dimethyl Sulfoxide (DMSO)	Sigma-Aldrich®, St Louis, MO	D2650 – 5X1ML
DMEM		D5648-10X1L
Ethanol	Servochem (PTY) LTD, Montague Gardens, Cape Town, RSA	no catalogue number
Fluoroshield with DAPI	Sigma-Aldrich®, St Louis, MO	F6057 – 20ml
Foetal Bovine Serum (FBS) (gamma irradiated) – 1	Gibco® by Life Technologies™, Paisley, UK	10499-044 – 500ml
Foetal Bovine Serum (FBS) Superior (heat inactivated) – 2	Biochrom GmbH, Berlin, Germany	S0615 – 500ml

Gentamicin solution	Sigma-Aldrich, St Louis, MO	G1272 – 10ml
Hydrocortisone		H0396-100MG
L-Glutamine		G-8540-100G
Medium 199 growth medium (liquid)		M4530
Mouse anti-human CD31 primary antibody (monoclonal)	Dako, Agilent Technologies, C.A.	M0823
MCDB-131 Medium	Sigma-Aldrich, St Louis, MO	M8537
Methylcellulose – 4000 centipoises		M-0512 100g
Heparin NaCl		H3393-50KU
Heparin sodium, mucosal (5000 I.U./ml)	Fresenius Kabi Manufacturing, Johannesberg, R.S.A	no catalogue number
Hoechst 33258	ThermoFischer Scientific, OR	H3569 – 10 ml
Hydrochloric acid (HCl), 25% w/v	Honeywell Riedel-deHaën, Seelze, Germany	30723 – 2.5L
Penicillin Streptomycin (10 000 U penicillin and 10 mg streptomycin/ml)	Sigma-Aldrich®, St Louis, MO	P0781 (100X concentration)
Penicillin Streptomycin (10 000 U/ml / 10 000 µg/ml)	Gibco® by Life Technologies, Carlsbad, CA	15140-122 (100 ml)
Sigmacote®	Sigma-Aldrich®, St Louis, MO	SL2-100mL
Sodium bicarbonate ($NaHCO_3$)		S-5761-1KG

Sodium Chloride (NaCl)		S-7653-1KG
Sodium Dodecyl Sulfate – SDS		L3771-100G
Sodium Hydroxide (NaOH)		S-5881-500G
Sodium Phosphate Dibasic Dodecahydrate ($Na_2HPO_4.12H_2O$)		71649-500G
Sodium Phosphate Monobasic Monohydrate ($NaH_2PO_4.H_2O$)		S9638-500G
Triethanolamine (TEOA) 99%	Saarchem-Holpro Analytic, Krugersdorp, R.S.A	6112040 -2.5L
Triton-X (used to permeabilise PEG)	Sigma Aldrich®, St Louis, MO	T8532 – 500ML
Trypan Blue		T8154-100ML
Trypsin-EDTA (10X) 100ml		59427C-100ML
Tween® 20		P1379

Appendix 4: Details of all consumables used

Table A13: Details of general consumables used

Product	Producer / Supplier	Product Catalogue Number
40 µl Cuvette Pack of 100 with stoppers	Malvern Instruments LTD., Worcestershire, UK	ZEN0040
0.6ml Graduated Microcentrifuge Tube with flat cap	Thermo Scientific QSP, San Diego, CA	502-GRD-Q
1.5ml Graduated Microcentrifuge Tube with flat cap		509-GRD-Q
2ml Graduated Microcentrifuge Tube with locking cap		L-508GRD-Q
24-well clear, flat bottomed, sterile tissue culture treated plate	Corning Inc., Corning, NY	Costar® 3524
96-well clear, flat bottomed, sterile tissue culture treated plate		3595
96-well clear, round bottomed, sterile plate, non-tissue culture treated	Thermo Scientific™ Nunc™, Roskilde, Denmark	268200
15ml centrifuge tube	Falcon by BD Biosciences, San Jose, CA	352096
50ml centrifuge tube	Thermo Scientific™ Nalgene™, Waltham, MA	352070

Mr Frosty freezing container, Nalgene	Sigma-Aldrich®, St Louis, MO	C1562
Parafilm M® 4 in. X 250 ft. roll	Bemis NA, Neenah, WI	PM 999
Straight-side Wide-Mouth Jar (1 L)– for umbilical cord incubation	Thermo Scientific™ Nalgene™, Waltham, MA	2116-1000

Appendix 5: Details of all equipment used

Table A14: Details of equipment used

Product	Producer / Supplier
Centrifuge – J2-21 with a JA20 rotor, for centrifuging methylcellulose	Beckman Coulter Life Sciences, Indianapolis, IN
Centrifuge – Megafuge 1.0R	Heraeus, Hanau, Germany
Centrifuge – 5415R (for microcentrifuge tubes)	Eppendorf, Hamburg, Germany
Freeze Dryer – VirTis	SP Industries, Gardiner, NY
Haemocytometer	Improved Neubauer, Baxter Scientific, Deerfield, IL
iMark plate reader	Biorad, Hercules, CA
Incubator (for all 37 °C cell culture)	HERA Cell by Heraeus, Hanau, Germany
MCO-175M, O_2/CO_2 Incubator	Osaka Sanyo Electric Co., Osaka, Japan
Microscope – Nikon Eclipse Ti-S Light microscope	Nikon, Tokyo, Japan
Microscope – Nikon Fluorescent Microscope (Nikon Eclipse 90i DS-Ri1)	
Microscope - ZEISS LSM510 Confocal microscope with MaiTai two photon laser	Carl Zeiss Microscopy GmbH, Göttingen, Germany
pH meter – 3510	Jenway by Bibby Scientific, Staffordshire, UK
Pipettes	Gilson, Inc. Middleton, WI

Rheometer - Kinexus Pro	Malvern Instruments, UK
Shaking incubator	IncoShake by Labotech, Cape Town, RSA
Water Bath – Grant Y14	Grant Instruments, Cambridge, UK
37°C incubator for tissue culture	MCO-175M, O2/CO2 Incubator, Osaka Sanyo Electric Co., Japan
	Heraeus, Hanau, Germany
-65 °C freezer	Snijders Scientific, Tilburg, Netherlands

6. Literature cited

[1] J.G. Mill, I. Stefanon, L. dos Santos, M.P. Baldo, Remodeling in the ischemic heart: the stepwise progression for heart failure, Brazilian Journal of Medical and Biological Research. 44 (2011) 890–898. doi:10.1590/S0100-879X2011007500096.

[2] D. Bradshaw, P. Groenewald, R. Laubscher, N. Nannan, B. Nojilana, R. Norman, D. Pieterse, M. Schneider, Initial Burden of Diseases Estimates for South Africa, 2000, (2003). http://www.mrc.ac.za/bod/initialbodestimates.pdf.

[3] G.A. Mensah, G.A. Roth, U.K.A. Sampson, A.E. Moran, V.I. Feigin, M.H. Forouzanfar, M. Naghavi, C.J.L. Murray, Mortality from cardiovascular diseases in sub-Saharan Africa, 1990–2013: a systematic analysis of data from the Global Burden of Disease Study 2013: cardiovascular topic, Cardiovascular Journal Of Africa. 26 (2015) S6–S10. doi:10.5830/CVJA-2015-036.

[4] World Health Organisation, Global status report on noncommunicable diseases 2010, (2011). http://www.who.int/nmh/publications/ncd_report_full_en.pdf (accessed January 11, 2018).

[5] A.K. Keates, A.O. Mocumbi, M. Ntsekhe, K. Sliwa, S. Stewart, Cardiovascular disease in Africa: epidemiological profile and challenges, Nature Reviews Cardiology. 14 (2017) 273–293. doi:10.1038/nrcardio.2017.19.

[6] S. Kathiresan, D. Srivastava, Genetics of Human Cardiovascular Disease, Cell. 148 (2012) 1242–1257. doi:10.1016/j.cell.2012.03.001.

[7] R.H. Eckel, J.M. Jakicic, J.D. Ard, J.M. de Jesus, N.H. Miller, V.S. Hubbard, I.-M. Lee, A.H. Lichtenstein, C.M. Loria, B.E. Millen, C.A. Nonas, F.M. Sacks, S.C. Smith, L.P. Svetkey, T.A. Wadden, S.Z. Yanovski, 2013 AHA/ACC Guideline on Lifestyle Management to Reduce Cardiovascular Risk: A Report of the American College of Cardiology/American Heart Association Task Force on Practice Guidelines, Circulation. 129 (2014) S76–S99. doi:10.1161/01.cir.0000437740.48606.d1.

[8] L. Masana, E. Ros, I. Sudano, D. Angoulvant, D. Ibarretxe Gerediaga, N. Murga Eizagaechevarria, V. Arrarte, A. García-Quintana, A. Zamora Cervantes, A. Mello e Silva, O. Weingärtner, A. Schlitt, M. Piedecausa, Is there a role for lifestyle changes in cardiovascular prevention? What, when and how?, Atherosclerosis Supplements. 26 (2017) 2–15. doi:10.1016/S1567-5688(17)30020-X.

[9] K. Sakakura, M. Nakano, F. Otsuka, E. Ladich, F.D. Kolodgie, R. Virmani, Pathophysiology of atherosclerosis plaque progression, Heart Lung Circ. 22 (2013) 399–411. doi:10.1016/j.hlc.2013.03.001.

[10] R. Virmani, F.D. Kolodgie, A.P. Burke, A. Farb, S.M. Schwartz, Lessons from sudden coronary death: a comprehensive morphological classification scheme for atherosclerotic lesions, Arteriosclerosis, Thrombosis, and Vascular Biology. 20 (2000) 1262–1275.

[11] A.C. van der Wal, A.E. Becker, C.M. van der Loos, P.K. Das, Site of intimal rupture or erosion of thrombosed coronary atherosclerotic plaques is characterized by an inflammatory process irrespective of the dominant plaque morphology, Circulation. 89 (1994) 36–44. doi:10.1161/01.CIR.89.1.36.

[12] C.L. Hastings, E.T. Roche, E. Ruiz-Hernandez, K. Schenke-Layland, C.J. Walsh, G.P. Duffy, Drug and cell delivery for cardiac regeneration, Advanced Drug Delivery Reviews. 84 (2015) 85–106. doi:10.1016/j.addr.2014.08.006.

[13] M.A. Laflamme, C.E. Murry, Regenerating the heart, Nature Biotechnology. 23 (2005) 845–856. doi:10.1038/nbt1117.

[14] M. Domenech, L. Polo-Corrales, J.E. Ramirez-Vick, D.O. Freytes, Tissue Engineering Strategies for Myocardial Regeneration: Acellular Versus Cellular Scaffolds?, Tissue Engineering Part B: Reviews. 22 (2016) 438–458. doi:10.1089/ten.teb.2015.0523.

[15] J.R. Venugopal, M.P. Prabhakaran, S. Mukherjee, R. Ravichandran, K. Dan, S. Ramakrishna, Biomaterial strategies for alleviation of myocardial infarction, Journal of The Royal Society Interface. 9 (2012) 1–19. doi:10.1098/rsif.2011.0301.

[16] L.C. Lee, Z. Zhihong, A. Hinson, J.M. Guccione, Reduction in Left Ventricular Wall Stress and Improvement in Function in Failing Hearts using Algisyl-LVR, Journal of Visualized Experiments. (2013). doi:10.3791/50096.

[17] L.H. Opie, P.J. Commerford, B.J. Gersh, M.A. Pfeffer, Controversies in ventricular remodelling, The Lancet. 367 (2006) 356–367. doi:10.1016/S0140-6736(06)68074-4.

[18] R.H. Woods, A Few Applications of a Physical Theorem to Membranes in the Human Body in a State of Tension, Journal of Anatomy and Physiology. 26 (1892) 362–370.

[19] I.L. Piña, E.A. Madigan, Section 1: The Syndrome of Heart Failure, Chapter 1: The Basics, in: J.S. Alpert, L.T. Braun (Eds.), Heart Failure: Strategies to Improve Outcomes, Cardiotext publishing, Minnesota, 2013: p. 102.

[20] K.C. Wollert, G.P. Meyer, J. Lotz, S. Ringes Lichtenberg, P. Lippolt, C. Breidenbach, S. Fichtner, T. Korte, B. Hornig, D. Messinger, L. Arseniev, B. Hertenstein, A. Ganser, H. Drexler, Intracoronary autologous bone-marrow cell transfer after myocardial infarction: the BOOST randomised controlled clinical trial, The Lancet. 364 (2004) 141–148. doi:10.1016/S0140-6736(04)16626-9.

[21] R.P. Giugliano, E. Braunwald, Selecting the Best Reperfusion Strategy in ST-Elevation Myocardial Infarction: It's All a Matter of Time, Circulation. 108 (2003) 2828–2830. doi:10.1161/01.CIR.0000106684.71725.98.

[22] D.M. Nelson, Z. Ma, K.L. Fujimoto, R. Hashizume, W.R. Wagner, Intra-myocardial biomaterial injection therapy in the treatment of heart failure: Materials, outcomes and challenges, Acta Biomaterialia. 7 (2011) 1–15. doi:10.1016/j.actbio.2010.06.039.

[23] P. Shah, P. Pellicori, J. Cuthbert, A.L. Clark, Pharmacological and Non-pharmacological Treatment for Decompensated Heart Failure: What Is New?, Current Heart Failure Reports. 14 (2017) 147–157. doi:10.1007/s11897-017-0328-x.

[24] D.L. Mann, Mechanisms and models in heart failure: A combinatorial approach, Circulation. 100 (1999) 999–1008.

[25] S. Mitsos, K. Katsanos, E. Koletsis, G.C. Kagadis, N. Anastasiou, A. Diamantopoulos, D. Karnabatidis, D. Dougenis, Therapeutic angiogenesis for myocardial ischemia revisited: basic biological concepts and focus on latest clinical trials, Angiogenesis. 15 (2012) 1–22. doi:10.1007/s10456-011-9240-2.

[26] I.L. Piña, E.A. Madigan, Section 1: The Syndrome of Heart Failure, Chapter 1: The Basics, in: J.S. Alpert, L.T. Braun (Eds.), Heart Failure: Strategies to Improve Outcomes, Cardiotext publishing, Minnesota, 2013: p. 121.

[27] G. Casu, P. Merella, Diuretic Therapy in Heart Failure: Current Approaches, European Cardiology Review. 10 (2015) 42. doi:10.15420/ecr.2015.10.01.42.

[28] W.F. Peacock, M.R. Costanzo, T. De Marco, M. Lopatin, J. Wynne, R.M. Mills, C.L. Emerman, Impact of Intravenous Loop Diuretics on Outcomes of Patients Hospitalized with Acute Decompensated Heart Failure: Insights from the ADHERE Registry, Cardiology. 113 (2009) 12–19. doi:10.1159/000164149.

[29] H. Valantine, Cardiac allograft vasculopathy after heart transplantation: risk factors and management, The Journal of Heart and Lung Transplantation. 23 (2004) S187–S193. doi:10.1016/j.healun.2004.03.009.

[30] N.R. Johnson, M. Kruger, K.P. Goetsch, P. Zilla, D. Bezuidenhout, Y. Wang, N.H. Davies, Coacervate Delivery of Growth Factors Combined with a Degradable Hydrogel Preserves Heart Function after Myocardial Infarction, ACS Biomaterials Science & Engineering. 1 (2015) 753–759. doi:10.1021/acsbiomaterials.5b00077.

[31] Y.-R. Yun, J.E. Won, E. Jeon, S. Lee, W. Kang, H. Jo, J.-H. Jang, U.S. Shin, H.-W. Kim, Fibroblast Growth Factors: Biology, Function, and Application for Tissue

Regeneration, Journal of Tissue Engineering. 1 (2010) 218142. doi:10.4061/2010/218142.

[32] L. Deveza, J. Choi, F. Yang, Therapeutic Angiogenesis for Treating Cardiovascular Diseases, Theranostics. 2 (2012) 801–814. doi:10.7150/thno.4419.

[33] G. Zhang, L.J. Suggs, Matrices and scaffolds for drug delivery in vascular tissue engineering, Advanced Drug Delivery Reviews. 59 (2007) 360–373. doi:10.1016/j.addr.2007.03.018.

[34] A.M. van der Laan, J.J. Piek, N. van Royen, Targeting angiogenesis to restore the microcirculation after reperfused MI, Nature Reviews Cardiology. 6 (2009) 515–523. doi:10.1038/nrcardio.2009.103.

[35] I. Shiojima, K. Sato, Y. Izumiya, S. Schiekofer, M. Ito, R. Liao, W.S. Colucci, K. Walsh, Disruption of coordinated cardiac hypertrophy and angiogenesis contributes to the transition to heart failure, Journal of Clinical Investigation. 115 (2005) 2108–2118. doi:10.1172/JCI24682.

[36] R. Passier, L.W. van Laake, C.L. Mummery, Stem-cell-based therapy and lessons from the heart, Nature. 453 (2008) 322–329. doi:10.1038/nature07040.

[37] S. Banquet, E. Gomez, L. Nicol, F. Edwards-Levy, J.-P. Henry, R. Cao, D. Schapman, B. Dautreaux, F. Lallemand, F. Bauer, Y. Cao, C. Thuillez, P. Mulder, V. Richard, E. Brakenhielm, Arteriogenic Therapy by Intramyocardial Sustained Delivery of a Novel Growth Factor Combination Prevents Chronic Heart Failure, Circulation. 124 (2011) 1059–1069. doi:10.1161/CIRCULATIONAHA.110.010264.

[38] K.K.L. Ho, J.L. Pinsky, W.B. Kannel, D. Levy, The epidemiology of heart failure: The Framingham Study, Journal of the American College of Cardiology. 22 (1993) A6–A13. doi:10.1016/0735-1097(93)90455-A.

[39] S. Takeshita, L.P. Zheng, E. Brogi, M. Kearney, L.Q. Pu, S. Bunting, N. Ferrara, J.F. Symes, J.M. Isner, Therapeutic angiogenesis. A single intraarterial bolus of vascular endothelial growth factor augments revascularization in a rabbit ischemic hind limb model., Journal of Clinical Investigation. 93 (1994) 662–670. doi:10.1172/JCI117018.

[40] R.J. Laham, M. Rezaee, M. Post, F.W. Sellke, R.A. Braeckman, D. Hung, M. Simons, Intracoronary and intravenous administration of basic fibroblast growth factor: myocardial and tissue distribution, Drug Metabolism and Disposition: The Biological Fate of Chemicals. 27 (1999) 821–826.

[41] P. Tayalia, D.J. Mooney, Controlled Growth Factor Delivery for Tissue Engineering, Advanced Materials. 21 (2009) 3269–3285. doi:10.1002/adma.200900241.

[42] M. Simons, J.A. Ware, Therapeutic angiogenesis in cardiovascular disease, Nature Reviews Drug Discovery. 2 (2003) 863–872. doi:10.1038/nrd1226.

[43] M.-A. Renault, D.W. Losordo, Therapeutic myocardial angiogenesis, Microvascular Research. 74 (2007) 159–171. doi:10.1016/j.mvr.2007.08.005.

[44] B.H. Annex, Therapeutic angiogenesis for critical limb ischaemia, Nature Reviews Cardiology. 10 (2013) 387–396. doi:10.1038/nrcardio.2013.70.

[45] E. Brogi, G. Schatteman, T. Wu, E.A. Kim, L. Varticovski, B. Keyt, J.M. Isner, Hypoxia-induced paracrine regulation of vascular endothelial growth factor receptor expression., Journal of Clinical Investigation. 97 (1996) 469–476. doi:10.1172/JCI118437.

[46] J. Waltenberger, U. Mayr, S. Pentz, V. Hombach, Functional upregulation of the vascular endothelial growth factor receptor KDR by hypoxia, Circulation. 94 (1996) 1647–1654.

[47] P. Carmeliet, R.K. Jain, Angiogenesis in cancer and other diseases, Nature. 407 (2000) 249–257. doi:10.1038/35025220.

[48] Y.-W. Kim, T.V. Byzova, Oxidative stress in angiogenesis and vascular disease, Blood. 123 (2014) 625–631. doi:10.1182/blood-2013-09-512749.

[49] R.M. Touyz, A.M. Briones, Reactive oxygen species and vascular biology: implications in human hypertension, Hypertension Research. 34 (2011) 5–14. doi:10.1038/hr.2010.201.

[50] J.F. Turrens, Mitochondrial formation of reactive oxygen species, The Journal of Physiology. 552 (2003) 335–344. doi:10.1113/jphysiol.2003.049478.

[51] M.D. Brand, C. Affourtit, T.C. Esteves, K. Green, A.J. Lambert, S. Miwa, J.L. Pakay, N. Parker, Mitochondrial superoxide: production, biological effects, and activation of uncoupling proteins, Free Radical Biology and Medicine. 37 (2004) 755–767. doi:10.1016/j.freeradbiomed.2004.05.034.

[52] M. Ushio-Fukai, Y. Nakamura, Reactive oxygen species and angiogenesis: NADPH oxidase as target for cancer therapy, Cancer Letters. 266 (2008) 37–52. doi:10.1016/j.canlet.2008.02.044.

[53] B.L. Krock, N. Skuli, M.C. Simon, Hypoxia-Induced Angiogenesis: Good and Evil, Genes & Cancer. 2 (2011) 1117–1133. doi:10.1177/1947601911423654.

[54] A. Mutoh, S. Ueda, Peroxidized unsaturated fatty acids stimulate Toll-like receptor 4 signaling in endothelial cells, Life Sciences. 92 (2013) 984–992. doi:10.1016/j.lfs.2013.03.019.

[55] P.C. Maisonpierre, C. Suri, P.F. Jones, S. Bartunkova, S.J. Wiegand, C. Radziejewski, D. Compton, J. McClain, T.H. Aldrich, N. Papadopoulos, T.J. Daly, S. Davis, T.N. Sato, G.D. Yancopoulos, Angiopoietin-2, a natural antagonist for Tie2 that disrupts in vivo angiogenesis, Science. 277 (1997) 55–60.

[56] L.M. Coussens, W.W. Raymond, G. Bergers, M. Laig-Webster, O. Behrendtsen, Z. Werb, G.H. Caughey, D. Hanahan, Inflammatory mast cells up-regulate angiogenesis during squamous epithelial carcinogenesis, Genes & Development. 13 (1999) 1382–1397.

[57] M.J. Cross, L. Claesson-Welsh, FGF and VEGF function in angiogenesis: signalling pathways, biological responses and therapeutic inhibition, Trends in Pharmacological Sciences. 22 (2001) 201–207. doi:10.1016/S0165-6147(00)01676-X.

[58] H. Gerhardt, M. Golding, M. Fruttiger, C. Ruhrberg, A. Lundkvist, A. Abramsson, M. Jeltsch, C. Mitchell, K. Alitalo, D. Shima, C. Betsholtz, VEGF guides angiogenic sprouting utilizing endothelial tip cell filopodia, The Journal of Cell Biology. 161 (2003) 1163–1177. doi:10.1083/jcb.200302047.

[59] S. Isogai, N.D. Lawson, S. Torrealday, M. Horiguchi, B.M. Weinstein, Angiogenic network formation in the developing vertebrate trunk, Development. 130 (2003) 5281–5290. doi:10.1242/dev.00733.

[60] L.E. Benjamin, D. Golijanin, A. Itin, D. Pode, E. Keshet, Selective ablation of immature blood vessels in established human tumors follows vascular endothelial growth factor withdrawal, Journal of Clinical Investigation. 103 (1999) 159–165. doi:10.1172/JCI5028.

[61] D. Von Tell, A. Armulik, C. Betsholtz, Pericytes and vascular stability, Experimental Cell Research. 312 (2006) 623–629. doi:10.1016/j.yexcr.2005.10.019.

[62] E. Dejana, E. Tournier-Lasserve, B.M. Weinstein, The Control of Vascular Integrity by Endothelial Cell Junctions: Molecular Basis and Pathological Implications, Developmental Cell. 16 (2009) 209–221. doi:10.1016/j.devcel.2009.01.004.

[63] M.L. Iruela-Arispe, G.E. Davis, Cellular and Molecular Mechanisms of Vascular Lumen Formation, Developmental Cell. 16 (2009) 222–231. doi:10.1016/j.devcel.2009.01.013.

[64] L.-K. Phng, H. Gerhardt, Angiogenesis: A Team Effort Coordinated by Notch, Developmental Cell. 16 (2009) 196–208. doi:10.1016/j.devcel.2009.01.015.

[65] M. Hellström, L.-K. Phng, J.J. Hofmann, E. Wallgard, L. Coultas, P. Lindblom, J. Alva, A.-K. Nilsson, L. Karlsson, N. Gaiano, K. Yoon, J. Rossant, M.L. Iruela-Arispe, M. Kalén, H. Gerhardt, C. Betsholtz, Dll4 signalling through Notch1 regulates formation

of tip cells during angiogenesis, Nature. 445 (2007) 776–780. doi:10.1038/nature05571.

[66] A.F. Siekmann, N.D. Lawson, Notch signalling limits angiogenic cell behaviour in developing zebrafish arteries, Nature. 445 (2007) 781–784. doi:10.1038/nature05577.

[67] S. Artavanis-Tsakonas, M.D. Rand, R.J. Lake, Notch signaling: cell fate control and signal integration in development, Science. 284 (1999) 770–776.

[68] T. Gridley, Notch Signaling in Vertebrate Development and Disease, Molecular and Cellular Neuroscience. 9 (1997) 103–108. doi:10.1006/mcne.1997.0610.

[69] S.J. Bray, Notch signalling: a simple pathway becomes complex, Nature Reviews Molecular Cell Biology. 7 (2006) 678–689. doi:10.1038/nrm2009.

[70] U.-M. Fiuza, A.M. Arias, Cell and molecular biology of Notch, Journal of Endocrinology. 194 (2007) 459–474. doi:10.1677/JOE-07-0242.

[71] S. Claxton, M. Fruttiger, Periodic Delta-like 4 expression in developing retinal arteries, Gene Expression Patterns. 5 (2004) 123–127. doi:10.1016/j.modgep.2004.05.004.

[72] C.J. Favre, M. Mancuso, K. Maas, J.W. McLean, P. Baluk, D.M. McDonald, Expression of genes involved in vascular development and angiogenesis in endothelial cells of adult lung, American Journal of Physiology-Heart and Circulatory Physiology. 285 (2003) H1917–H1938. doi:10.1152/ajpheart.00983.2002.

[73] J.J. Hofmann, M.L. Iruela-Arispe, Notch Signaling in Blood Vessels: Who Is Talking to Whom About What?, Circulation Research. 100 (2007) 1556–1568. doi:10.1161/01.RES.0000266408.42939.e4.

[74] N. Villa, L. Walker, C.E. Lindsell, J. Gasson, M.L. Iruela-Arispe, G. Weinmaster, Vascular expression of Notch pathway receptors and ligands is restricted to arterial vessels, Mech. Dev. 108 (2001) 161–164.

[75] V. Tarallo, L. Tudisco, S. De Falco, A placenta growth factor 2 variant acts as dominant negative of vascular endothelial growth factor A by heterodimerization mechanism, American Journal of Cancer Research. 1 (2011) 265–274.

[76] N. Takehara, Y. Tsutsumi, K. Tateishi, T. Ogata, H. Tanaka, T. Ueyama, T. Takahashi, T. Takamatsu, M. Fukushima, M. Komeda, M. Yamagishi, H. Yaku, Y. Tabata, H. Matsubara, H. Oh, Controlled delivery of basic fibroblast growth factor promotes human cardiosphere-derived cell engraftment to enhance cardiac repair for

chronic myocardial infarction, Journal of the American College of Cardiology. 52 (2008) 1858–1865. doi:10.1016/j.jacc.2008.06.052.

[77] N. Ferrara, H.-P. Gerber, J. LeCouter, The biology of VEGF and its receptors, Nature Medicine. 9 (2003) 669–676. doi:10.1038/nm0603-669.

[78] R. Blanco, H. Gerhardt, VEGF and Notch in Tip and Stalk Cell Selection, Cold Spring Harbor Perspectives in Medicine. 3 (2013) a006569–a006569. doi:10.1101/cshperspect.a006569.

[79] C. Fischer, M. Mazzone, B. Jonckx, P. Carmeliet, FLT1 and its ligands VEGFB and PlGF: drug targets for anti-angiogenic therapy?, Nature Reviews Cancer. 8 (2008) 942–956. doi:10.1038/nrc2524.

[80] R. Benedito, C. Roca, I. Sörensen, S. Adams, A. Gossler, M. Fruttiger, R.H. Adams, The Notch Ligands Dll4 and Jagged1 Have Opposing Effects on Angiogenesis, Cell. 137 (2009) 1124–1135. doi:10.1016/j.cell.2009.03.025.

[81] P. Carmeliet, L. Moons, A. Luttun, V. Vincenti, V. Compernolle, M. De Mol, Y. Wu, F. Bono, L. Devy, H. Beck, D. Scholz, T. Acker, T. DiPalma, M. Dewerchin, A. Noel, I. Stalmans, A. Barra, S. Blacher, T. Vandendriessche, A. Ponten, U. Eriksson, K.H. Plate, J.-M. Foidart, W. Schaper, D.S. Charnock-Jones, D.J. Hicklin, J.-M. Herbert, D. Collen, M.G. Persico, Synergism between vascular endothelial growth factor and placental growth factor contributes to angiogenesis and plasma extravasation in pathological conditions, Nature Medicine. 7 (2001) 575–583. doi:10.1038/87904.

[82] M. Shibuya, N. Ito, L. Claesson-Welsh, Structure and function of vascular endothelial growth factor receptor-1 and -2, Current Topics in Microbiology and Immunology. 237 (1999) 59–83.

[83] G. Neufeld, T. Cohen, S. Gengrinovitch, Z. Poltorak, Vascular endothelial growth factor (VEGF) and its receptors, FASEB Journal: Official Publication of the Federation of American Societies for Experimental Biology. 13 (1999) 9–22.

[84] Y. Cao, P. Linden, D. Shima, F. Browne, J. Folkman, In vivo angiogenic activity and hypoxia induction of heterodimers of placenta growth factor/vascular endothelial growth factor., Journal of Clinical Investigation. 98 (1996) 2507–2511. doi:10.1172/JCI119069.

[85] J. DiSalvo, M.L. Bayne, G. Conn, P.W. Kwok, P.G. Trivedi, D.D. Soderman, T.M. Palisi, K.A. Sullivan, K.A. Thomas, Purification and Characterization of a Naturally Occurring Vascular Endothelial Growth Factor · Placenta Growth Factor Heterodimer, Journal of Biological Chemistry. 270 (1995) 7717–7723. doi:10.1074/jbc.270.13.7717.

[86] M. Autiero, J. Waltenberger, D. Communi, A. Kranz, L. Moons, D. Lambrechts, J. Kroll, S. Plaisance, M. De Mol, F. Bono, S. Kliche, G. Fellbrich, K. Ballmer-Hofer, D. Maglione, U. Mayr-Beyrle, M. Dewerchin, S. Dombrowski, D. Stanimirovic, P. Van Hummelen, C. Dehio, D.J. Hicklin, G. Persico, J.-M. Herbert, D. Communi, M. Shibuya, D. Collen, E.M. Conway, P. Carmeliet, Role of PlGF in the intra- and intermolecular cross talk between the VEGF receptors Flt1 and Flk1, Nature Medicine. 9 (2003) 936–943. doi:10.1038/nm884.

[87] S.S. Said, J.G. Pickering, K. Mequanint, Advances in Growth Factor Delivery for Therapeutic Angiogenesis, Journal of Vascular Research. 50 (2013) 35–51. doi:10.1159/000345108.

[88] C.A. Staton, Preface, in: C. Staton, C.E. Lewis, R.J. Bicknell (Eds.), Angiogenesis Assays: A Critical Appraisal of Current Techniques, J. Wiley & Sons, Chichester, England, 2006: p. xv.

[89] D.M. McDonald, Foreword, in: C. Staton, C.E. Lewis, R.J. Bicknell (Eds.), Angiogenesis Assays: A Critical Appraisal of Current Techniques, J. Wiley & Sons, Chichester, England, 2006: p. xii.

[90] A.M. Goodwin, In vitro assays of angiogenesis for assessment of angiogenic and anti-angiogenic agents, Microvascular Research. 74 (2007) 172–183. doi:10.1016/j.mvr.2007.05.006.

[91] C.A. Staton, M.W.R. Reed, N.J. Brown, A critical analysis of current in vitro and in vivo angiogenesis assays: Current in vitro and in vivo angiogenesis assays, International Journal of Experimental Pathology. 90 (2009) 195–221. doi:10.1111/j.1365-2613.2008.00633.x.

[92] H. Wemme, S. Pfeifer, R. Heck, J. Müller-Quernheim, Measurement of Lymphocyte Proliferation: Critical Analysis of Radioactive and Photometric Methods, Immunobiology. 185 (1992) 78–89. doi:10.1016/S0171-2985(11)80319-0.

[93] N.W. Roehm, G.H. Rodgers, S.M. Hatfield, A.L. Glasebrook, An improved colorimetric assay for cell proliferation and viability utilizing the tetrazolium salt XTT, Journal of Immunological Methods. 142 (1991) 257–265. doi:10.1016/0022-1759(91)90114-U.

[94] M.G. Lampugnani, Cell Migration into a Wounded Area In Vitro, in: Adhesion Protein Protocols, Humana Press, New Jersey, 1999: pp. 177–182. doi:10.1385/1-59259-258-9:177.

[95] S. Boyden, The chemotactic effect of mixtures of antibody and antigen on polymorphonuclear leucocytes, The Journal of Experimental Medicine. 115 (1962) 453–466.

[96] G. Alessandri, K. Raju, P.M. Gullino, Mobilization of Capillary Endothelium in Vitro Induced by Effectors of Angiogenesis in Vivo, Cancer Research. 43 (1983) 1790–1797.

[97] W. Falk, R.H. Goodwin, E.J. Leonard, A 48-well micro chemotaxis assembly for rapid and accurate measurement of leukocyte migration, Journal of Immunological Methods. 33 (1980) 239–247.

[98] F.A. Saleh, M. Whyte, P.G. Genever, Effects of endothelial cells on human mesenchymal stem cell activity in a three-dimensional in vitro model, European Cells & Materials. 22 (2011) 242–257.

[99] A. Hadjizadeh, C.J. Doillon, Directional migration of endothelial cells towards angiogenesis using polymer fibres in a 3D co-culture system, Journal of Tissue Engineering and Regenerative Medicine. 4 (2010) 524–531. doi:10.1002/term.269.

[100] D. Antoni, H. Burckel, E. Josset, G. Noel, Three-Dimensional Cell Culture: A Breakthrough in Vivo, International Journal of Molecular Sciences. 16 (2015) 5517–5527. doi:10.3390/ijms16035517.

[101] V. Nehls, D. Drenckhahn, A Novel, Microcarrier-Based in Vitro Assay for Rapid and Reliable Quantification of Three-Dimensional Cell Migration and Angiogenesis, Microvascular Research. 50 (1995) 311–322. doi:10.1006/mvre.1995.1061.

[102] B.A. Juliar, M.T. Keating, Y.P. Kong, E.L. Botvinick, A.J. Putnam, Sprouting angiogenesis induces significant mechanical heterogeneities and ECM stiffening across length scales in fibrin hydrogels, Biomaterials. 162 (2018) 99–108. doi:10.1016/j.biomaterials.2018.02.012.

[103] N.H. Davies, Discussion on technical challenges of the microcarried bead assay, (2018).

[104] N. Kramer, A. Walzl, C. Unger, M. Rosner, G. Krupitza, M. Hengstschläger, H. Dolznig, In vitro cell migration and invasion assays, Mutation Research/Reviews in Mutation Research. 752 (2013) 10–24. doi:10.1016/j.mrrev.2012.08.001.

[105] T. Korff, H.G. Augustin, Integration of endothelial cells in multicellular spheroids prevents apoptosis and induces differentiation, The Journal of Cell Biology. 143 (1998) 1341–1352.

[106] P. Kaaijk, D. Troost, P.K. Das, S. Leenstra, D.A. Bosch, Long-term culture of organotypic multicellular glioma spheroids: a good culture model for studying gliomas, Neuropathology and Applied Neurobiology. 21 (1995) 386–391.

[107] L. Xiao, T. Tsutsui, Characterization of human dental pulp cells-derived spheroids in serum-free medium: Stem cells in the core: Stem Cell Distribution in Spheroid, Journal of Cellular Biochemistry. 114 (2013) 2624–2636. doi:10.1002/jcb.24610.

[108] S. Blacher, C. Erpicum, B. Lenoir, J. Paupert, G. Moraes, S. Ormenese, E. Bullinger, A. Noel, Cell Invasion in the Spheroid Sprouting Assay: A Spatial Organisation Analysis Adaptable to Cell Behaviour, PLoS ONE. 9 (2014) e97019. doi:10.1371/journal.pone.0097019.

[109] M. Heiss, M. Hellstrom, M. Kalen, T. May, H. Weber, M. Hecker, H.G. Augustin, T. Korff, Endothelial cell spheroids as a versatile tool to study angiogenesis in vitro, The FASEB Journal. 29 (2015) 3076–3084. doi:10.1096/fj.14-267633.

[110] T. Korff, S. Kimmina, G. Martiny-Baron, H.G. Augustin, Blood vessel maturation in a 3-dimensional spheroidal coculture model: direct contact with smooth muscle cells regulates endothelial cell quiescence and abrogates VEGF responsiveness, The FASEB Journal. 15 (2001) 447–457. doi:10.1096/fj.00-0139com.

[111] W.G. Chang, J.W. Andrejecsk, M.S. Kluger, W.M. Saltzman, J.S. Pober, Pericytes modulate endothelial sprouting, Cardiovascular Research. 100 (2013) 492–500. doi:10.1093/cvr/cvt215.

[112] K.M. Welch-Reardon, S.M. Ehsan, K. Wang, N. Wu, A.C. Newman, M. Romero-Lopez, A.H. Fong, S.C. George, R.A. Edwards, C.C.W. Hughes, Angiogenic sprouting is regulated by endothelial cell expression of Slug, Journal of Cell Science. 127 (2014) 2017–2028. doi:10.1242/jcs.143420.

[113] E. Urich, C. Patsch, S. Aigner, M. Graf, R. Iacone, P.-O. Freskgård, Multicellular Self-Assembled Spheroidal Model of the Blood Brain Barrier, Scientific Reports. 3 (2013). doi:10.1038/srep01500.

[114] C. Gebhard, C. Gabriel, I. Walter, Morphological and Immunohistochemical Characterization of Canine Osteosarcoma Spheroid Cell Cultures, Anatomia, Histologia, Embryologia. 45 (2016) 219–230. doi:10.1111/ahe.12190.

[115] A.Y. Hsiao, Y.-C. Tung, X. Qu, L.R. Patel, K.J. Pienta, S. Takayama, 384 hanging drop arrays give excellent Z-factors and allow versatile formation of co-culture spheroids, Biotechnology and Bioengineering. 109 (2012) 1293–1304. doi:10.1002/bit.24399.

[116] L. Pfisterer, T. Korff, Spheroid-Based In Vitro Angiogenesis Model, in: S.G. Martin, P.W. Hewett (Eds.), Angiogenesis Protocols, Springer New York, New York, NY, 2016: pp. 167–177. doi:10.1007/978-1-4939-3628-1_11.

[117] R. Auerbach, R. Lewis, B. Shinners, L. Kubai, N. Akhtar, Angiogenesis assays: a critical overview, Clinical Chemistry. 49 (2003) 32–40.

[118] A.E. Birsner, O. Benny, R.J. D'Amato, The Corneal Micropocket Assay: A Model of Angiogenesis in the Mouse Eye, Journal of Visualized Experiments. (2014). doi:10.3791/51375.

[119] P. Rous, J.B. Murphy, Tumour implantations in the developing embryo, Journal of the American Medical Association. LVI (1911) 741. doi:10.1001/jama.1911.02560100033015.

[120] K.P. Goetsch, M. Bracher, D. Bezuidenhout, P. Zilla, N.H. Davies, Regulation of tissue ingrowth into proteolytically degradable hydrogels, Acta Biomaterialia. (2015). doi:10.1016/j.actbio.2015.06.009.

[121] D. Coltrini, E. Di Salle, R. Ronca, M. Belleri, C. Testini, M. Presta, Matrigel plug assay: evaluation of the angiogenic response by reverse transcription-quantitative PCR, Angiogenesis. 16 (2013) 469–477. doi:10.1007/s10456-012-9324-7.

[122] A.H. Zisch, M.P. Lutolf, M. Ehrbar, G.P. Raeber, S.C. Rizzi, N.H. Davies, H. Schmökel, D. Bezuidenhout, V. Djonov, P. Zilla, J.A. Hubbell, Cell-demanded release of VEGF from synthetic, biointeractive cell-ingrowth matrices for vascularized tissue growth, The Journal of the Federation of American Societies for Experimental Biology. 17 (2003) 2260–2285. doi:10.1096/fj.02-1041fje.

[123] J. Jedelská, B. Strehlow, U. Bakowsky, A. Aigner, S. Höbel, M. Bette, M. Roessler, N. Franke, A. Teymoortash, J.A. Werner, B. Eivazi, R. Mandic, The chorioallantoic membrane assay is a promising ex vivo model system for the study of vascular anomalies, In Vivo: International Journal of Experimental and Clinical Pathophysiology and Drug Research. 27 (2013) 701–705.

[124] V. Hamburger, H.L. Hamilton, A series of normal stages in the development of the chick embryo, Journal of Morphology. 88 (1951) 49–92. doi:10.1002/jmor.1050880104.

[125] L.L.Y. Chiu, M. Radisic, Scaffolds with covalently immobilized VEGF and Angiopoietin-1 for vascularization of engineered tissues, Biomaterials. 31 (2010) 226–241. doi:10.1016/j.biomaterials.2009.09.039.

[126] Y. Bai, Y. Leng, G. Yin, X. Pu, Z. Huang, X. Liao, X. Chen, Y. Yao, Effects of combinations of BMP-2 with FGF-2 and/or VEGF on HUVECs angiogenesis in vitro and CAM angiogenesis in vivo, Cell and Tissue Research. 356 (2014) 109–121. doi:10.1007/s00441-013-1781-9.

[127] I. Moreno-Jiménez, J.M. Kanczler, G. Hulsart-Billstrom, S. Inglis, R.O.C. Oreffo, The Chorioallantoic Membrane Assay for Biomaterial Testing in Tissue Engineering: A Short-Term In Vivo Preclinical Model, Tissue Engineering Part C: Methods. 23 (2017) 938–952. doi:10.1089/ten.tec.2017.0186.

[128] W. Leene, M.J. Duyzings, C. van Steeg, Lymphoid stem cell identification in the developing thymus and bursa of Fabricius of the chick, Z Zellforsch Mikrosk Anat. 136 (1973) 521–533.

[129] D. Ribatti, B. Nico, A. Vacca, M. Presta, The gelatin sponge–chorioallantoic membrane assay, Nature Protocols. 1 (2006) 85–91. doi:10.1038/nprot.2006.13.

[130] R. Auerbach, Chapter 19: An overview of current angiogenesis assays: Choice of assay, precautions in interpretation, future, requirements and directions, in: C. Staton, C.E. Lewis, R.J. Bicknell (Eds.), Angiogenesis Assays: A Critical Appraisal of Current Techniques, J. Wiley & Sons, Chichester, England, 2006: p. xv.

[131] C.S. Kue, K.Y. Tan, M.L. Lam, H.B. Lee, Chick embryo chorioallantoic membrane (CAM): an alternative predictive model in acute toxicological studies for anti-cancer drugs, Experimental Animals. 64 (2015) 129–138. doi:10.1538/expanim.14-0059.

[132] M.A. Gimbrone, S.B. Leapman, R.S. Cotran, J. Folkman, Tumor dormancy in vivo by prevention of neovascularization, The Journal of Experimental Medicine. 136 (1972) 261–276.

[133] B.M. Kenyon, E.E. Voest, C.C. Chen, E. Flynn, J. Folkman, R.J. D'Amato, A model of angiogenesis in the mouse cornea, Investigative Ophthalmology & Visual Science. 37 (1996) 1625–1632.

[134] C. Claaßen, L. Sewald, G. Tovar, K. Borchers, Controlled Release of Vascular Endothelial Growth Factor from Heparin-Functionalized Gelatin Type A and Albumin Hydrogels, Gels. 3 (2017) 35. doi:10.3390/gels3040035.

[135] E.A. Horner, J. Kirkham, X.B. Yang, Chapter 35: Animal Models, in: J.M. Polak, S. Mantalaris, S.E. Harding (Eds.), Advances in Tissue Engineering, Imperial College Press, London, 2008: pp. 763–779. http://public.eblib.com/choice/publicfullrecord.aspx?p=1193570 (accessed May 11, 2018).

[136] D. Bezuidenhout, N. Davies, M. Black, C. Schmidt, A. Oosthuysen, P. Zilla, Covalent Surface Heparinization Potentiates Porous Polyurethane Scaffold Vascularization, Journal of Biomaterials Applications. 24 (2010) 401–418. doi:10.1177/0885328208097565.

[137] E.A. Jones, X. Yang, P.V. Giannoudis, D. McGonagle, Chapter 5: Animal Models for Investigating MSC Involvement in Bone and Cartilage Repair, in: Mesenchymal Stem Cells and Skeletal Regeneration, 2013: p. 27.

[138] S.P. Andrade, M.A.N.D. Ferreira, T. Fan, Chapter 9: Implantation of sponges and polymers, in: C. Staton, C.E. Lewis, R.J. Bicknell (Eds.), Angiogenesis Assays: A

Critical Appraisal of Current Techniques, J. Wiley & Sons, Chichester, England, 2006: p. 189.

[139] M. Gnecchi, H. He, O.D. Liang, L.G. Melo, F. Morello, H. Mu, N. Noiseux, L. Zhang, R.E. Pratt, J.S. Ingwall, V.J. Dzau, Paracrine action accounts for marked protection of ischemic heart by Akt-modified mesenchymal stem cells, Nature Medicine. 11 (2005) 367–368. doi:10.1038/nm0405-367.

[140] A. Stempien-Otero, D. Helterline, T. Plummer, S. Farris, A. Prouse, N. Polissar, D. Stanford, N.A. Mokadam, Mechanisms of bone marrow-derived cell therapy in ischemic cardiomyopathy with left ventricular assist device bridge to transplant, Journal of the American College of Cardiology. 65 (2015) 1424–1434. doi:10.1016/j.jacc.2015.01.042.

[141] A.A. Ucuzian, A.A. Gassman, A.T. East, H.P. Greisler, Molecular Mediators of Angiogenesis, Journal of Burn Care & Research. 31 (2010) 158–175. doi:10.1097/BCR.0b013e3181c7ed82.

[142] S. De Falco, The discovery of placenta growth factor and its biological activity, Experimental and Molecular Medicine. 44 (2012) 1. doi:10.3858/emm.2012.44.1.025.

[143] Y. Shing, J. Folkman, R. Sullivan, C. Butterfield, J. Murray, M. Klagsbrun, Heparin affinity: purification of a tumor-derived capillary endothelial cell growth factor, Science. 223 (1984) 1296–1299. doi:10.1126/science.6199844.

[144] M. Presta, M. Rusnati, A. Gualandris, P. Dell'Era, C. Urbinati, D. Coltrini, E. Tanghetti, M. Belleri, Human Basic Fibroblast Growth Factor: Structure-Function Relationship of an Angiogenic Molecule, in: M.E. Maragoudakis, P.M. Gullino, P.I. Lelkes (Eds.), Angiogenesis, Springer, Boston, MA, 1994: pp. 39–50. doi:10.1007/978-1-4757-9188-4_5.

[145] N. Turner, R. Grose, Fibroblast growth factor signalling: from development to cancer, Nature Reviews Cancer. 10 (2010) 116–129. doi:10.1038/nrc2780.

[146] M. Wiedemann, B. Trueb, Characterization of a Novel Protein (FGFRL1) from Human Cartilage Related to FGF Receptors, Genomics. 69 (2000) 275–279. doi:10.1006/geno.2000.6332.

[147] M. Rusnati, M. Presta, Interaction of angiogenic basic fibroblast growth factor with endothelial cell heparan sulfate proteoglycans. Biological implications in neovascularization, International Journal of Clinical & Laboratory Research. 26 (1996) 15–23.

[148] I. Lang, C. Hoffmann, H. Olip, M.A. Pabst, T. Hahn, G. Dohr, G. Desoye, Differential mitogenic responses of human macrovascular and microvascular

endothelial cells to cytokines underline their phenotypic heterogeneity, Cell Proliferation. 34 (2001) 143–155.

[149] M. Presta, P. Dell'Era, S. Mitola, E. Moroni, R. Ronca, M. Rusnati, Fibroblast growth factor/fibroblast growth factor receptor system in angiogenesis, Cytokine & Growth Factor Reviews. 16 (2005) 159–178. doi:10.1016/j.cytogfr.2005.01.004.

[150] M. Presta, D. Moscatelli, J. Joseph-Silverstein, D.B. Rifkin, Purification from a human hepatoma cell line of a basic fibroblast growth factor-like molecule that stimulates capillary endothelial cell plasminogen activator production, DNA synthesis, and migration, Molecular and Cellular Biology. 6 (1986) 4060–4066.

[151] M. Murakami, L.T. Nguyen, Z.W. Zhang, K.L. Moodie, P. Carmeliet, R.V. Stan, M. Simons, The FGF system has a key role in regulating vascular integrity, Journal of Clinical Investigation. 118 (2008) 3355–3366. doi:10.1172/JCI35298.

[152] A. Ahn, W.H. Frishman, A. Gutwein, J. Passeri, M. Nelson, Therapeutic Angiogenesis: A New Treatment Approach for Ischemic Heart Disease—Part II, Cardiology in Review. 16 (2008) 219–229. doi:10.1097/CRD.0b013e3181620e50.

[153] K.E. Johnson, T.A. Wilgus, Vascular Endothelial Growth Factor and Angiogenesis in the Regulation of Cutaneous Wound Repair, Advances in Wound Care. 3 (2014) 647–661. doi:10.1089/wound.2013.0517.

[154] A. Amoroso, F. Del Porto, C. Di Monaco, P. Manfredini, A. Afeltra, Vascular endothelial growth factor: a key mediator of neoangiogenesis. A review, European Review for Medical and Pharmacological Sciences. 1 (1997) 17–25.

[155] G.V. Sherbet, Vascular Endothelial Growth Factor, in: Growth Factors and Their Receptors in Cell Differentiation, Cancer and Cancer Therapy, Elsevier, 2011: pp. 55–64. doi:10.1016/B978-0-12-387819-9.00004-9.

[156] J. Igarashi, P.A. Erwin, A.P.V. Dantas, H. Chen, T. Michel, VEGF induces S1P1 receptors in endothelial cells: Implications for cross-talk between sphingolipid and growth factor receptors, Proceedings of the National Academy of Sciences. 100 (2003) 10664–10669. doi:10.1073/pnas.1934494100.

[157] F. Liu, A.D. Verin, P. Wang, R. Day, R.P. Wersto, F.J. Chrest, D.K. English, J.G.N. Garcia, Differential Regulation of Sphingosine-1-Phosphate- and VEGF-Induced Endothelial Cell Chemotaxis: Involvement of Gia2-Linked Rho Kinase Activity, American Journal of Respiratory Cell and Molecular Biology. 24 (2001) 711–719. doi:10.1165/ajrcmb.24.6.4323.

[158] A.Z. Faranesh, M.T. Nastley, C. Perez de la Cruz, M.F. Haller, P. Laquerriere, K.W. Leong, E.R. McVeigh, In vitro release of vascular endothelial growth factor from

gadolinium-doped biodegradable microspheres, Magnetic Resonance in Medicine. 51 (2004) 1265–1271. doi:10.1002/mrm.20092.

[159] B. Wang, R. Cheheltani, J. Rosano, D.L. Crabbe, M.F. Kiani, Oxygen Transport to Tissue XXXIV: Targeted Delivery of VEGF to Treat Myocardial Infarction, in: W.J. Welch, F. Palm, D.F. Bruley, D.K. Harrison (Eds.), Advances in Experimental Medicine and Biology, Springer New York, New York, 2013: pp. 307–314. http://link.springer.com/10.1007/978-1-4614-4989-8_43 (accessed February 24, 2016).

[160] M. Wu, P. Claus, N. Vanden Driessche, G. Reyns, P. Pokreisz, H. Gillijns, E. Caluwe, J. Bogaert, D. Collen, S. Janssens, Placental growth factor 2 — A potential therapeutic strategy for chronic myocardial ischemia, International Journal of Cardiology. 203 (2015) 534–542. doi:10.1016/j.ijcard.2015.10.177.

[161] D. Maglione, V. Guerriero, G. Viglietto, M.G. Ferraro, O. Aprelikova, K. Alitalo, S. Del Vecchio, K.J. Lei, J.Y. Chou, M.G. Persico, Two alternative mRNAs coding for the angiogenic factor, placenta growth factor (PlGF), are transcribed from a single gene of chromosome 14, Oncogene. 8 (1993) 925–931.

[162] Y. Cao, W.-R. Ji, P. Qi, Å. Rosin, Y. Cao, Placenta Growth Factor: Identification and Characterization of a Novel Isoform Generated by RNA Alternative Splicing, Biochemical and Biophysical Research Communications. 235 (1997) 493–498. doi:10.1006/bbrc.1997.6813.

[163] W. Yang, H. Ahn, M. Hinrichs, R.J. Torry, D.S. Torry, Evidence of a novel isoform of placenta growth factor (PlGF-4) expressed in human trophoblast and endothelial cells, Journal of Reproductive Immunology. 60 (2003) 53–60.

[164] S. Hauser, H.A. Weich, A heparin-binding form of placenta growth factor (PlGF-2) is expressed in human umbilical vein endothelial cells and in placenta, Growth Factors. 9 (1993) 259–268.

[165] D. Maglione, V. Guerriero, G. Viglietto, P. Delli-Bovi, M.G. Persico, Isolation of a human placenta cDNA coding for a protein related to the vascular permeability factor, Proceedings of the National Academy of Sciences of the United States of America. 88 (1991) 9267–9271.

[166] M. Migdal, B. Huppertz, S. Tessler, A. Comforti, M. Shibuya, R. Reich, H. Baumann, G. Neufeld, Neuropilin-1 is a placenta growth factor-2 receptor, The Journal of Biological Chemistry. 273 (1998) 22272–22278.

[167] Z.M. Binsalamah, A.A. Khan, S. Prakash, D. Shum-Tim, Intramyocardial sustained delivery of placental growth factor using nanoparticles as a vehicle for delivery in

the rat infarct model, International Journal of Nanomedicine. (2011) 2667. doi:10.2147/IJN.S25175.

[168] A. Luttun, M. Tjwa, L. Moons, Y. Wu, A. Angelillo-Scherrer, F. Liao, J.A. Nagy, A. Hooper, J. Priller, B. De Klerck, V. Compernolle, E. Daci, P. Bohlen, M. Dewerchin, J.-M. Herbert, R. Fava, P. Matthys, G. Carmeliet, D. Collen, H.F. Dvorak, D.J. Hicklin, P. Carmeliet, Revascularization of ischemic tissues by PlGF treatment, and inhibition of tumor angiogenesis, arthritis and atherosclerosis by anti-Flt1, Nature Medicine. (2002). doi:10.1038/nm731.

[169] H. Bompais, J. Chagraoui, X. Canron, M. Crisan, X.H. Liu, A. Anjo, C. Tolla-Le Port, M. Leboeuf, P. Charbord, A. Bikfalvi, G. Uzan, Human endothelial cells derived from circulating progenitors display specific functional properties compared with mature vessel wall endothelial cells, Blood. 103 (2004) 2577–2584. doi:10.1182/blood-2003-08-2770.

[170] R.D. Levit, N. Landázuri, E.A. Phelps, M.E. Brown, A.J. García, M.E. Davis, G. Joseph, R. Long, S.A. Safley, J.D. Suever, A.N. Lyle, C.J. Weber, W.R. Taylor, Cellular encapsulation enhances cardiac repair, Journal of the American Heart Association. 2 (2013) e000367. doi:10.1161/JAHA.113.000367.

[171] M.K.L. Chuah, D. Collen, T. VandenDriessche, Biosafety of adenoviral vectors, Current Gene Therapy. 3 (2003) 527–543.

[172] H. Chu, Y. Wang, Therapeutic angiogenesis: controlled delivery of angiogenic factors, Therapeutic Delivery. 3 (2012) 693–714.

[173] M.D. Hariawala, J.R. Horowitz, D. Esakof, D.D. Sheriff, D.H. Walter, B. Keyt, J.M. Isner, J.F. Symes, VEGF Improves Myocardial Blood Flow but Produces EDRF-Mediated Hypotension in Porcine Hearts, Journal of Surgical Research. 63 (1996) 77–82. doi:10.1006/jsre.1996.0226.

[174] R.J. Laham, N.A. Chronos, M. Pike, M.E. Leimbach, J.E. Udelson, J.D. Pearlman, R.I. Pettigrew, M.J. Whitehouse, C. Yoshizawa, M. Simons, Intracoronary basic fibroblast growth factor (FGF-2) in patients with severe ischemic heart disease: results of a phase I open-label dose escalation study, Journal of the American College of Cardiology. 36 (2000) 2132–2139.

[175] M. Simons, B.H. Annex, R.J. Laham, N. Kleiman, T. Henry, H. Dauerman, J.E. Udelson, E.V. Gervino, M. Pike, M.J. Whitehouse, T. Moon, N.A. Chronos, Pharmacological treatment of coronary artery disease with recombinant fibroblast growth factor-2: double-blind, randomized, controlled clinical trial, Circulation. 105 (2002) 788–793.

[176] M.A. Bush, E. Samara, M.J. Whitehouse, C. Yoshizawa, D.L. Novicki, M. Pike, R.J. Laham, M. Simons, N.A. Chronos, Pharmacokinetics and pharmacodynamics of recombinant FGF-2 in a phase I trial in coronary artery disease, Journal of Clinical Pharmacology. 41 (2001) 378–385.

[177] R.K. Jain, Molecular regulation of vessel maturation, Nature Medicine. 9 (2003) 685–693.

[178] B. Jiang, E.M. Brey, Chapter 22: Formation of Stable Vascular Networks in Engineered Tissues, in: D. Eberli (Ed.), Regenerative Medicine and Tissue Engineering - Cells and Biomaterials, InTech, 2011. doi:10.5772/23223.

[179] D. Hanahan, Signaling Vascular Morphogenesis and Maintenance, Science. 277 (1997) 48–50. doi:10.1126/science.277.5322.48.

[180] G. Thurston, C. Suri, K. Smith, J. McClain, T.N. Sato, G.D. Yancopoulos, D.M. McDonald, Leakage-resistant blood vessels in mice transgenically overexpressing angiopoietin-1, Science. 286 (1999) 2511–2514.

[181] L.T. Cooper, W.R. Hiatt, M.A. Creager, J.G. Regensteiner, W. Casscells, J.M. Isner, J.P. Cooke, A.T. Hirsch, Proteinuria in a placebo-controlled study of basic fibroblast growth factor for intermittent claudication, Vascular Medicine. 6 (2001) 235–239. doi:10.1177/1358836X0100600406.

[182] K. Samoto, K. Ikezaki, M. Ono, T. Shono, K. Kohno, M. Kuwano, M. Fukui, Expression of Vascular Endothelial Growth Factor and Its Possible Relation with Neovascularization in Human Brain Tumors, Cancer Research. 55 (1995) 1189.

[183] R.J. Lee, M.L. Springer, W.E. Blanco-Bose, R. Shaw, P.C. Ursell, H.M. Blau, VEGF Gene Delivery to Myocardium : Deleterious Effects of Unregulated Expression, Circulation. 102 (2000) 898–901. doi:10.1161/01.CIR.102.8.898.

[184] A.P. Levy, N.S. Levy, M.A. Goldberg, Post-transcriptional regulation of vascular endothelial growth factor by hypoxia, The Journal of Biological Chemistry. 271 (1996) 2746–2753.

[185] I. Stein, M. Neeman, D. Shweiki, A. Itin, E. Keshet, Stabilization of vascular endothelial growth factor mRNA by hypoxia and hypoglycemia and coregulation with other ischemia-induced genes, Molecular and Cellular Biology. 15 (1995) 5363–5368.

[186] D.F. Lazarous, E.F. Unger, S.E. Epstein, A. Stine, J.L. Arevalo, E.Y. Chew, A.A. Quyyumi, Basic fibroblast growth factor in patients with intermittent claudication: results of a phase I trial, Journal of the American College of Cardiology. 36 (2000) 1239–1244. doi:10.1016/S0735-1097(00)00882-2.

[187] D.F. Lazarous, M. Scheinowitz, M. Shou, E. Hodge, M.A.S. Rajanayagam, S. Hunsberger, W.G. Robison, J.A. Stiber, R. Correa, S.E. Epstein, E.F. Unger, Effects of Chronic Systemic Administration of Basic Fibroblast Growth Factor on Collateral Development in the Canine Heart, Circulation. 91 (1995) 145–153. doi:10.1161/01.CIR.91.1.145.

[188] D.T. Shima, U. Deutsch, P.A. D'Amore, Hypoxic induction of vascular endothelial growth factor (VEGF) in human epithelial cells is mediated by increases in mRNA stability, FEBS Letters. 370 (1995) 203–208. doi:10.1016/0014-5793(95)00831-S.

[189] S.M. Eppler, D.L. Combs, T.D. Henry, J.J. Lopez, S.G. Ellis, J.-H. Yi, B.H. Annex, E.R. McCluskey, T.F. Zioncheck, A target-mediated model to describe the pharmacokinetics and hemodynamic effects of recombinant human vascular endothelial growth factor in humans*, Clinical Pharmacology & Therapeutics. 72 (2002) 20–32. doi:10.1067/mcp.2002.126179.

[190] Z. Huang, C. Ni, Y. Chu, S. Wang, S. Yang, X. Wu, X. Wang, X. Li, W. Feng, S. Lin, Chemical modification of recombinant human keratinocyte growth factor 2 with polyethylene glycol improves biostability and reduces animal immunogenicity, Journal of Biotechnology. 142 (2009) 242–249. doi:10.1016/j.jbiotec.2009.05.004.

[191] H.-W. Ryou, J.-W. Lee, K.A. Yoon, E.-S. Park, S.-C. Chi, Effect of protease inhibitors on degradation of recombinant human epidermal growth factor in skin tissue, Archives of Pharmacal Research. 20 (1997) 34–38. doi:10.1007/BF02974039.

[192] D.F. Lazarous, M. Shou, J.A. Stiber, D.M. Dadhania, V. Thirumurti, E. Hodge, E.F. Unger, Pharmacodynamics of basic fibroblast growth factor: route of administration determines myocardial and systemic distribution, Cardiovascular Research. 36 (1997) 78–85.

[193] A.H. Zisch, M.P. Lutolf, J.A. Hubbell, Biopolymeric delivery matrices for angiogenic growth factors, Cardiovascular Pathology. 12 (2003) 295–310. doi:10.1016/S1054-8807(03)00089-9.

[194] I. Vlodavsky, R. Bar-Shavit, R. Ishar-Michael, P. Bashkin, Z. Fuks, Extracellular sequestration and release of fibroblast growth factor: a regulatory mechanism?, Trends in Biochemical Sciences. 16 (1991) 268–271. doi:10.1016/0968-0004(91)90102-2.

[195] S.P. Baldwin, W.M. Saltzman, Materials for protein delivery in tissue engineering, Advanced Drug Delivery Reviews. 33 (1998) 71–86. doi:10.1016/S0169-409X(98)00021-0.

[196] H. Iwaguro, J. Yamaguchi, C. Kalka, S. Murasawa, H. Masuda, S. Hayashi, M. Silver, T. Li, J.M. Isner, T. Asahara, Endothelial progenitor cell vascular endothelial

growth factor gene transfer for vascular regeneration, Circulation. 105 (2002) 732–738.

[197] H.-F. Duan, C.-T. Wu, D.-L. Wu, Y. Lu, H.-J. Liu, X.-Q. Ha, Q.-W. Zhang, H. Wang, X.-X. Jia, L.-S. Wang, Treatment of myocardial ischemia with bone marrow-derived mesenchymal stem cells overexpressing hepatocyte growth factor, Mol. Ther. 8 (2003) 467–474.

[198] E. Jabbarzadeh, T. Starnes, Y.M. Khan, T. Jiang, A.J. Wirtel, M. Deng, Q. Lv, L.S. Nair, S.B. Doty, C.T. Laurencin, Induction of angiogenesis in tissue-engineered scaffolds designed for bone repair: A combined gene therapy-cell transplantation approach, Proceedings of the National Academy of Sciences. 105 (2008) 11099–11104. doi:10.1073/pnas.0800069105.

[199] National Institutes of Health, Assessment of Adenoviral Vector Safety and Toxicity: Report of the National Institutes of Health Recombinant DNA Advisory Committee, Human Gene Therapy. 13 (2002) 3–13. doi:10.1089/10430340152712629.

[200] A. Bostanci, Blood test flags agent in death of Penn subject, Science. 295 (2002) 604–605.

[201] S. Hacein-Bey-Abina, F. Le Deist, F. Carlier, C. Bouneaud, C. Hue, J.-P. De Villartay, A.J. Thrasher, N. Wulffraat, R. Sorensen, S. Dupuis-Girod, A. Fischer, E.G. Davies, W. Kuis, L. Leiva, M. Cavazzana-Calvo, Sustained Correction of X-Linked Severe Combined Immunodeficiency by ex Vivo Gene Therapy, New England Journal of Medicine. 346 (2002) 1185–1193. doi:10.1056/NEJMoa012616.

[202] S. Hacein-Bey-Abina, C. von Kalle, M. Schmidt, F. Le Deist, N. Wulffraat, E. McIntyre, I. Radford, J.-L. Villeval, C.C. Fraser, M. Cavazzana-Calvo, A. Fischer, A Serious Adverse Event after Successful Gene Therapy for X-Linked Severe Combined Immunodeficiency, New England Journal of Medicine. 348 (2003) 255–256. doi:10.1056/NEJM200301163480314.

[203] Z. Wang, Z. Wang, W.W. Lu, W. Zhen, D. Yang, S. Peng, Novel biomaterial strategies for controlled growth factor delivery for biomedical applications, NPG Asia Materials. 9 (2017) e435. doi:10.1038/am.2017.171.

[204] J.M. Singelyn, J.A. DeQuach, S.B. Seif-Naraghi, R.B. Littlefield, P.J. Schup-Magoffin, K.L. Christman, Naturally derived myocardial matrix as an injectable scaffold for cardiac tissue engineering, Biomaterials. 30 (2009) 5409–5416. doi:10.1016/j.biomaterials.2009.06.045.

[205] S. Zhang, H. Uludağ, Nanoparticulate Systems for Growth Factor Delivery, Pharmaceutical Research. 26 (2009) 1561–1580. doi:10.1007/s11095-009-9897-z.

[206] H. Li, J.H. Song, J.S. Park, K. Han, Polyethylene glycol-coated liposomes for oral delivery of recombinant human epidermal growth factor, International Journal of Pharmaceutics. 258 (2003) 11–19.

[207] H. Li, J.H. An, J.-S. Park, K. Han, Multivesicular liposomes for oral delivery of recombinant human epidermal growth factor, Archives of Pharmacal Research. 28 (2005) 988–994.

[208] S.-O. Jeon, H.-J. Hwang, D.-H. Oh, J.-E. Seo, K.-H. Chun, S.-M. Hong, M.-J. Kim, W.-C. Kim, M.-S. Park, C.-H. Yoon, K.-H. Min, C.-W. Suh, S. Lee, Enhanced percutaneous delivery of recombinant human epidermal growth factor employing nano-liposome system, Journal of Microencapsulation. 29 (2012) 234–241. doi:10.3109/02652048.2011.646327.

[209] R.C. Scott, J.M. Rosano, Z. Ivanov, B. Wang, P.L.-G. Chong, A.C. Issekutz, D.L. Crabbe, M.F. Kiani, Targeting VEGF-encapsulated immunoliposomes to MI heart improves vascularity and cardiac function, The FASEB Journal. 23 (2009) 3361–3367. doi:10.1096/fj.08-127373.

[210] Y. Misao, G. Takemura, M. Arai, T. Ohno, H. Onogi, T. Takahashi, S. Minatoguchi, T. Fujiwara, H. Fujiwara, Importance of recruitment of bone marrow-derived CXCR4+ cells in post-infarct cardiac repair mediated by G-CSF, Cardiovascular Research. 71 (2006) 455–465. doi:10.1016/j.cardiores.2006.05.002.

[211] R.C. Scott, B. Wang, R. Nallamothu, C.B. Pattillo, G. Perez-Liz, A. Issekutz, L.D. Valle, G.C. Wood, M.F. Kiani, Targeted delivery of antibody conjugated liposomal drug carriers to rat myocardial infarction, Biotechnology and Bioengineering. 96 (2007) 795–802. doi:10.1002/bit.21233.

[212] T.M. Taylor, J. Weiss, P.M. Davidson, B.D. Bruce, Liposomal Nanocapsules in Food Science and Agriculture, Critical Reviews in Food Science and Nutrition. 45 (2005) 587–605. doi:10.1080/10408390591001135.

[213] D. Papahadjopoulos, T.M. Allen, A. Gabizon, E. Mayhew, K. Matthay, S.K. Huang, K.D. Lee, M.C. Woodle, D.D. Lasic, C. Redemann, Sterically stabilized liposomes: improvements in pharmacokinetics and antitumor therapeutic efficacy., Proceedings of the National Academy of Sciences. 88 (1991) 11460–11464. doi:10.1073/pnas.88.24.11460.

[214] A.L. Klibanov, K. Maruyama, V.P. Torchilin, L. Huang, Amphipathic polyethyleneglycols effectively prolong the circulation time of liposomes, FEBS Letters. 268 (1990) 235–237. doi:10.1016/0014-5793(90)81016-H.

[215] T.M. Allen, C. Hansen, F. Martin, C. Redemann, A. Yau-Young, Liposomes containing synthetic lipid derivatives of poly(ethylene glycol) show prolonged

circulation half-lives in vivo, Biochimica et Biophysica Acta (BBA) - Biomembranes. 1066 (1991) 29–36. doi:10.1016/0005-2736(91)90246-5.

[216] K. Lee, E.A. Silva, D.J. Mooney, Growth factor delivery-based tissue engineering: general approaches and a review of recent developments, Journal of The Royal Society Interface. 8 (2011) 153–170. doi:10.1098/rsif.2010.0223.

[217] E.M. Ahmed, Hydrogel: Preparation, characterization, and applications: A review, Journal of Advanced Research. 6 (2015) 105–121. doi:10.1016/j.jare.2013.07.006.

[218] N.A. Peppas, J.Z. Hilt, A. Khademhosseini, R. Langer, Hydrogels in Biology and Medicine: From Molecular Principles to Bionanotechnology, Advanced Materials. 18 (2006) 1345–1360. doi:10.1002/adma.200501612.

[219] K.H. Bae, M. Kurisawa, Emerging hydrogel designs for controlled protein delivery, Biomaterials Science. 4 (2016) 1184–1192. doi:10.1039/C6BM00330C.

[220] V. Pérez-Luna, O. González-Reynoso, Encapsulation of Biological Agents in Hydrogels for Therapeutic Applications, Gels. 4 (2018) 61. doi:10.3390/gels4030061.

[221] S.R. Caliari, J.A. Burdick, A practical guide to hydrogels for cell culture, Nature Methods. 13 (2016) 405–414. doi:10.1038/nmeth.3839.

[222] T.D. Johnson, K.L. Christman, Injectable hydrogel therapies and their delivery strategies for treating myocardial infarction, Expert Opinion on Drug Delivery. 10 (2013) 59–72. doi:10.1517/17425247.2013.739156.

[223] N.K. Singh, D.S. Lee, In situ gelling pH- and temperature-sensitive biodegradable block copolymer hydrogels for drug delivery, Journal of Controlled Release. 193 (2014) 214–227. doi:10.1016/j.jconrel.2014.04.056.

[224] N. Landa, L. Miller, M.S. Feinberg, R. Holbova, M. Shachar, I. Freeman, S. Cohen, J. Leor, Effect of Injectable Alginate Implant on Cardiac Remodeling and Function After Recent and Old Infarcts in Rat, Circulation. 117 (2008) 1388–1396. doi:10.1161/CIRCULATIONAHA.107.727420.

[225] W. Dai, S.L. Hale, G.L. Kay, A.J. Jyrala, R.A. Kloner, Delivering stem cells to the heart in a collagen matrix reduces relocation of cells to other organs as assessed by nanoparticle technology, Regenerative Medicine. 4 (2009) 387–395. doi:10.2217/rme.09.2.

[226] H.K. Awada, N.R. Johnson, Y. Wang, Sequential delivery of angiogenic growth factors improves revascularization and heart function after myocardial infarction, Journal of Controlled Release. 207 (2015) 7–17. doi:10.1016/j.jconrel.2015.03.034.

[227] S. Sahoo, C. Chung, S. Khetan, J.A. Burdick, Hydrolytically Degradable Hyaluronic Acid Hydrogels with Controlled Temporal Structures, Biomacromolecules. 9 (2008) 1088–1092. doi:10.1021/bm800051m.

[228] H. Geckil, F. Xu, X. Zhang, S. Moon, U. Demirci, Engineering hydrogels as extracellular matrix mimics, Nanomedicine. 5 (2010) 469–484. doi:10.2217/nnm.10.12.

[229] Q. Xing, K. Yates, C. Vogt, Z. Qian, M.C. Frost, F. Zhao, Increasing Mechanical Strength of Gelatin Hydrogels by Divalent Metal Ion Removal, Scientific Reports. 4 (2014). doi:10.1038/srep04706.

[230] M. Kumagai, K. Minakata, H. Masumoto, M. Yamamoto, A. Yonezawa, T. Ikeda, K. Uehara, K. Yamazaki, T. Ikeda, K. Matsubara, M. Yokode, A. Shimizu, Y. Tabata, R. Sakata, K. Minatoya, A therapeutic angiogenesis of sustained release of basic fibroblast growth factor using biodegradable gelatin hydrogel sheets in a canine chronic myocardial infarction model, Heart and Vessels. 33 (2018) 1251–1257. doi:10.1007/s00380-018-1185-6.

[231] A. Marui, Y. Tabata, S. Kojima, M. Yamamoto, K. Tambara, T. Nishina, Y. Saji, K. Inui, T. Hashida, S. Yokoyama, R. Onodera, T. Ikeda, M. Fukushima, M. Komeda, A novel approach to therapeutic angiogenesis for patients with critical limb ischemia by sustained release of basic fibroblast growth factor using biodegradable gelatin hydrogel: an initial report of the phase I-IIa study, Circulation Journal: Official Journal of the Japanese Circulation Society. 71 (2007) 1181–1186.

[232] P.A. Janmey, J.P. Winer, J.W. Weisel, Fibrin gels and their clinical and bioengineering applications, Journal of The Royal Society Interface. 6 (2009) 1–10. doi:10.1098/rsif.2008.0327.

[233] J. Leijten, J. Seo, K. Yue, G. Trujillo-de Santiago, A. Tamayol, G.U. Ruiz-Esparza, S.R. Shin, R. Sharifi, I. Noshadi, M.M. Álvarez, Y.S. Zhang, A. Khademhosseini, Spatially and temporally controlled hydrogels for tissue engineering, Materials Science and Engineering: R: Reports. 119 (2017) 1–35. doi:10.1016/j.mser.2017.07.001.

[234] S. Nie, W. Xiao, Q. Shi-bin, Z. Qiu-tang, J. Ju-quan, L. Xiao-qing, Z. Xiang-ming, C. Guo-xiang, M. Chang-sheng, Improved myocardial perfusion and cardiac function by controlled-release basic fibroblast growth factor using fibrin glue in a canine infarct model, Journal of Zhejiang University SCIENCE B. 11 (2010) 895–904. doi:10.1631/jzus.B1000302.

[235] D. Dippold, A. Cai, M. Hardt, A.R. Boccaccini, R.E. Horch, J.P. Beier, D.W. Schubert, Investigation of the batch-to-batch inconsistencies of Collagen in PCL-

Collagen nanofibers, Materials Science and Engineering: C. 95 (2019) 217–225. doi:10.1016/j.msec.2018.10.057.

[236] C.S. Hughes, L.M. Postovit, G.A. Lajoie, Matrigel: A complex protein mixture required for optimal growth of cell culture, PROTEOMICS. 10 (2010) 1886–1890. doi:10.1002/pmic.200900758.

[237] E.E. Antoine, P.P. Vlachos, M.N. Rylander, Review of Collagen I Hydrogels for Bioengineered Tissue Microenvironments: Characterization of Mechanics, Structure, and Transport, Tissue Engineering Part B: Reviews. 20 (2014) 683–696. doi:10.1089/ten.teb.2014.0086.

[238] L.E. Dickinson, M.E. Allen, S.K. Akiyama, Guiding endothelial progenitor cell tube formation using patterned fibronectin surfaces, Soft Matter. 6 (2010) 5109–5119. doi:10.1039/c0sm00233j.

[239] M.P. Lutolf, J.A. Hubbell, Synthetic biomaterials as instructive extracellular microenvironments for morphogenesis in tissue engineering, Nature Biotechnology. 23 (2005) 47–55. doi:10.1038/nbt1055.

[240] D. Hanjaya-Putra, K.T. Wong, K. Hirotsu, S. Khetan, J.A. Burdick, S. Gerecht, Spatial control of cell-mediated degradation to regulate vasculogenesis and angiogenesis in hyaluronan hydrogels, Biomaterials. 33 (2012) 6123–6131. doi:10.1016/j.biomaterials.2012.05.027.

[241] T.D. Sargeant, A.P. Desai, S. Banerjee, A. Agawu, J.B. Stopek, An in situ forming collagen–PEG hydrogel for tissue regeneration, Acta Biomaterialia. 8 (2012) 124–132. doi:10.1016/j.actbio.2011.07.028.

[242] J.L. Drury, D.J. Mooney, Hydrogels for tissue engineering: scaffold design variables and applications, Biomaterials. 24 (2003) 4337–4351. doi:10.1016/S0142-9612(03)00340-5.

[243] J. Cauich-Rodriguez, Effect of cross-linking agents on the dynamic mechanical properties of hydrogel blends of poly(acrylic acid)-poly(vinyl alcohol-vinyl acetate), Biomaterials. 17 (1996) 2259–2264. doi:10.1016/0142-9612(96)00058-0.

[244] T.P. Martens, A.F.G. Godier, J.J. Parks, L.Q. Wan, M.S. Koeckert, G.M. Eng, B.I. Hudson, W. Sherman, G. Vunjak-Novakovic, Percutaneous Cell Delivery Into the Heart Using Hydrogels Polymerizing In Situ, Cell Transplantation. 18 (2009) 297–304. doi:10.3727/096368909788534915.

[245] B.E.B. Jensen, I. Dávila, A.N. Zelikin, Poly(vinyl alcohol) Physical Hydrogels: Matrix-Mediated Drug Delivery Using Spontaneously Eroding Substrate, The Journal of Physical Chemistry B. 120 (2016) 5916–5926. doi:10.1021/acs.jpcb.6b01381.

[246] M.P. Lutolf, J.A. Hubbell, Synthesis and Physicochemical Characterization of End-Linked Poly(ethylene glycol)-co-peptide Hydrogels Formed by Michael-Type Addition, Biomacromolecules. 4 (2003) 713–722. doi:10.1021/bm025744e.

[247] C.D. Pritchard, T.M. O'Shea, D.J. Siegwart, E. Calo, D.G. Anderson, F.M. Reynolds, J.A. Thomas, J.R. Slotkin, E.J. Woodard, R. Langer, An injectable thiol-acrylate poly(ethylene glycol) hydrogel for sustained release of methylprednisolone sodium succinate, Biomaterials. 32 (2011) 587–597. doi:10.1016/j.biomaterials.2010.08.106.

[248] J. Zhu, Bioactive modification of poly(ethylene glycol) hydrogels for tissue engineering, Biomaterials. 31 (2010) 4639–4656. doi:10.1016/j.biomaterials.2010.02.044.

[249] M.P. Lutolf, N. Tirelli, S. Cerritelli, L. Cavalli, J.A. Hubbell, Systematic Modulation of Michael-Type Reactivity of Thiols through the Use of Charged Amino Acids, Bioconjugate Chemistry. 12 (2001) 1051–1056. doi:10.1021/bc015519e.

[250] M. Bracher, D. Bezuidenhout, M.P. Lutolf, T. Franz, M. Sun, P. Zilla, N.H. Davies, Cell specific ingrowth hydrogels, Biomaterials. 34 (2013) 6797–6803. doi:10.1016/j.biomaterials.2013.05.057.

[251] M. Morpurgo, F.M. Veronese, D. Kachensky, J.M. Harris, Preparation and Characterization of Poly(ethylene glycol) Vinyl Sulfone, Bioconjugate Chemistry. 7 (1996) 363–368. doi:10.1021/bc9600224.

[252] V.S. Khire, T.Y. Lee, C.N. Bowman, Surface Modification Using Thiol−Acrylate Conjugate Addition Reactions, Macromolecules. 40 (2007) 5669–5677. doi:10.1021/ma070146j.

[253] P.M. Kharkar, M.S. Rehmann, K.M. Skeens, E. Maverakis, A.M. Kloxin, Thiol–ene Click Hydrogels for Therapeutic Delivery, ACS Biomaterials Science & Engineering. 2 (2016) 165–179. doi:10.1021/acsbiomaterials.5b00420.

[254] A. Janse van Rensburg, N.H. Davies, A. Oosthuysen, C. Chokoza, P. Zilla, D. Bezuidenhout, Improved vascularization of porous scaffolds through growth factor delivery from heparinized polyethylene glycol hydrogels, Acta Biomaterialia. 49 (2017) 89–100. doi:10.1016/j.actbio.2016.11.036.

[255] K. Kadner, S. Dobner, T. Franz, D. Bezuidenhout, M.S. Sirry, P. Zilla, N.H. Davies, The beneficial effects of deferred delivery on the efficiency of hydrogel therapy post myocardial infarction, Biomaterials. 33 (2012) 2060–2066. doi:10.1016/j.biomaterials.2011.11.031.

[256] A. Abbotto, L. Beverina, G. Chirico, A. Facchetti, P. Ferruti, M. Gilberti, G.A. Pagani, Crosslinked Poly(amido-amine)s as Superior Matrices for Chemical

Incorporation of Highly Efficient Organic Nonlinear Optical Dyes, Macromolecular Rapid Communications. 24 (2003) 397–402. doi:10.1002/marc.200390057.

[257] B.D. Mather, K. Viswanathan, K.M. Miller, T.E. Long, Michael addition reactions in macromolecular design for emerging technologies, Progress in Polymer Science. 31 (2006) 487–531. doi:10.1016/j.progpolymsci.2006.03.001.

[258] J. Kim, Y.P. Kong, S.M. Niedzielski, R.K. Singh, A.J. Putnam, A. Shikanov, Characterization of the crosslinking kinetics of multi-arm poly(ethylene glycol) hydrogels formed via Michael-type addition, Soft Matter. 12 (2016) 2076–2085. doi:10.1039/C5SM02668G.

[259] S.P. Zustiak, J.B. Leach, Hydrolytically Degradable Poly(Ethylene Glycol) Hydrogel Scaffolds with Tunable Degradation and Mechanical Properties, Biomacromolecules. 11 (2010) 1348–1357. doi:10.1021/bm100137q.

[260] S. Dobner, D. Bezuidenhout, P. Govender, P. Zilla, N.H. Davies, A Synthetic Non-degradable Polyethylene Glycol Hydrogel Retards Adverse Post-infarct Left Ventricular Remodeling, Journal of Cardiac Failure. 15 (2009) 629–636. doi:10.1016/j.cardfail.2009.03.003.

[261] M.C. Ciuffreda, G. Malpasso, C. Chokoza, D. Bezuidenhout, K.P. Goetsch, M. Mura, F. Pisano, N.H. Davies, M. Gnecchi, Synthetic extracellular matrix mimic hydrogel improves efficacy of mesenchymal stromal cell therapy for ischemic cardiomyopathy, Acta Biomaterialia. 70 (2018) 71–83. doi:10.1016/j.actbio.2018.01.005.

[262] M.P. Lutolf, J.L. Lauer-Fields, H.G. Schmoekel, A.T. Metters, F.E. Weber, G.B. Fields, J.A. Hubbell, Synthetic matrix metalloproteinase-sensitive hydrogels for the conduction of tissue regeneration: Engineering cell-invasion characteristics, Proceedings of the National Academy of Sciences of the United States of America. 100 (2003) 5413–5418. doi:10.1073 pnas.0737381100.

[263] T.D. Zaveri, J.S. Lewis, N.V. Dolgova, M.J. Clare-Salzler, B.G. Keselowsky, Integrin-directed modulation of macrophage responses to biomaterials, Biomaterials. 35 (2014) 3504–3515. doi:10.1016/j.biomaterials.2014.01.007.

[264] R.M. Schweller, Z.J. Wu, B. Klitzman, J.L. West, Stiffness of Protease Sensitive and Cell Adhesive PEG Hydrogels Promotes Neovascularization In Vivo, Annals of Biomedical Engineering. 45 (2017) 1387–1398. doi:10.1007/s10439-017-1822-8.

[265] B.C. Jackson, D.W. Nebert, V. Vasiliou, Update of human and mouse matrix metalloproteinase families, Human Genomics. 4 (2010) 194–201. doi:10.1186/1479-7364-4-3-194.

[266] H. Nagase, G.B. Fields, Human matrix metalloproteinase specificity studies using collagen sequence-based synthetic peptides, Biopolymers. 40 (1996) 399–416. doi:10.1002/(SICI)1097-0282(1996)40:4<399::AID-BIP5>3.0.CO;2-R.

[267] S.K. Akiyama, Integrins in cell adhesion and signaling, Hum. Cell. 9 (1996) 181–186.

[268] M.D. Pierschbacher, E. Ruoslahti, Variants of the cell recognition site of fibronectin that retain attachment-promoting activity, Proceedings of the National Academy of Sciences of the United States of America. 81 (1984) 5985–5988.

[269] E. Ruoslahti, RGD and other recognition sequences for integrins, Annual Review of Cell and Developmental Biology. 12 (1996) 697–715. doi:10.1146/annurev.cellbio.12.1.697.

[270] G. Maheshwari, G. Brown, D.A. Lauffenburger, A. Wells, L.G. Griffith, Cell adhesion and motility depend on nanoscale RGD clustering, Journal of Cell Science. 113 (2000) 1677–1686.

[271] D.L. Hern, J.A. Hubbell, Incorporation of adhesion peptides into nonadhesive hydrogels useful for tissue resurfacing, Journal of Biomedical Materials Research. 39 (1998) 266–276.

[272] B.T. Burgess, J.L. Myles, R.B. Dickinson, Quantitative Analysis of Adhesion-Mediated Cell Migration in Three-Dimensional Gels of RGD-Grafted Collagen, Annals of Biomedical Engineering. 28 (2000) 110–118. doi:10.1114/1.259.

[273] A.K.A. Silva, C. Richard, M. Bessodes, D. Scherman, O.-W. Merten, Growth Factor Delivery Approaches in Hydrogels, Biomacromolecules. 10 (2009) 9–18. doi:10.1021/bm801103c.

[274] F. Brandl, F. Sommer, A. Goepferich, Rational design of hydrogels for tissue engineering: Impact of physical factors on cell behavior, Biomaterials. 28 (2007) 134–146. doi:10.1016/j.biomaterials.2006.09.017.

[275] D.E. Ingber, Cellular mechanotransduction: putting all the pieces together again, The FASEB Journal. 20 (2006) 811–827. doi:10.1096/fj.05-5424rev.

[276] M. Ehrbar, A. Sala, P. Lienemann, A. Ranga, K. Mosiewicz, A. Bittermann, S.C. Rizzi, F.E. Weber, M.P. Lutolf, Elucidating the role of matrix stiffness in 3D cell migration and remodeling, Biophysical Journal. 100 (2011) 284–293. doi:10.1016/j.bpj.2010.11.082.

[277] H.H. Winter, M. Mours, Rheology of Polymers Near Liquid-Solid Transitions, in: Neutron Spin Echo Spectroscopy Viscoelasticity Rheology, Springer, Berlin, 1997: pp. 165–234. doi:10.1007/3-540-68449-2_3.

[278] U. Freudenberg, A. Hermann, P.B. Welzel, K. Stirl, S.C. Schwarz, M. Grimmer, A. Zieris, W. Panyanuwat, S. Zschoche, D. Meinhold, A. Storch, C. Werner, A star-PEG–heparin hydrogel platform to aid cell replacement therapies for neurodegenerative diseases, Biomaterials. 30 (2009) 5049–5060. doi:10.1016/j.biomaterials.2009.06.002.

[279] B. Mulloy, J. Hogwood, E. Gray, R. Lever, C.P. Page, Pharmacology of Heparin and Related Drugs, Pharmacological Reviews. 68 (2016) 76–141. doi:10.1124/pr.115.011247.

[280] J.E. Scott, Extracellular matrix, supramolecular organisation and shape, Journal of Anatomy. 187 (Pt 2) (1995) 259–269.

[281] S.-C. Hung, X.-A. Lu, J.-C. Lee, M.D.-T. Chang, S. Fang, T. Fan, M.M.L. Zulueta, Y.-Q. Zhong, Synthesis of heparinoligosaccharides and their interaction with eosinophil-derived neurotoxin, Organic & Biomolecular Chemistry. 10 (2012) 760–772. doi:10.1039/C1OB06415K.

[282] J.D. Esko, Chapter 29: Glycosaminoglycan-binding Proteins, in: A. Varki, R. Cummings, J. Esko, H. Freeze, G. Hart, J. Marth (Eds.), Essentials of Glycobiology, Cold Spring Harbor Laboratory Press, Cold Spring Harbor, NY, 1999.

[283] I.R. Williams, Fibroblasts, in: Encyclopedia of Immunology, Elsevier, 1998: pp. 905–909. doi:10.1006/rwei.1999.0237.

[284] M. Doyon, Rapports du foie avec la coagulation du sang. Conditions de l'incoagulabilite du sang circulant., Journal de Physiologie et de Pathologie General. 14 (1912).

[285] M. Doyon, Rapports du foie avec la coagulation du sang. Conditions de l'incoagubilite du sang circulant, Journal de Physiologie. (1912) 229–240.

[286] S. Taylor, J. Folkman, Protamine is an inhibitor of angiogenesis, Nature. 297 (1982) 307–312.

[287] A.B. Schreiber, J. Kenney, W.J. Kowalski, R. Friesel, T. Mehlman, T. Maciag, Interaction of endothelial cell growth factor with heparin: characterization by receptor and antibody recognition, Proc. Natl. Acad. Sci. U.S.A. 82 (1985) 6138–6142.

[288] D.M. Ornitz, A. Yayon, J.G. Flanagan, C.M. Svahn, E. Levi, P. Leder, Heparin is Required for Cell-Free Binding of Basic Fibroblast Growth Factor to a Soluble Receptor and for Mitogenesis in Whole Cells, Molecular and Cellular Biology. 12 (1992) 240–247.

[289] G.C. Steffens, C. Yao, P. Prével, M. Markowicz, P. Schenck, E.M. Noah, N. Pallua, Modulation of Angiogenic Potential of Collagen Matrices by Covalent Incorporation of Heparin and Loading with Vascular Endothelial Growth Factor, Tissue Engineering. 10 (2004) 1502–1509. doi:10.1089/ten.2004.10.1502.

[290] D.L. Elbert, A.B. Pratt, M.P. Lutolf, S. Halstenberg, J.A. Hubbell, Protein delivery from materials formed by self-selective conjugate addition reactions, Journal of Controlled Release: Official Journal of the Controlled Release Society. 76 (2001) 11–25.

[291] N.H. Davies, C. Schmidt, D. Bezuidenhout, P. Zilla, Sustaining Neovascularization of a Scaffold Through Staged Release of Vascular Endothelial Growth Factor-A and Platelet-Derived Growth Factor-BB, Tissue Engineering Part A. 18 (2012) 26–34. doi:10.1089/ten.tea.2011.0192.

[292] Q. Wang, J.L. Mynar, M. Yoshida, E. Lee, M. Lee, K. Okuro, K. Kinbara, T. Aida, High-water-content mouldable hydrogels by mixing clay and a dendritic molecular binder, Nature. 463 (2010) 339–343. doi:10.1038/nature08693.

[293] L.A. Pruitt, Structural Biomedical Polymers (Nondegradable), in: P. Ducheyne, K.E. Healy, D.W. Hutmacher, D.W. Grainger, C.J. Kirkpatrick (Eds.), Comprehensive Biomaterials, Elsevier, Amsterdam, 2011: p. 374.

[294] G.A. Hudalla, W.L. Murphy, Biomaterials that Regulate Growth Factor Activity via Bioinspired Interactions, Advanced Functional Materials. 21 (2011) 1754–1768. doi:10.1002/adfm.201002468.

[295] S. Browne, A. Pandit, Engineered systems for therapeutic angiogenesis, Current Opinion in Pharmacology. 36 (2017) 34–43. doi:10.1016/j.coph.2017.07.002.

[296] M.W. Laschke, Y. Harder, M. Amon, I. Martin, J. Farhadi, A. Ring, N. Torio-Padron, R. Schramm, M. Rücker, D. Junker, J.M. Häufel, C. Carvalho, M. Heberer, G. Germann, B. Vollmar, M.D. Menger, Angiogenesis in Tissue Engineering: Breathing Life into Constructed Tissue Substitutes, Tissue Engineering. 12 (2006) 2093–2104. doi:10.1089/ten.2006.12.2093.

[297] N.H. Davies, S. Dobner, D. Bezuidenhout, C. Schmidt, M. Beck, A.H. Zisch, P. Zilla, The dosage dependence of VEGF stimulation on scaffold neovascularisation, Biomaterials. 29 (2008) 3531–3538. doi:10.1016/j.biomaterials.2008.05.007.

[298] Y. Zhu, H. Jiang, S.-H. Ye, T. Yoshizumi, W.R. Wagner, Tailoring the degradation rates of thermally responsive hydrogels designed for soft tissue injection by varying the autocatalytic potential, Biomaterials. 53 (2015) 484–493. doi:10.1016/j.biomaterials.2015.02.100.

[299] S. Nishio, S. Takeda, K. Kosuga, M. Okada, E. Kyo, T. Tsuji, E. Takeuchi, T. Terashima, Y. Inuzuka, T. Hata, Y. Takeuchi, T. Harita, J. Seki, S. Ikeguchi, Decade of Histological Follow-Up for a Fully Biodegradable Poly-l-lactic Acid Coronary Stent (Igaki-Tamai Stent) in Humans: Are Bioresorbable Scaffolds the Answer?, Circulation. 129 (2014) 534–535. doi:10.1161/CIRCULATIONAHA.113.003769.

[300] F. Witte, The history of biodegradable magnesium implants: A review☆, Acta Biomaterialia. 6 (2010) 1680–1692. doi:10.1016/j.actbio.2010.02.028.

[301] S. Sokic, G. Papavasiliou, FGF-1 and proteolytically mediated cleavage site presentation influence three-dimensional fibroblast invasion in biomimetic PEGDA hydrogels, Acta Biomaterialia. 8 (2012) 2213–2222. doi:10.1016/j.actbio.2012.03.017.

[302] D. Druecke, E.N. Lamme, S. Hermann, J. Pieper, P.S. May, H.-U. Steinau, L. Steinstraesser, Modulation of scar tissue formation using different dermal regeneration templates in the treatment of experimental full-thickness wounds, Wound Repair and Regeneration. 12 (2004) 518–527. doi:10.1111/j.1067-1927.2004.012504.x.

[303] G.P. Raeber, M.P. Lutolf, J.A. Hubbell, Molecularly Engineered PEG Hydrogels: A Novel Model System for Proteolytically Mediated Cell Migration, Biophysical Journal. 89 (2005) 1374–1388. doi:10.1529/biophysj.104.050682.

[304] B. Choi, X.J. Loh, A. Tan, C.K. Loh, E. Ye, M.K. Joo, B. Jeong, Introduction to In Situ Forming Hydrogels for Biomedical Applications, in: X.J. Loh (Ed.), In-Situ Gelling Polymers, Springer Singapore, Singapore, 2015: pp. 5–35. doi:10.1007/978-981-287-152-7_2.

[305] M. Rubinstein, R.H. Colby, Section 7: Networks and gels, in: Polymer Physics, Oxford University Press, Oxford ; New York, 2003: p. 292.

[306] Y. Maruyama, The human endothelial cell in tissue culture, Zeitschrift Fur Zellforschung Und Mikroskopische Anatomie (Vienna, Austria: 1948). 60 (1963) 69–79.

[307] N. Jiménez, V.J.D. Krouwer, J.A. Post, A new, rapid and reproducible method to obtain high quality endothelium in vitro, Cytotechnology. 65 (2013) 1–14. doi:10.1007/s10616-012-9459-9.

[308] E.A. Jaffe, R.L. Nachman, C.G. Becker, C.R. Minick, Culture of Human Endothelial Cells Derived from Umbilical Veins. Identification by morphologic and immunologic criteria, Journal of Clinical Investigation. 52 (1973) 2745–2756. doi:10.1172/JCI107470.

[309] K. Cooper, V. Shah, N. Sapre, E. Sharma, C. Mistry, C. Viswanathan, Defining Permissible Time Lapse between Umbilical Cord Tissue Collection and Commencement of Cell Isolation, International Journal of Hematology-Oncology and Stem Cell Research. 7 (2013) 15–23.

[310] B. Baudin, A. Bruneel, N. Bosselut, M. Vaubourdolle, A protocol for isolation and culture of human umbilical vein endothelial cells, Nature Protocols. 2 (2007) 481–485. doi:10.1038/nprot.2007.54.

[311] E.F. Smeets, E.J.U. von Asmuth, C.J. van der Linden, J.F.M. Leeuwenberg, W.A. Buurman, A Comparison of Substrates for Human Umbilical Vein Endothelial Cell Culture, Biotechnic & Histochemistry. 67 (1992) 241–250. doi:10.3109/10520299209110072.

[312] D.B. Cines, E.S. Pollak, C.A. Buck, J. Loscalzo, G.A. Zimmerman, R.P. McEver, J.S. Pober, T.M. Wick, B.A. Konkle, B.S. Schwartz, E.S. Barnathan, K.R. McCrae, B.A. Hug, A.M. Schmidt, D.M. Stern, Endothelial cells in physiology and in the pathophysiology of vascular disorders, Blood. 91 (1998) 3527–3561.

[313] L. Fina, H.V. Molgaard, D. Robertson, N.J. Bradley, P. Monaghan, D. Delia, D.R. Sutherland, M.A. Baker, M.F. Greaves, Expression of the CD34 gene in vascular endothelial cells, Blood. 75 (1990) 2417–2426.

[314] S. Baumhueter, N. Dybdal, C. Kyle, L.A. Lasky, Global vascular expression of murine CD34, a sialomucin-like endothelial ligand for L-selectin, Blood. 84 (1994) 2554–2565.

[315] J.A. Ryan, Evolution of Cell Culture Surfaces, Sigma-Aldrich. (2008). https://www.sigmaaldrich.com/technical-documents/articles/biofiles/evolution-of-cell.html.

[316] M. Elena Diaz, R.L. Cerro, Transition from split streamlines to dip-coating during Langmuir–Blodgett film deposition, Thin Solid Films. 460 (2004) 274–278. doi:10.1016/j.tsf.2004.02.002.

[317] S.H. Lee, E. Ruckenstein, Chapter 25: Surface restructuring of polymers, in: Wetting Experiments, CRC Press, 2018.

[318] A. Stahl, X. Wu, A. Wenger, M. Klagsbrun, P. Kurschat, Endothelial progenitor cell sprouting in spheroid cultures is resistant to inhibition by osteoblasts: A model for bone replacement grafts, FEBS Letters. 579 (2005) 5338–5342. doi:10.1016/j.febslet.2005.09.005.

[319] S. Sokic, G. Papavasiliou, Controlled Proteolytic Cleavage Site Presentation in Biomimetic PEGDA Hydrogels Enhances Neovascularization *In Vitro*, Tissue Engineering Part A. 18 (2012) 2477–2486. doi:10.1089/ten.tea.2012.0173.

[320] F. Tetzlaff, A. Fischer, Human Endothelial Cell Spheroid-based Sprouting Angiogenesis Assay in Collagen, Bio-Protocol. 8 (2018). doi:10.21769/BioProtoc.2995.

[321] P. Correa de Sampaio, D. Auslaender, D. Krubasik, A.V. Failla, J.N. Skepper, G. Murphy, W.R. English, A Heterogeneous In Vitro Three Dimensional Model of Tumour-Stroma Interactions Regulating Sprouting Angiogenesis, PLoS ONE. 7 (2012) e30753. doi:10.1371/journal.pone.0030753.

[322] A. Wenger, A. Stahl, H. Weber, G. Finkenzeller, H.G. Augustin, G.B. Stark, U. Kneser, Modulation of in vitro Angiogenesis in a Three-Dimensional Spheroidal Coculture Model for Bone Tissue Engineering, Tissue Engineering. 10 (2004) 1536–1547. doi:10.1089/ten.2004.10.1536.

[323] T. Korff, H.G. Augustin, Tensional forces in fibrillar extracellular matrices control directional capillary sprouting, Journal of Cell Science. 112 (Pt 19) (1999) 3249–3258.

[324] Y. Yang, L.M. Leone, L.J. Kaufman, Elastic Moduli of Collagen Gels Can Be Predicted from Two-Dimensional Confocal Microscopy, Biophysical Journal. 97 (2009) 2051–2060. doi:10.1016/j.bpj.2009.07.035.

[325] R.C. Arevalo, J.S. Urbach, D.L. Blair, Size-Dependent Rheology of Type-I Collagen Networks, Biophysical Journal. 99 (2010) L65–L67. doi:10.1016/j.bpj.2010.08.008.

[326] R.K. Willits, S.L. Skornia, Effect of collagen gel stiffness on neurite extension, Journal of Biomaterials Science. Polymer Edition. 15 (2004) 1521–1531.

[327] E.E. Antoine, P.P. Vlachos, M.N. Rylander, Tunable Collagen I Hydrogels for Engineered Physiological Tissue Micro-Environments, PLOS ONE. 10 (2015) e0122500. doi:10.1371/journal.pone.0122500.

[328] D.C. Hoffmann, S. Willenborg, M. Koch, D. Zwolanek, S. Müller, A.-K.A. Becker, S. Metzger, M. Ehrbar, P. Kurschat, M. Hellmich, J.A. Hubbell, S.A. Eming, Proteolytic Processing Regulates Placental Growth Factor Activities, Journal of Biological Chemistry. 288 (2013) 17976–17989. doi:10.1074/jbc.M113.451831.

[329] A. Kiba, N. Yabana, M. Shibuya, A Set of Loop-1 and -3 Structures in the Novel Vascular Endothelial Growth Factor (VEGF) Family Member, VEGF-E NZ-7 , Is Essential for the Activation of VEGFR-2 Signaling, Journal of Biological Chemistry. 278 (2003) 13453–13461. doi:10.1074/jbc.M210931200.

[330] J. Morales-Sanfrutos, J. Lopez-Jaramillo, M. Ortega-Muñoz, A. Megia-Fernandez, F. Perez-Balderas, F. Hernandez-Mateo, F. Santoyo-Gonzalez, Vinyl sulfone: a versatile function for simple bioconjugation and immobilization, Organic & Biomolecular Chemistry. 8 (2010) 667–675. doi:10.1039/B920576D.

[331] H. Gitay-Goren, S. Soker, I. Vlodavsky, G. Neufeld, The binding of vascular endothelial growth factor to its receptors is dependent on cell surface-associated heparin-like molecules, The Journal of Biological Chemistry. 267 (1992) 6093–6098.

[332] K. Ono, H. Hattori, S. Takeshita, A. Kurita, M. Ishihara, Structural features in heparin that interact with VEGF165 and modulate its biological activity, Glycobiology. 9 (1999) 705–711. doi:10.1093/glycob/9.7.705.

[333] O. Oliviero, M. Ventre, P.A. Netti, Functional porous hydrogels to study angiogenesis under the effect of controlled release of vascular endothelial growth factor, Acta Biomaterialia. 8 (2012) 3294–3301. doi:10.1016/j.actbio.2012.05.019.

[334] G.S. Schultz, A. Wysocki, Interactions between extracellular matrix and growth factors in wound healing, Wound Repair and Regeneration. 17 (2009) 153–162. doi:10.1111/j.1524-475X.2009.00466.x.

[335] L. Macri, D. Silverstein, R. Clark, Growth factor binding to the pericellular matrix and its importance in tissue engineering☆, Advanced Drug Delivery Reviews. 59 (2007) 1366–1381. doi:10.1016/j.addr.2007.08.015.

[336] N.A. Peppas, K.M. Wood, J.O. Blanchette, Hydrogels for oral delivery of therapeutic proteins, Expert Opinion on Biological Therapy. 4 (2004) 881–887. doi:10.1517/14712598.4.6.881.

[337] A. Marui, A. Kanematsu, K. Yamahara, K. Doi, T. Kushibiki, M. Yamamoto, H. Itoh, T. Ikeda, Y. Tabata, M. Komeda, Simultaneous application of basic fibroblast growth factor and hepatocyte growth factor to enhance the blood vessels formation, Journal of Vascular Surgery. 41 (2005) 82–90. doi:10.1016/j.jvs.2004.10.029.

[338] D.C. Hoffmann, Functional characterization of the PlGF-2 heparin-binding domain, PhD, University of Cologne, 2011.

[339] M.M. Martino, P.S. Briquez, E. Guc, F. Tortelli, W.W. Kilarski, S. Metzger, J.J. Rice, G.A. Kuhn, R. Muller, M.A. Swartz, J.A. Hubbell, Growth Factors Engineered for Super-Affinity to the Extracellular Matrix Enhance Tissue Healing, Science. 343 (2014) 885–888. doi:10.1126/science.1247663.

[340] O.A. Ibrahimi, F. Zhang, S.C. Lang Hrstka, M. Mohammadi, R.J. Linhardt, Kinetic Model for FGF, FGFR, and Proteoglycan Signal Transduction Complex Assembly, Biochemistry. 43 (2004) 4724–4730. doi:10.1021/bi0352320.

[341] A. Zieris, S. Prokoph, K.R. Levental, P.B. Welzel, M. Grimmer, U. Freudenberg, C. Werner, FGF-2 and VEGF functionalization of starPEG–heparin hydrogels to modulate biomolecular and physical cues of angiogenesis, Biomaterials. 31 (2010) 7985–7994. doi:10.1016/j.biomaterials.2010.07.021.

[342] M.V. Tsurkan, K. Chwalek, K.R. Levental, U. Freudenberg, C. Werner, Modular StarPEG-Heparin Gels with Bifunctional Peptide Linkers, Macromolecular Rapid Communications. 31 (2010) 1529–1533. doi:10.1002/marc.201000155.

[343] S.E. Sakiyama-Elbert, Incorporation of heparin into biomaterials, Acta Biomaterialia. 10 (2014) 1581–1587. doi:10.1016/j.actbio.2013.08.045.

[344] S.M. Marino, V.N. Gladyshev, Cysteine Function Governs Its Conservation and Degeneration and Restricts Its Utilization on Protein Surfaces, Journal of Molecular Biology. 404 (2010) 902–916. doi:10.1016/j.jmb.2010.09.027.

[345] D. Gospodarowicz, J. Cheng, Heparin protects basic and acidic FGF from inactivation, Journal of Cellular Physiology. 128 (1986) 475–484. doi:10.1002/jcp.1041280317.

[346] D.L. Rabenstein, Heparin and heparan sulfate: structure and function, Natural Product Reports. 19 (2002) 312–331.

[347] M. Klagsbrun, A. Baird, A dual receptor system is required for basic fibroblast growth factor activity, Cell. 67 (1991) 229–231.

[348] F.W. Sellke, J. Li, A. Stamler, J.J. Lopez, K.A. Thomas, M. Simons, Angiogenesis induced by acidic fibroblast growth factor as an alternative method of revascularization for chronic myocardial ischemia, Surgery. 120 (1996) 182–188.

[349] D.E. Discher, P. Janmey, Y. Wang, Tissue Cells Feel and Respond to the Stiffness of Their Substrate, Science. 310 (2005) 1139–1143. doi:10.1126/science.1116995.

[350] C. Chokoza, C.A. Gustafsson, K.P. Goetsch, P. Zilla, N. Thierfelder, F. Pisano, M. Mura, M. Gnecchi, D. Bezuidenhout, N.H. Davies, Tuning Tissue Ingrowth into Proangiogenic Hydrogels via Dual Modality Degradation, ACS Biomaterials Science & Engineering. (2019). doi:10.1021/acsbiomaterials.9b01220.

[351] D.F. Williams, On the nature of biomaterials, Biomaterials. 30 (2009) 5897–5909. doi:10.1016/j.biomaterials.2009.07.027.

[352] C.S. Bahney, C.-W. Hsu, J.U. Yoo, J.L. West, B. Johnstone, A bioresponsive hydrogel tuned to chondrogenesis of human mesenchymal stem cells, The Journal of the Federation of American Societies for Experimental Biology. 25 (2011) 1486–1496. doi:10.1096/fj.10-165514.

[353] C.-Y. Lin, J.C. Liu, Modular protein domains: an engineering approach toward functional biomaterials, Current Opinion in Biotechnology. 40 (2016) 56–63. doi:10.1016/j.copbio.2016.02.011.

[354] M.P. Staiger, A.M. Pietak, J. Huadmai, G. Dias, Magnesium and its alloys as orthopedic biomaterials: A review, Biomaterials. 27 (2006) 1728–1734. doi:10.1016/j.biomaterials.2005.10.003.

[355] L.S. Nair, C.T. Laurencin, Biodegradable polymers as biomaterials, Progress in Polymer Science. 32 (2007) 762–798. doi:10.1016/j.progpolymsci.2007.05.017.

[356] T. Sugiura, S. Tara, H. Nakayama, T. Yi, Y.-U. Lee, T. Shoji, C.K. Breuer, T. Shinoka, Fast-degrading bioresorbable arterial vascular graft with high cellular infiltration inhibits calcification of the graft, Journal of Vascular Surgery. 66 (2017) 243–250. doi:10.1016/j.jvs.2016.05.096.

[357] S. Chatani, D.P. Nair, C.N. Bowman, Relative reactivity and selectivity of vinyl sulfones and acrylates towards the thiol–Michael addition reaction and polymerization, Polymer Chemistry. 4 (2013) 1048–1055. doi:10.1039/C2PY20826A.

[358] N.A. Peppas, Y. Huang, M. Torres-Lugo, J.H. Ward, J. Zhang, Physicochemical Foundations and Structural Design of Hydrogels in Medicine and Biology, Annual Review of Biomedical Engineering. 2 (2000) 9–29. doi:10.1146/annurev.bioeng.2.1.9.

[359] C. Hiemstra, L.J. van der Aa, Z. Zhong, P.J. Dijkstra, J. Feijen, Rapidly in Situ-Forming Degradable Hydrogels from Dextran Thiols through Michael Addition, Biomacromolecules. 8 (2007) 1548–1556. doi:10.1021/bm061191m.

[360] K.S. Anseth, A.T. Metters, S.J. Bryant, P.J. Martens, J.H. Elisseeff, C.N. Bowman, In situ forming degradable networks and their application in tissue engineering and drug delivery, Journal of Controlled Release: Official Journal of the Controlled Release Society. 78 (2002) 199–209.

[361] J. Zandstra, C. Hiemstra, A.H. Petersen, J. Zuidema, M.M. van Beuge, S. Rodriguez, A.A. Lathuile, G.J. Veldhuis, R. Steendam, R.A. Bank, E.R. Popa, Microsphere size influences the foreign body reaction, European Cells & Materials. 28 (2014) 335–347.

[362] A.J. Singer, R.A.F. Clark, Cutaneous Wound Healing, New England Journal of Medicine. 341 (1999) 738–746. doi:10.1056/NEJM199909023411006.

[363] J.D. Bryers, C.M. Giachelli, B.D. Ratner, Engineering biomaterials to integrate and heal: The biocompatibility paradigm shifts, Biotechnology and Bioengineering. 109 (2012) 1898–1911. doi:10.1002/bit.24559.

[364] B. Baudin, A. Bruneel, N. Bosselut, M. Vaubourdolle, A protocol for isolation and culture of human umbilical vein endothelial cells, Nature Protocols. 2 (2007) 481–485. doi:10.1038/nprot.2007.54.

[365] J.K. Lucas, Umbilical Venous Catheters (Insertion and Removal), in: L. Ganti (Ed.), Atlas of Emergency Medicine Procedures, Springer New York, New York, 2016: pp. 699–704. doi:10.1007/978-1-4939-2507-0_121.

[366] D. Bezuidenhout, N. Davies, P. Zilla, Effect of well defined dodecahedral porosity on inflammation and angiogenesis, American Society for Artificial Internal Organs. 48 (2002) 465–471.